# STUDY REPORT

# IN VITRO ASSESSMENT OF ACUTE EXPOSURE OF THS2.2 AEROSOL ON ORGANOTYPIC ACUTE HUMAN NASAL CULTURES (STUDY PLAN NUMBER 172200)

TABLE OF CONTENTS

TABLE OF CONTENTS ..... 2
TABLE OF FIGURES ..... 7
TABLE OF TABLES ..... 8
1 APPROVAL ..... 9
1.1 STUDY DIRECTOR'S STATEMENT OF COMPLIANCE ..... 9
1.2 QUALITY ASSURANCE STATEMENT ..... 9
2 GENERAL INFORMATION ..... 10
2.1 NAMES AND ADDRESSES ..... 10
2.2 STUDY SCHEDULE ..... 12
2.3 TEST GUIDELINES ..... 12
3 STUDY PLAN DEVIATIONS ..... 13
4 ABSTRACT / EXECUTIVE SUMMARY ..... 18
5 INTRODUCTION ..... 19
6 OBJECTIVE ..... 22
7 EXPERIMENTAL DESIGN ..... 23
7.1 TEST AND REFERENCE ITEMS ..... 23
7.1.1 Identification and Description ..... 23
7.1.2 Item Storage ..... 25
7.1.3 Item Conditioning ..... 25
7.1.4 Carbonyl Levels Deposited in the Cultivation Base Module of the Vitrocell® 24/48 Exposure System following 28 min Exposure to Reference Smoke and Test Aerosol ..... 26
7.2 TEST SYSTEM ..... 28
7.3 SAMPLE GENERATION ..... 29
7.3.1 Experimental Repetitions: The Impact Assessment of THS2.2 Aerosol as Compared with 3R4F Smoke Exposure ..... 29
7.3.2 Dose Range Assessment of THS2.2 Aerosol ..... 32
7.4 TESTING PROCEDURE ..... 32
7.4.1 Aerosol/Smoke Generation and *in vitro* Exposure Regimens ..... 32
7.4.2 Nicotine Determination in Whole Smoke/Aerosol ..... 32
7.4.3 Carbonyl Concentrations Deposited in the Vitocell Base Mocule Following Whole Smoke/Aerosol Exposure ..... 33
7.4.4 Maintenance of Nasal MucilAir™ 3D-organotypic Cultures (Air-Liquid Interface Cultures) ..... 33
7.4.5 Apical Wash of MucilAir™ 3D-organotypic Culture (Air-Liquid Interface Cultures) ..... 34
7.4.6 Adenylate Kinase (AK) Cytotoxicity Assay ..... 35
7.4.7 Measurement of Secreted Pro-Inflammatory Mediators ..... 36
7.4.8 Culture Processing, Embedding, Sectioning, and Staining ..... 38
7.4.9 Immunohistochemistry (IHC) Analysis ..... 38
7.4.10 Cytochrome P450 (CYP) 1A1/1B1 Activity Assay ..... 39

7.4.11 RNA/microRNA Purification ..... 39
7.4.12 mRNA Profiling Analysis using GeneChips ..... 39
7.4.13 MiRNA profiling ..... 40
8 STATISTICAL AND COMPUTATIONAL METHODS ..... 41
8.1 STATISTICAL METHODS ..... 41
8.1.1 Experimental Unit ..... 41
8.1.2 Derived Variables ..... 41
8.1.2.1 Normalized Cytotoxicity Levels ..... 41
8.1.2.2 Normalized CYP Activity Levels ..... 42
8.1.3 Data Transformation ..... 42
8.1.4 Statistical Comparisons ..... 42
8.2 COMPUTATIONAL METHODS: AFFYMETRIX GENE EXPRESSION ANALYSIS ..... 42
8.2.1 Processing and Quality Control (QC) of Raw CEL Files ..... 42
8.2.2 Gene-Level Analysis ..... 43
8.2.3 Statistical Analysis: Network-Level Analysis ..... 43
8.2.3.1 Network Perturbation Amplitude (NPA) ..... 43
8.2.3.2 Biological Impact Factor (BIF) ..... 45
8.2.4 Gene-Set Analysis ..... 46
8.3 COMPUTATIONAL METHODS: AFFYMETRIX MIRNA EXPRESSION ANALYSIS ..... 47
8.3.1 Processing and Quality Control of Raw CEL Files ..... 47
8.3.2 Probe Set Filtering ..... 47
8.3.3 Determining a Differential miRNA Expression ..... 47
9 RESULTS ..... 49
9.1 NICOTINE CONCENTRATIONS IN THE SMOKE/AEROSOL ..... 49
9.2 HISTOLOGICAL EVALUATION ..... 51
9.2.1 Morphological Evaluation ..... 51
9.2.2 Immunohistochemistry (IHC) Analysis ..... 53
9.3 CYTOTOXICITY ..... 58
9.4 CYTOCHROME P450 (CYP) 1A1/1B1 ACTIVITY ..... 59
9.5 SECRETION OF PRO-INFLAMMATORY MEDIATORS ..... 60
9.6 TRANSCRIPTOME OF NASAL EPITHELIAL CULTURES ..... 62
9.6.1 Differentially Expressed Genes ..... 62
9.6.2 Biological Impact Factor ..... 64
9.6.3 Network Perturbation Amplitude ..... 68
9.6.4 Alterations of the Expression Levels of Genes Regulating Cell Stress and Inflammation ..... 70
9.7 MIRNA TRANSCRIPTOME OF THE NASAL EPITHELIAL CULTURES ..... 73
9.8 CORRELATION OF THE OUTCOMES ACROSS THE EXPERIMENTAL REPETITIONS ..... 76

9.8.1 Correlation of Immunohistochemistry, Cytotoxicity, CYP1A1/1B1 Activity, and Pro-Inflammatory Mediators across the Experimental Repetitions ..... 76
9.8.2 Correlation of the Gene Expression Fold-Changes across the Experimental Repetitions ..... 78
9.8.3 Correlation of the miRNA Expression Fold-Changes across the Experimental Repetitions ..... 80
9.9 DOSE RANGE ASSESSMENT OF THS2.2 BASED ON THE CYTOTOXICITY AND CULTURE HISTOLOGY ..... 82
10 DISCUSSION AND CONCLUSION ..... 85
11 ARCHIVING ..... 88
12 REFERENCES ..... 89
12.1 LITERATURE ..... 89
12.2 LIST OF STANDARD OPERATING PROCEDURES (SOP) AND WORK INSTRUCTIONS (WKI) ..... 94
12.3 PHILIP MORRIS INTERNATIONAL (PMI) INTERNAL DOCUMENTS ..... 96
13 ABBREVIATIONS ..... 98
14 TABLES AND SUPPLEMENTARY FIGURES ..... 102
14.1 SUPPLEMENTARY TABLES ..... 102
14.1.1 **Supplementary Table 1**. Descriptive Statistics of Formaldehyde Levels Deposited in the Cultivation Base Module of the Vitrocell® 24/48 exposure system ..... 102
14.1.2 **Supplementary Table 2**. Descriptive Statistics of Acetaldehyde Levels Deposited in the Cultivation Base Module of the Vitrocell® 24/48 exposure system ..... 102
14.1.3 **Supplementary Table 3**. Descriptive Statistics of Acetone Levels Deposited in the Cultivation Base Module of the Vitrocell® 24/48 exposure system ..... 103
14.1.4 **Supplementary Table 4**. Descriptive Statistics of Acrolein Levels Deposited in the Cultivation Base Module of the Vitrocell® 24/48 exposure system ..... 103
14.1.5 **Supplementary Table 5**. Descriptive Statistics of Propionaldehyde Levels Deposited in the Cultivation Base Module of the Vitrocell® 24/48 exposure system ..... 104
14.1.6 **Supplementary Table 6**. Descriptive Statistics of Crotonaldehyde Levels Deposited in the Cultivation Base Module of the Vitrocell® 24/48 exposure system ..... 104
14.1.7 **Supplementary Table 7**. Descriptive Statistics of Methyl Ethyl Ketone Levels Deposited in the Cultivation Base Module of the Vitrocell® 24/48 exposure system ..... 105
14.1.8 **Supplementary Table 8**. Descriptive Statistics of Butyraldehyde Levels Deposited in the Cultivation Base Module of the Vitrocell® 24/48 exposure system ..... 105
14.1.9 **Supplementary Table 9**. Descriptive Statistics: Cytotoxicity, CYP Activity, and Inflammatory Mediators Levels of the 3R4F (0.20) Group ..... 106
14.1.10 **Supplementary Table 10**. Descriptive Statistics of Immunohistochemistry Quantification on P63 Positive Staining (%) ..... 107
14.1.11 **Supplementary Table 11**. Descriptive Statistics of Immunohistochemistry Quantification on Ki67 Positive Staining (%) ..... 107
14.1.12 **Supplementary Table 12**. Descriptive Statistics of Immunohistochemistry Quantification on FoxJ1 Positive Staining (%) ..... 108
14.1.13 **Supplementary Table 13.** Descriptive Statistics: Cytotoxicity (RLU) ..... 109
14.1.14 **Supplementary Table 14.** Descriptive Statistics: CYP1A1/1B1 Activity (RLU) ... 110

14.1.15 **Supplementary Table 15.** Descriptive Statistics: EGF (Epidermal Growth Factor) Protein in the Basolateral Media ..... 111
14.1.16 **Supplementary Table 16**. Descriptive Statistics: CXCL1 (Chemokine (C-X-C motif) Ligand 1) Protein in the Basolateral Media ..... 112
14.1.17 **Supplementary Table 17.** Descriptive Statistics: IL6 (Interleukin 6) Protein in the Basolateral Media ..... 113
14.1.18 **Supplementary Table 18.** Descriptive Statistics: CXCL8 (Chemokine (C-X-C motif) Ligand 8) Protein in the Basolateral Media ..... 114
14.1.19 **Supplementary Table 19.** Descriptive Statistics: CCL20 (Chemokine (C-C motif) Ligand 20) Protein in the Basolateral Media ..... 115
14.1.20 **Supplementary Table 20.** Descriptive Statistics: MMP1 (Matrix Metalloproteinase 1) Protein in the Basolateral Media ..... 116
14.1.21 **Supplementary Table 21.** Descriptive Statistics: MMP9 (Matrix Metalloproteinase 9) Protein in the Basolateral Media ..... 117
14.1.22 **Supplementary Table 22.** Descriptive Statistics: sICAM1 (soluble Inter-Cellular Adhesion Molecule 1) Protein in the Basolateral Media ..... 118
14.1.23 **Supplementary Table 23.** Descriptive Statistics: TIMP1 (Tissue Inhibitor of Metalloproteinase 1) Protein in the Basolateral Media ..... 119
14.1.24 **Supplementary Table 24**. Descriptive Statistics: TNFA (Tumor Necrosis Factor Alpha) Protein in the Basolateral Media ..... 120
14.1.25 **Supplementary Table 25**. Descriptive Statistics of VEGFA (Vascular Endothelial Growth Factor Alpha) Protein in the Basolateral Media ..... 121
14.1.26 **Supplementary Table 26**. Descriptive Statistics of CCL11 (Chemokine (C-C motif) Ligand 11) Protein in the Basolateral Media ..... 122
14.1.27 **Supplementary Table 27**. Descriptive Statistics of CSF3 (colony-stimulating factor 3) Protein in the Basolateral Media ..... 122
14.1.28 **Supplementary Table 28**. Descriptive Statistics of CSF2 (colony-stimulating factor 2) Protein in the Basolateral Media ..... 123
14.1.29 **Supplementary Table 29**. Descriptive Statistics of IL1A (Interleukin 1 Alpha) Protein in the Basolateral Media ..... 123
14.1.30 **Supplementary Table 30**. Descriptive Statistics of IL1B (Interleukin 1 Beta) Protein in the Basolateral Media ..... 124
14.1.31 **Supplementary Table 31**. Descriptive Statistics of IL10 (Interleukin 10) Protein in the Basolateral Media ..... 125
14.1.32 **Supplementary Table 32**. Descriptive Statistics of IL13 (Interleukin 13) Protein in the Basolateral Media ..... 125
14.1.33 **Supplementary Table 33**. Descriptive Statistics of CXCL10 (chemokine (C-X-C motif) ligand)) Protein in the Basolateral Media ..... 126
14.1.34 **Supplementary Table 34**. Descriptive Statistics of CCL2 (Chemokine (C-C motif) Ligand 2) Protein in the Basolateral Media ..... 126
14.1.35 **Supplementary Table 35**. Descriptive Statistics of CCL5 (Chemokine (C-C motif) Ligand 5) Protein in the Basolateral Media ..... 127
14.1.36 **Supplementary Table 36**. Descriptive Statistics of TSLP (Thymic Stromal Lymphopoietin) Protein in the Basolateral Media ..... 127
14.1.37 **Supplementary Table 37**. Descriptive Statistics: Cytotoxicity (%) in Dose Range Assessment of THS2.2 ..... 128

14.2 SUPPLEMENTARY FIGURES ..... 129

14.2.1 **Supplementary Figure 1**. Individual Plots of the Inflammatory Mediators Secreted into the Basolateral Media ..... 129
14.2.2 **Supplementary Figure 2**. Volcano Plots of the Differentially Expressed Genes (DEGs) in All Experimental Groups Relative to Air Controls ..... 131
14.2.3 **Supplementary Figure 3**. Gene-set Analysis of the Differentially Expressed Genes 132
14.2.4 **Supplementary Figure 4**. Volcano Plots of the Differentially Expressed miRNAs in All Experimental Groups Relative to Air Controls ..... 133
14.2.5 **Supplementary Figure 5**. Quantile-Quantile (QQ) Plots of the Differentially Expressed miRNA in All Experimental Groups ..... 134

TABLE OF FIGURES

**Figure 1. Cigarette smoke-induced changes in mucosal immune responses.** ..... 19
**Figure 2. Concentrations of representative carbonyls deposited in the Cultivation Base Module of Vitrocell® 24/48 exposure system following exposures to the reference cigarette smoke and test item aerosol.** ..... 27
**Figure 3. Schematic representation of exposure runs for 3R4F and THS2.2.** ..... 30
**Figure 4. Histology following exposure of the human organotypic 3D nasal cultures to 3R4F smoke/THS2.2 aerosol.** ..... 52
**Figure 5. IHC images of FoxJ1, Ki67, and p63 immunostaining.** ..... 55
**Figure 6. Quantitative analysis of FoxJ1, Ki67, and p63 immunostaining of exposed organotypic nasal cultures** ..... 57
**Figure 7 Cytotoxicity in organotypic cultures following 3R4F and THS2.2 exposure.** ..... 58
**Figure 8. CYP1A1/CYP1B1 activity following 3R4F and THS2.2 exposure in the organotypic nasal cultures.** ..... 59
**Figure 9. Fold changes of secretion levels of pro-inflammatory mediators into the basolateral medium of the organotypic nasal cultures following exposure.** ..... 61
**Figure 10. Volcano plots of the differentially expressed genes in nasal epithelial cultures following exposure.** ..... 63
**Figure 11. Relative biological impact factor (BIF) derived from cumulated network perturbations impacted by 3R4F and THS2.2 exposure compared with the air controls.** ..... 65
**Figure 12. Contribution of individual network perturbations to the biological impact factor (BIF) analysis.** ..... 67
**Figure 13. Heatmap of network perturbation amplitude (NPA) scores of biological networks impacted by 3R4F and THS2.2 exposure.** ..... 69
**Figure 14. Altered expression levels of genes regulating cellular stress after 3R4F and THS2.2 exposure.** ..... 71
**Figure 15. Altered expression levels of genes regulating inflammation after 3R4F and THS2.2 exposure.** ..... 72
**Figure 16. Volcano plots of the differentially expressed miRNAs in nasal epithelial cultures following exposure.** ..... 74
**Figure 17. Heatmap of differentially expressed miRNAs after 3R4F smoke and THS2.2 aerosol exposure.** ..... 75
**Figure 18. Correlation plots of the immunohistochemistry, cytotoxicity, CYP1A1/1B1 activity, and pro-inflammatory mediators across the experimental repetitions.** ..... 77
**Figure 19. Correlation plots of gene fold-changes generated from the microarray analysis.** ..... 79
**Figure 20. Correlation plots of miRNA fold-changes generated from the miRNA array analysis.** ..... 81
**Figure 21. Cytotoxicity following exposure to various dilutions of THS2.2 aerosol.** ..... 83
**Figure 22. Histology following exposure to various dilutions of THS2.2 aerosol.** ..... 84

TABLE OF TABLES

**Table 1. Study Plan Deviations** ..... 13
**Table 2. Test and Reference Items** ..... 23
**Table 3. Reference and Test Items Used in Experimental Repetitions** ..... 24
**Table 4. Specifications of the Different Batches of Nasal Culture Used in the Experimental Repetitions** ..... 28
**Table 5. Target Nicotine Concentrations in the Smoke/Aerosol (mg nicotine/L smoke or aerosol) Applied in the Study** ..... 29
**Table 6. Post-Exposure Endpoints** ..... 31
**Table 7. Concentrations of diluted Aerosol (%) Applied and Endpoints Assessed in the Dose Range Assessment of THS2.2** ..... 32
**Table 8. Cytotoxicity Kits Used in the Study** ..... 35
**Table 9. Summary of Milliplex® Kits used in the Experimental Repetitions** ..... 37
**Table 10. Network and Network Models Used in the Analysis** ..... 44
**Table 11. Target and Actual Nicotine Concentrations in the Smoke/Aerosol** ..... 50
**Table 12. Actual Nicotine Concentrations in the THS2.2 Aerosol from the Various Dilutions Applied for the Dose Range Assessment of THS2.2** ..... 82

# 1 APPROVAL

## 1.1 Study Director's Statement of Compliance

The accountability of this study was with the study director(s). The study director(s) take accountability for the study having being executed as defined in the study plan.
The laboratory heads and supervisors take account for the data generated in their labs.

| Name | Date / Signature |
|---|---|
| Study Director<br>Anita Iskandar | 01-Jul-2016 |
| Lab Head Cellular Research<br>Stefan Frentzel | 01-Jul-2016 |
| Lab Head Proteomics<br>Ashraf Elamin | 01-Jul-2016 |
| Supervisor Gene Expression<br>Emmanuel Guedj | 01.Jul.2016 |
| Supervisor Tissue Research<br>Keyur Trivedi | 01-JUL-2016 |
| Statistician<br>Patrice Leroy | 01-JUL-2016 |
| Computational Scientist<br>Florian Martin | 21-JUL-2016 |
| Program Manager<br>Julia Hoeng | 7-July 2016 |

## 1.2 Quality Assurance Statement

Not Applicable. This study is a non-GLP study.

# 2 GENERAL INFORMATION

## 2.1 Names and Addresses

| | |
|---|---|
| **Sponsor** | Manuel C. Peitsch<br>Philip Morris Products S. A.<br>Research & Development Philip Morris International (PMI)<br>Quai Jeanrenaud 5<br>2000 Neuchatel<br>Switzerland |
| **Test Facility** | Philip Morris Products S. A.<br>Research & Development<br>PMI Product Testing<br>Quai Jeanrenaud 5<br>2000 Neuchâtel<br>Switzerland |
| **Former Study Director(s)** | - Experiment 1 (Repetition Phase (RP) also referred to as Main Phase 2): Maciej Cabanski<br>- Experiment 2 (also referred to as Main Phase 3): Maciej Cabanski<br>- Experiment 3 (also referred to as Main Phase 4): Carole Mathis<br>- Experiment 4 (also referred to as Main Phase 5): Carole Mathis<br>- Experiment 5 (also referred to as Main Phase 6): Carole Mathis<br>- Dose Range Assessment (also referred to as DRA): Carole Mathis |
| **Former Study Director Deputy(s)** | - Experiment 1 (Repetition Phase (RP) also referred to as Main Phase 2): Carole Mathis<br>- Experiment 2 (also referred to as Main Phase 3): Carole Mathis<br>- Experiment 3 (also referred to as Main Phase 4): Anita Iskandar<br>- Experiment 4 (also referred to as Main Phase 5): Anita Iskandar<br>- Experiment 5 (also referred to as Main Phase 6): Anita Iskandar<br>- Dose Range Assessment (also referred to as DRA): Carole Mathis |

| | |
|---|---|
| **Other Scientists/Technicians Involved in the Study (in an alphabetical order)** | Martin Almstetter, Camille Basile, Karine Baumer, Abdelkader Benyagoub, Flavia Buchler, Maica Corciulo, Remi Dulize, Philippe Alexandre Guy, Lola Hamied, Stephanie Johne, Samuel Kleinhans, Diana Kuehn, Shoaib Majeed, Maude Mayer, Celine Merg, Fabio Talamo, Laura Ortega Torres, Dariusz Peric, Sophie Scheuner, Alain Sewer, Gregory Vuillaume, Yang Xiang, Filippo Zanetti. |

## 2.2 Study Schedule

| | |
|---|---|
| **Experimental starting date:** | 22.11.2013 |
| **Experimental completion date:** | 12.08.2015 |

## 2.3 Test Guidelines

- Health Canada Intense Smoking Regimen, Official Method T-115, Determination of "Tar", Nicotine and Carbon Monoxide in Mainstream Tobacco Smoke, December 31, 1999 (Adapted to meet the special conditions for the Vitrocell® 24/48 exposure system).
- International Organization for Standardization: International Standard ISO 3402, Tobacco and tobacco products – Atmosphere for conditioning and testing, 4th ed., 1999.

## 3 STUDY PLAN DEVIATIONS

During the execution of study S172000, deviations from the Study Plan 1722_Organotypic_Nasal_SP are outlined below (Table 1).

**Table 1. Study Plan Deviations**

| Number | Description | Justification of impact on study data and integrity |
|---|---|---|
| **1** | **Concerning the Test System.**<br>Deviating from the study plan 1722_Organotypic_Nasal_SP (section 4.3)—in which nasal epithelial MucilAir™ cultures (mono-culture, no fibroblast, from Epithelix Sàrl, Geneva, Switzerland) were delivered on 22-Nov-2013 (for a study referred to as Main Phase 1 in the calendar week of (CW) 48, 2013)—, more shipments of culture batches of nasal epithelial MucilAir™ were organized. The reason for this change was to conduct a series of experimental repetitions, thus reducing the chance that the observed effect was a coincidence that was caused merely by experimental variability (e.g., time of the experiment, culture batch, and technicians). Additional shipments were organized for the additional experimental repetitions:<br>- Experiment 1 (Repetition Phase (RP) also referred to as Main Phase 2), for which the cultures were delivered on 07-Apr-2014.<br>- Experiment 2 (also referred to as Main Phase 3), for which the cultures were delivered on 23-Jun-2014.<br>- Experiment 3 (also referred to as Main Phase 4), for which the cultures were delivered on 23-Mar-2015.<br>- Experiment 4 (also referred to as Main Phase 5), for which the cultures were delivered on 20-Apr-2015.<br>- Experiment 5 (also referred to as Main Phase 6), for which the cultures were delivered on 15-Apr-2015.<br>- Dose Range Assessment (also referred to as DRA, or at times referred to Dose Range Finding (DRF)), for which the cultures were delivered on 24-Apr-2015. This Dose Range Assessment (DRA) phase was conducted to determine the biological impact of a broader range of THS2.2 concentrations/dilutions on nasal cultures. The reason for this change is to assess the impact of a higher dose of the test item THS2.2 aerosol to evaluate the likelihood and severity of adverse cytotoxic effects related to the test aerosol exposure.<br><br>Moreover, deviating from the study plan 1722_Organotypic_Nasal_SP (section 4.2.1)—in which a specific donor was specified to be delivered on 22-Nov-2013 (for a study referred to as Main Phase 1 on CW48 2013)—, for the additional experimental repetitions, the nasal cultures were reconstituted from a different donor as those. The reason for the change was because the quality of the first batch of tissue inserts delivered on 22-Nov-2013 was not optimal (the cultures did not pass quality controls) and that the epithelial cells from this donor were limited, thus could not be used to reconsititute additional cultures, as confirmed by the supplier Epithelix Sàrl (recorded in an Email Correspondence Regarding the Batch Issue). | The additional experimental repetitions were planned to increase the number of samples and to repeat the experiments. The data obtained in Main Phase 1, where the cultures did not pass quality control, were not considered. Therefore, it was considered that these deviations would not have a negative impact on the data integrity. |
| **2** | **Concerning the Test Item: Product Description.**<br>Deviating from the study plan (section 4.1.1)—in whicht the test item was referred to as a modified risk tobacco product (MRTP), ZRH_4.2 (also known as Zurich)—, in the additional experimental repetition, the test item were also referred to as THS2.2. The reason for the change is to be consistent with the naming convention across various studies. | The alias of the test item name was provided to align the naming convention across various studies. The batch certificates were |

Table continues

| | | |
|---|---|---|
| | **Concerning the Test Item: Batch Number.**<br>Deviating from the study plan 1722_Organotypic_Nasal_SP (section 4.1.1)—in which the batch of the test item is B-05879—, the batches of the test items used in the series of experimental repetitions were different. New batches were used accordingly (e.g. when certain batches passed the expiration dates). The certificate of each of the batches were recorded to ensure that the quality of the items were consistent across the different batches. | used to ensure the comparable quality of the test items used during the experimental repetitions. Therefore, it was considered that these deviations would not have a negative impact on the data integrity. |
| **3** | **Concerning the Experimental Design: Doses of the Reference and Test Items.**<br>Deviating from the study plan1722_Organotypic_Nasal_SP (section 4.1.4.2)—in in which the doses of the reference and test items applied in the Dilution/Distribution Module of the the Vitrocell® 24/48 exposure system were expressed at the levels of the smoke or aerosol concentrations (%)—, for the data analysis, the doses of the reference and test items were also expressed at the levels of the nicotine concentrations (mg nicotine/L smoke or mg nicotine/L aerosol). To achieve the same nicotine concentration, the percentage of the reference smoke applied in the Dilution/Distribution Module was not identical to that of the test aerosol. Therefore, to allow a better assessment when comparing the biological impact of the reference smoke and test aerosol on the nasal cultures, the nicotine concentrations (mg nicotine/L smoke or mg nicotine/L aerosol) were used to express the doses being tested. The nicotine concentrations in the smoke or aerosol were determined based on the trapping experiments using EXtrelut® columns (described in the study plan section 4.1.4.1.c Nicotine determination).<br><br>Deviating from the study plan 1722_Organotypic_Nasal_SP (section 4.1.4.2)—in which two doses of THS2.2 were tested—for the additional experimental repetitions where the impact of THS2.2 aerosol was compared with that of 3R4F smoke, an additional dose of THS2.2 (at a higher concentration of nicotine) were tested. The additional dose was included to better assess a dose-response effects upon THS2.2 exposure.<br><br>Moreover, the Dose Range Assessment (DRA) phase was conducted to determine the biological impact of a broader range of THS2.2 concentrations/dilutions on nasal cultures.<br><br>**Concerning the Experimental Design: Number of Exposure Runs per Experimental Repetition**<br>Deviating from the study plan 1722_Organotypic_Nasal_SP (Section 4.3)—in which the metadatasheet and exposure plan were applicable for the Main Phase 1 only (conducted in the CW 48, 2013)—, for the additional experimental repetitions, the metadatasheets and exposure plans were documented in a dedicated study folder: Folder of 00_S172200_Study_Documents.<br><br>Deviating from the study plan 1722_Organotypic_Nasal_SP (section 4.3)—in which only one exposure run were conducted using three replicates of culture inserts—, in each of the additional experimental repetitions, the number of the exposure runs was increased to three runs (with one replicate for each of the endpoints and/or post-exposure time points, per exposure run). The reason for this change was to increase the robustness of the observed effect across the different exposure runs. The decision was taken | The change regarding the expression of the doses applied, and regarding the additional concentration of THS2.2 that were tested did not change the objectives of the study. The change regarding the exposure procedures (increasing the number of exposure runs) was aimed at reducing the chance that the observed effects were due to chance. Therefore, it was considered that these deviations would not have a negative impact on the data integrity. |

Table continues

| | | |
|---|---|---|
| | because it was considered that the variability of the exposure runs would be greater than the variability of the cultures (one culture insert to another). | |
| **4** | **Concerning Reagents: Negative Controls.**<br>Deviating from the study plan 1722_Organotypic_Nasal_SP (section 4.1.2)—in which in which PBS-treated controls were used as negative controls for adenylate kinase (AK) assay—, for the additional experimental repetitions, untreated cultures were used as the negative controls for the AK assay. The reason for this change is to have an appropriate negative control to compare with the positive control (i.e. Triton X-100-treated cultures). The treatment of Triton X-100 to the cultures was done by adding the solution directly to the culture media (without any vehicle matrix); therefore, it was considered that untreated cultures would be more appropriate as compared with PBS-treated cultures. Moreover, the data supported that the AK levels between PBS-treated cultures and untreated cultures were comparable.<br><br>Deviating from the study plan 1722_Organotypic_Nasal_SP (section 4.1.2)—in which a negative control for multi analytes profiling (MAP) for pro-inflammatory marker release measurement (Luminex-based measurement of mediators) was not specified—, for the additional experiment repetitions, PBS-treated cultures were used as the negative controls for the MAP assay. The reason for this change was to have an appropriate negative control for the MAP assay to compare with the positive controls (i.e. Tumor necrosis alpha (TNFA) and interleukin (IL) 1 beta mixture (each at 10 ng/mL PBS) added to the basolateral media of the cultures).<br><br>**Concerning Reagents: AK Cytotoxicity Assay Kits.**<br>Deviating from the study plan 1722_Organotypic_Nasal_SP (section 4.4.5)—in which a Bioluminescence Cytotoxicity Assay (BioVision Inc.) kit was specified—, in the additional experimental repetitions, another kit (i.e. ToxLight™ Bioassay Kit from Lonza) was also used to measure cytotoxicity levels following exposure. The use of the specific kits for a given experimental repetition were recorded in the lab notebook. The reason for this change was to have alternatives for the assessment of cytotoxicity (e.g. in case of reagent failure from a particular lot). | The changes regarding the reagents used for negative controls were done to have more appropriate controls (more compatible to be compared to their positive controls). Moreover, although two different kits were used for the AK assay, only one specific brand of the kit were used within a particular experimental repetition, and the cytotoxicity levels were always normalized to their positive and negative controls within the specific experimental repetition. Therefore, it was considered that these deviations would not have a negative impact on the data integrity. |
| **5** | **Concerning Endpoint and Procedure: Trans-Epithelial Electrical Resistance (TEER).**<br>Deviating from the study plan 1722_Organotypic_Nasal_SP (section 4.3, Table 5, and section 4.4.4)—in which TEER values were considered as an endpoint to assess the exposure impact—, for the experimental repetitions, the results of the TEER assays was only considered as a quality control check. The quality control check based on the TEER values refers to the TEER measurements that were done from randomly chosen inserts on the day of nasal cultures delivery. These TEER values were considered as a confirmationto the information provided by the supplier in the Certificate of Analysis for each of the batch delivered. The reason for this change was because TEER did not provide a robust readout as an endpoint (not sufficiently sensitive to infer the impact of exposure).<br><br>**Concerning Endpoint and Procedures: Pro-inflammatory Markers Release (Multi Analyte Profiling, MAP) Assay.**<br>Deviating from the study plan 1722_Organotypic_Nasal_SP (section 4.3, Table 5, and section 4.4.7)—in which particular kits of the MAP assay were | The changes regarding the specific endpoints and/or collection time points were done to prevent unreliable reading that might come from i) inaccurate measurements/readings, or ii) preliminary observations as the methods have not been optimized. Therefore, it was considered that these deviations would not have a negative impact on the data integrity. |

Table continues

| | | |
|---|---|---|
| | specified—, for the additional experimental repetitions, different MAP kits (panels) were used. The specific panels used in a given experimental repetition were recorded in the lab notebook. The reason for this change was to prioritize the list of analytes to be measured, i.e. only for the analytes which concentrations (in the basolaterl media) fell above the limit of detection were prioritized.<br><br>Moreover, deviating from the study plan 1722_Organotypic_Nasal_SP (section 4.3, Table 5)—in which the measurement of pro-inflammatory markers (MAP assay) was done using basolateral medium samples collected at 4, 24, 48, and 72 h post-exposure time points—, for the additional experimental repetitions, the measurement of pro-inflammatory markers were done using the basolateral media collected at 24, 48, and 72 h post-exposure only (excluding the samples collected at 4 h post-exposure). The reason for this change was because the concentration of the analytes in at the samples collected at 4 h post-exposure was considerably lower than those collected at the later time points.<br><br>**Concerning Endpoint and Procedure: Cytochrome P450 (CYP) Assay.**<br>Deviating from the study plan 1722_Organotypic_Nasal_SP (section 4.3, Table 5, and section 4.4.10)—in which the activity of CYP1A1 and CYP1B1 (combined) were measured in the cultures at 4, 24, 48, and 72 h post-exposure—, for the additional experimental repetitions, the combined CYP1A1 and CYP1B1 activity were measured at 24, 48, and 72 h post-exposure time points (excluding the 4 h post-exposure time point). The reason for this change was because the luciferase substrate (Luciferin-CEE) would need to be added to the basolateral media of the cultures at least for 24 h (starting from the time when the exposure experiment was completed), making the measurement at 4 h post-exposure not feasible.<br><br>Additionally, deviating from the study plan 1722_Organotypic_Nasal_SP (section 4.4.10)—in which the protein levels of CYP1A1 and CYP1B1 were considered as an endpoint to assess the impact of exposure—, for the additional experimental repetitions, the measurement of CYP1A1 and CYP1B1 protein levels were only done as a method development. The protocol to measure CYP1A1 and CYP1B1 protein levels in nasal organotypic cultures has not been established. Thus, the results were only considered preliminary.<br><br>**Concerning Endpoint and Procedure: TPM (Total Particulate Matter).**<br>Deviating from the study plan 1722_Organotypic_Nasal_SP (section 4.4.11)—in which the deposition of particles on a microbalance was planned to be conducted during the 28-minute exposure—, for the additional experimental repetitions, the microbalance measurement (for particle deposition) were only considered as an exploratory endpoint. The reason for this change was because of the high content of liquid droplets in the test item THS2.2 aerosol. Therefore, the microbalance measurement could not reflect an accurate reading regarding the total particle deposition during the exposure. | |
| **6** | **Concerning Study Timelines.**<br>Deviating from the study plan 1722_Organotypic_Nasal_SP (section 6.1)—in which the timeline of the study would be finished in 03-Mar-2014—, the completion of the study would be delayed because of the additional experimental repetitions that were conducted. | The additional experimental repetitions were planned to to repeat the experiments and to increase the number of |

Table continues

| | | |
|---|---|---|
| | | samples. Therefore, it was considered that these deviations would not have a negative impact on the data integrity. |
| 7 | **Concerning New Assays.**<br>Deviating from the study plan 1722_Organotypic_Nasal_SP section (6.1)—in experiment 5 (a.k.a Main Phase 6) and experiment 6 (a.k.a. Main Phase 7), new assays including proteomics analysis, mucociliary clearance, and enzyme-linked lectin assay, were conducted. However, they are performed as method development; and thus, the results considrered as preliminary data and not included in this present report. | The additional assays were performed as part of a new method development and not included in this report. Therefore, it was considered that these deviations would not have a negative impact on the data integrity. |

## 4 ABSTRACT / EXECUTIVE SUMMARY

The nose is the main entry point to the respiratory system. Cells in the nasal cavity are one of the first targets for inhaled toxic insults such as cigarette smoke (CS). Exposure to CS is associated with nasal inflammation; thus the nasal epithelium is relevant for evaluating the pathophysiological impact of CS. The recently developed human three-dimensional (3D) organotypic nasal culture models offer a better recapitulation of the *in vivo* nasal epithelium. These models exhibit a pseudostratified epithelium with polarity and tight junctions. This current study aimed to assess the biological impact of exposure to smoke generated from a conventional reference cigarette 3R4F and aerosol generated from a candidate modified risk tobacco product (MRTP), the Tobacco Heating System (THS) 2.2 using a human organotypic nasal culture MucilAir™ model.

The human 3D nasal epithelial cultures were exposed to 3R4F smoke and THS2.2 aerosol for 28 minutes at the air-liquid interface. A series of experimental repetitions was conducted to obtain reproducible measurements throughout approximately a one year period. For the exposure experiment, the nasal cultures were exposed to different concentrations 3R4F smoke and THS2.2 aerosols. A low concentration of 3R4F smoke was applied and matched with a low concentration of THS2.2 aerosol (at a target nicotine concentration of 0.15 mg nicotine/L 3R4F smoke or 0.15 mg nicotine/L THS2.2 aerosol, respectively). A high concentration of 3R4F smoke was matched with a medium concentration of THS2.2 (at a target nicotine concentration of 0.25 mg nicotine/L 3R4F smoke or 0.27 mg nicotine/L THS2.2 aerosol, respectively). Additionally, a higher concentration of THS2.2 was applied at a target nicotine concentration of 0.44 mg nicotine/L THS2.2 aerosol). Various endpoints were assessed at different time points after exposure (i.e., histological examination, cytotoxicity, activity of cytochrome P450 (CYP) 1A1/1B1, and expression profiles of mRNAs and microRNAs). Systems toxicological approaches leveraging gene expression data and biological network models were used to investigate the biological impact of the exposure. Moreover, a dose-range assessment of THS2.2 aerosol was conducted to evaluate the likelihood and severity of adverse cytotoxic effects related to an exposure to broader concentrations of THS2.2 aerosol.

The results showed that the impact of 3R4F smoke exposure on the various endpoints was more pronounced than that of THS2.2 aerosol at all tested concentrations. At the equivalent nicotine concentrations of 3R4F smoke and THS2.2 aerosol, greater cytotoxicity levels were observed upon 3R4F smoke exposure than those upon THS2.2 aerosol exposure. The histological evaluation of the nasal cultures showed epithelium thinning following 3R4F smoke at a nicotine concentration of 0.25 mg/L smoke. Following THS2.2 aerosol, thinning of the epithelium was only observed when the aerosol was applied at the nicotine concentrations above 1 mg nicotine/L THS2.2 aerosol. Greater concentrations of secreted inflammatory mediators were found in the basolateral media following the exposure to 3R4F smoke, as compared with those following THS2.2 aerosols when they were applied at the comparable nicotine concentrations. Possible toxicity-related mechanisms associated with the exposure—which were investigated using a network-approach based on gene expression data—revealed greater perturbations of various biological networks in the 3R4F-exposed cultures than in the THS2.2-exposed cultures when assessed at the comparable nicotine concentrations. Greater alterations in the miRNA expression levels were found in cultures-exposed to 3R4F smoke than those exposed to THS2.2 aerosol. The overall results supports that 3R4F smoke exposure had greater biological impact on the nasal cultures as compared with THS2.2 aerosol exposure when assessed at the comparable nicotine concentrations.

## 5 INTRODUCTION

The nose is the main entry point to the human respiratory system. Cells in the nasal cavity are one of the first targets for pathogens, allergens, and inhaled toxic insults. The nasal epithelial cells can initiate and regulate respiratory immune responses by releasing soluble mediators and expressing ligands/receptors on their surface (Figure 1). Therefore, toxicant-induced nasal injury can lead to the increased risk of infection and susceptibility to diseases of the lower respiratory tract (Harkema 2006). Exposure to cigarette smoke (CS) has been implicated in the etiology of several nasal disorders, including inflammation, acute and chronic rhinitis, and sinonasal cancer (Harvey 2007, Huvenne 2010, Lee 2013). CS can cause irritation influencing the local inflammatory and physiological processes in the upper airway epithelial tissues, such as cytokine release and transport mechanisms (Huvenne 2010), as well as proliferation, differentiation, and apoptosis (Lee 2013). Toxic reactive oxygen species (ROS) in CS cause not only inflammation, but also oxidative stress in the epithelial cells lining the airway (Goldkorn 2014). Nasal and sinus inflammation are commonly found in smokers and individuals with chronic obstructive pulmonary disease (COPD) (Kim 2007, Lieu 2000). Because the nasal epithelial cells also function as an essential protective and immunological barrier, diseases in the nasal cavity (e.g. nasal inflammation, rhinitis, and sinonasal cancer) have also been associated with impaired epithelial barrier function (Benninger 1999, Jaspers 2014, Nelson 2004, Schamberger 2013, Soyka 2012).

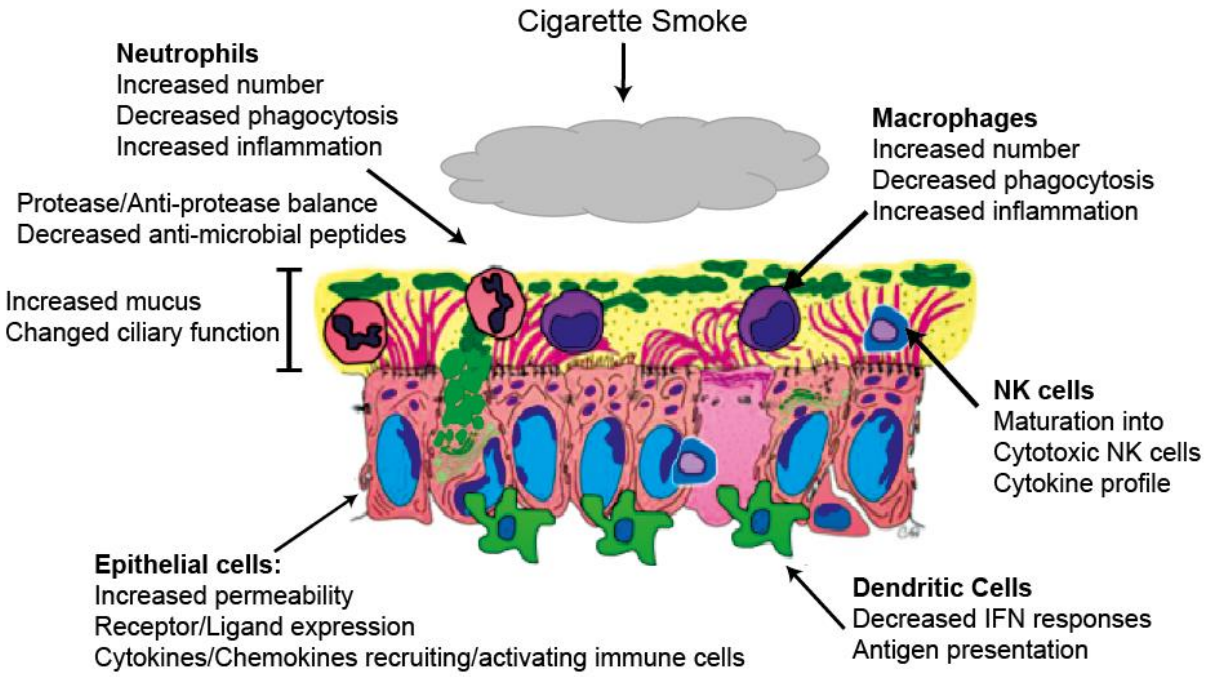



**Figure 1. Cigarette smoke-induced changes in mucosal immune responses.**

Adapted from (Jaspers 2014).

Moreover, the mucociliary apparatus is an initial defense mechanism clearing the nasal passages of inhaled toxicants, including pathogens, particulate matter, and other substances (Harkema 2006). Perturbations of either component of mucociliary clearance leads to chronic sinus disease, cough, and

increased risk of pathogenic infection (Moller 2006). Normal mucociliary clearance is dependent upon proper ciliary beating frequency (CBF) and the composition and viscosity of the airway surface liquid, which is regulated by active transport of ions (Virgin 2010). CBF has been shown to reflect the capacity of mucociliary clearance and can contribute to retention of secretions, cough, and potential airway infection in these patients (Jorissen 2013, Kern 2013, Yaghi 2012). CS has been associated with alterations of mucociliary clearance (Bascom 1995). Using nasal cilia samples obtained from brushings of male and female COPD patients, Yaghi et al. investigated the relation of disease severity to changes in ciliary function and the effect of pharmacologic agents on CBF (Yaghi 2012).

Evaluating the response of lower airway (bronchial) epithelium to inhaled toxicants is valuable; however, the effort is hampered by lack of accessible and relevant tissue samples. To facilitate these type of studies, finding suitable surrogate tissues have become an attractive strategy (McDougall 2008). The upper airway tissues (e.g. buccal and nasal) mucosa, which can be collected more easily than those of the lower airway, have been used to predict the responses of lower airway epithelial tissues to inhaled pathogens, irritants, and particulate matter (Sridhar 2008). Similar changes of the gene expression induced by CS in the field of injury—oral, bronchial, and nasal epithelia—have been reported; their altered patterns of gene expression of the upper airway tissue resemble those of the lower airway (Sridhar 2008). Moreover, the variety of inflammatory mediators released by nasal airway epithelial cells, such as interleukin (IL)-6, regulated on activation normal T-cell expressed and secreted (RANTES), vascular endothelial growth factor (VEGF), monocyte chemoattractant protein (MCP-1), matrix metalloproteinase (MMP)-9, and TIMP was similar to that released by bronchial airway epithelial tissues under normal conditions or under cytokine stimulation (IL-1β and TNF-α) (McDougall 2008). The expression of cell surface receptors (e.g. CD44, intracellular adhesion molecule (ICAM)-1, and αVβ5 integrins) was similar between the tissues (McDougall 2008). These receptors function in diverse processes such as the response to lung injury, antigen presentation and mobilization of leukocytes to inflammatory sites, and cellular signaling (McDougall 2008).

These similarities between the easily collected buccal or nasal epithelium and the less accessible respiratory tissues (such as the bronchial epithelium) could be utilized to develop potential non-invasive biomarkers of CS exposure. Such biomarkers could be useful for risk assessment approaches, diagnosis, treatment, and prevention of smoking-induced lung diseases. The biomarkers could be used for screening of individual susceptibility to CS-induced lung disease and identifying high-risk smokers who might benefit from chemoprophylaxis (Sridhar 2008). Therefore, studying the impact of smoke and inhaled aerosols using *in vitro* nasal models will lead to a better understanding of how the upper respiratory tissue responds following smoking and other inhaled aerosols.

Traditionally, most *in vitro* cell cultures are grown as monocultures in two-dimensional (2D) environments. They are grown on flat dishes made of synthetic plastic to which the cells adhere and spread by forming unnatural attachments to the culture surface (Werner 1996, Yoo 2003). These adherent cells adapt to the new microenvironment through alterations at the genetic, transcriptional, and protein levels. Immortalized cell lines have often been used as the *in vitro* models to study the respiratory tract because they are easy to handle; however, they are often unable to differentiate into heterogeneous cell populations (i.e., unable to form polarized, ciliated, and mucus-producing cells) that resemble the *in vivo* tissue. As an alternative to better mimic the *in vivo* characteristics of the respiratory epithelium, primary human cells of nasal epithelium can be cultured as a monolayer model

of a partially differentiated nasal epithelium. Because they originate from primary cells, they mimic many of the *in vivo* features of nasal epithelium. Nonetheless, these monolayer cultures cannot resemble the structural organization and functionality of the *in vivo* tissue. They remain as 2D culture models that are maintained under liquid media. Therefore, physiologically, they are less relevant for an exposure study of inhaled toxicants.

To address these gaps, organotypic three dimensional (3D) culture models have been developed. These 3D culture models are grown at the air-liquid interface (ALI). The airway epithelial cells grown at ALI can differentiate in a time-dependent manner while grown on a collagen-type membrane (Dimova 2005). These models are composed of polarized, differentiated cells resembling a pseudostratified pattern that closely mimics the *in vivo* epithelial morphology (i.e., all cells are in contact with the basement membrane but only some reach the luminal surface), and exhibit ciliated cells (Kim 2008). They manifest barrier functionality by expressing tight junctions, allowing the epithelial cells to adhere to each other while maintaining their polarity. The tight junctions between the polarized cells prevent lateral diffusion, maintain the extracellular osmotic balance, and ensure functional transcellular transport. Therefore, these tissue models exhibit two distinct compartments: apical (the air-directed side *in vitro*) and basolateral (the medium-directed side *in vitro*). The apical side of the tissue mimics the characteristics of the *in vivo* mucociliary surface covered by a physiological mucus layer. Therefore, the 3D culture models exhibit morphological and functional properties that more closely resemble the *in vivo* airway morphology as compared with submerged cultures (Dimova 2005). Such systems are more physiologically relevant for studing the exposure impact via inhalation (Dimova 2005, Werner 1996).

Potentially, the 3D airway epithelial models can be used to analyze smoking-related responses linked to disease mechanisms, such as inflammation, and tissue remodeling and repair. The system provides a more relevant physiological environment, allowing a better assessment approach for studying the impat of complex aerosol exposure (such as CS). Studies have reported that the differential gene expression of the organotypic culture models in response to CS can be assigned to functional categories and mapped to signaling pathways related to xenobiotic metabolism, the oxidant/antioxidant balance, and DNA damage and repair (Mathis 2015, Maunders 2007). Using network-based analysis, we have further evaluated the perturbation of xenobiotic metabolism, oxidative stress, cell proliferation, apoptosis, senescence, DNA damage response, and epithelial barrier defense in response to CS exposure using human organotypic nasal and bronchial cultures (Iskandar 2013, Iskandar 2015, Talikka 2014). Collectively, these studies indicate that human organotypic nasal culture is a relevant in *vitro* model for assessing new products using a systems toxicology approach.

## 6 OBJECTIVE

The objectives of the study were:
To determine the biological impact of THS2.2 aerosol exposure on a human organotypic 3D nasal culture model, as compared with that of 3R4F smoke. The biological impact assessment was done by combining results obtained from analyses using well-known cellular and functional assays, and using systems biology approaches (leveraging mRNA and miRNA profile, as well as computational biology analyses).

The biological impact of THS2.2 aerosol and 3R4F smoke exposure on the test system human 3D nasal cultures were explored in terms of:

- Dose-dependent responses of the test system after exposure
- Time-dependent responses of the test system after exposure (whether the impact transient or sustained over the post-exposure time)
- The possible biological pathway/processes perturbed in the test system after exposure

Moreover, the dose-range assessment of a broader concentrations of THS2.2 aerosol exposure was done to assess the concentration of THS2.2 aerosol at which overt cytotoxicity and morphological alterations of the human 3D nasal cultures were observed.

This is an exploratory study. All the above objectives were exploratory.

# 7 EXPERIMENTAL DESIGN

## 7.1 Test and Reference Items

### 7.1.1 Identification and Description

THS2.2 and 3R4F were designated as the test and reference items, respectively (Table 2).

**Table 2. Test and Reference Items**

| Short Name | Description | Type |
|---|---|---|
| **THS2.2** | ZRH/DDA1/C3/CAST LEAF– CL/Flavor/Reynaldo | Test |
| **3R4F** | Conventional reference cigarette | Reference |

Information on the test item characteristics including composition, stability, and homogeneity was provided by the sponsor. The 3R4F reference cigarette was purchased from the University of Kentucky (Kentucky Tobacco Research & Development Center). The specifications of the test and reference items used in this study are described in Table 3.

## Table 3. Reference and Test Items Used in Experimental Repetitions

| | Experimental Phase | | | | | |
|---|---|---|---|---|---|---|
| | Experiment 1 | Experiment 2 | Experiment 3 | Experiment 4 | Experiment 5 | Dose Range Assessment |
| | 07-Apr-2014 | 23-Jun-2014 | 23-Mar-2015 | 20-Apr-2015 | 15-Jun-2015 | 27-Apr-2015 |
| **Reference Item (3R4F)** | | | | | | |
| **Stick Information on 3R4F** | | | | | | |
| ***Pack No*** | V347Y61B5 | V347Y61B5 | V350Y61B5 | V350Y61B5 | V350Y61B5 | NA |
| ***Receiving Date*** | Jul-2012 | Jul-2012 | Dec-2014 | Dec-2014 | Dec-2014 | NA |
| ***Expiry Date*** | Dec-2014 | Dec-2014 | May-2017 | May-2017 | May-2017 | NA |
| **Test Item (THS2.2)** | | | | | | |
| **Stick Information on THS2.2** | | | | | | |
| ***Batch No*** | THS2.2 Batch B-08163 | THS2.2 Batch B-11433 | THS2.2 Batch B-13055 | THS2.2 Batch B-13055 | THS2.2 Batch B-13055 | THS2.2 Batch B-13055 |
| ***Receiving Date*** | Nov-2013 | Oct-2014 | Dec-2014 | Dec-2014 | Dec-2014 | Dec-2014 |
| ***Expiry Date*** | 10-Oct-2014 | 26-Mar-2015* | 24-Jun-2015 | 24-Jun-2015 | 24-Jun-2015 | 24-Jun-2015 |
| **Device Information on THS2.2** | | | | | | |
| ***Product Code*** | Device THS2.2 B-06050 | Device THS2.2 B-06050 | Device THS2.2 No. B-18731 | Device THS2.2 No. B-18731 | Device THS2.2 No. B-18731 | Device THS2.2 No. B-18731 |
| ***Receiving Date*** | 04-Sep-2013 | 04-Sep-2013 | 27-Feb-2015 | 27-Feb-2015 | 27-Feb-2015 | 27-Feb-2015 |
| ***Specific Description*** | Aerosol generation | | | | | |
| ***Batch Description*** | DC.000067.RD (1)/ZRH/FPD4.2/3.2.2/C28/FDP 4.2 Cigarette Holder/3.2.2 software upgrade/Configuration without forced-cleaning feature. Aerosol generation. | | | | | |

*Expiry date based on a quality control retest. Abbreviations: NA, not available (i.e., not tested). Information on the 3R4F reference item is provided by the supplier (Kentucky Tobacco Research & Development Center).

### 7.1.2 Item Storage

After the items were received, they were stored in a fridge at 5 ± 3°C with uncontrolled humidity conditions in their original packaging.

### 7.1.3 Item Conditioning

All test items were conditioned between 7 and 21 days under controlled conditions at a temperature of 22 ± 1ºC and a relative humidity of 60 ± 3% according to ISO guidelines.

### 7.1.4 Carbonyl Levels Deposited in the Cultivation Base Module of the Vitrocell® 24/48 Exposure System following 28 min Exposure to Reference Smoke and Test Aerosol

Figure 2 shows the concentrations of representative carbonyls deposited in the Base Module of the Vitrocell® 24/48 exposure system following exposure to the reference cigarette smoke and test item aerosols at the corresponding target nicotine concentrations used in this study (i.e., the concentration applied in the five experimental repetitions described in section Sample Generation: Experimental Repetitions). The descriptive statistics reporting the values obtained in every sampling are given in Supplementary Table 1-Supplementary Table 8.

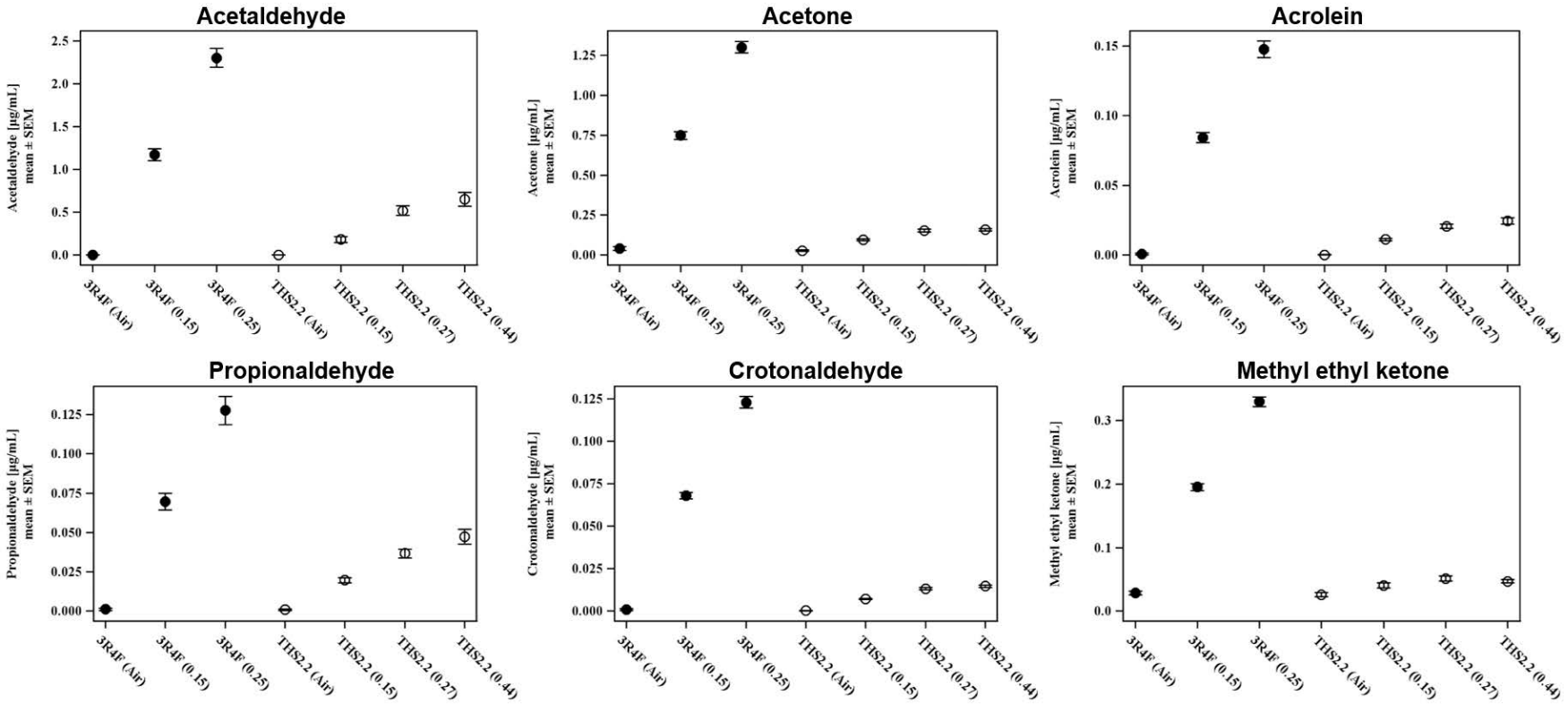



**Figure 2. Concentrations of representative carbonyls deposited in the Cultivation Base Module of Vitrocell® 24/48 exposure system following exposures to the reference cigarette smoke and test item aerosol.**

The mean of a carbonyl in PBS-filled inserts (µg/mL) ± SEM (N = 10 samplings from 2014-2015) are shown. The PBS-filled inserts were placed in the Cultivation Base Module of Vitrocell® 24/48 exposure system and exposed to 3R4F smoke and THS2.2 aerosol according to the concentrations used in this study. Representative carbonyls are shown. The descriptive statistics are given in Supplementary Table 1-Supplementary Table 8. Abbreviations: N, number of samples; SEM, standard error mean.

### 7.2 Test System

The human organotypic nasal culture model MucilAir™ (Product code EP01, Epithelix Sàrl, Geneva, Switzerland) was used as the test system in this study. The cultures were grown in a 6.5 mm Transwell® with a 0.4 µm polyester sterile membrane insert (Product No. 3470, Corning Inc.) and maintained in MucilAir™ media (Product code EP04, Epithelix Sàrl). For each culture batch used in each experimental repetition, "Certificate of Analysis" documentations were provided by the supplier. Table 4 summarizes the information provided in the certificates from the supplier.

**Table 4. Specifications of the Different Batches of Nasal Culture Used in the Experimental Repetitions**

| | Experiment 1 | Experiment 2 | Experiment 3 | Experiment 4 | Experiment 5 | Dose Range Assessment |
|---|---|---|---|---|---|---|
| **Week of Experiment** | **07-Apr-2014** | **23-Jun-2014** | **23-Mar-2015** | **20-Apr-2015** | **15-Jun-2015** | **27-Apr-2015** |
| **Culture Delivery Date** | 04-Apr-2014 | 20-Jun-2014 | 20-Mar-2015 | 17-Apr-2015 | 12-Jun-2015 | 24-Apr-2015 |
| **Supplier** | Epithelix | Epithelix | Epithelix | Epithelix | Epithelix | Epithelix |
| **Donor ID** | MD041701 | MD041701 | MD041701 | MD041701 | MD041701 | MD041701 |
| **Batch ID (Seeding Date)** | 25-Feb-2014 | 05-May-2014 | 05-Feb-2015 | 09-Mar-2015 | 28-Apr-2015 | 16-Mar-2015 |
| **Cell Type** | hAEC/Nasal | hAEC/Nasal | hAEC/Nasal | hAEC/Nasal | hAEC/Nasal | hAEC/Nasal |
| **Age of Donor (Years)** | 30 | 30 | 30 | 30 | 30 | 30 |
| **Sex of Donor** | Male | Male | Male | Male | Male | Male |
| **Origin of Donor** | Caucasian | Caucasian | Caucasian | Caucasian | Caucasian | Caucasian |
| **Smoking Status of Donor** | Non-smoker | Non-smoker | Non-smoker | Non-smoker | Non-smoker | Non-smoker |
| **Pathology Status of Donor** | None reported | None reported | None reported | None reported | None reported | None reported |
| **Sterility** | Yes | Yes | Yes | Yes | Yes | Yes |
| **Mycoplasma** | Negative | Negative | Negative | Negative | Negative | Negative |
| **TEER (Ω cm²)*** | 369 ± 9 | 401 ± 9 | 296 ± 9 | 287 ± 10 | 415 ± 13 | 355 ± 10 |
| **CBF (Hz)*** | 7.8 ± 0.1 | 7.9 ± 0.1 | 7.6 ± 0.1 | 7.3 ± 0.1 | 7.9 ± 0.1 | 7.3 ± 0.1 |
| **Morphology** | Normal | Normal | Normal | Normal | Normal | Normal |
| **Mucus** | Present | Present | Present | Present | Present | Present |
| **HIV-1 and HIV-2** | Negative | Negative | Negative | Negative | Negative | Negative |
| **Hepatitis B** | Negative | Negative | Negative | Negative | Negative | Negative |
| **Hepatitis C** | Negative | Negative | Negative | Negative | Negative | Negative |
| **Certificate of Analysis (CoA)** | CoA_Seeded_25-Feb-2014 | CoA_Seeded_05-May-2014 | CoA_Seeded_05-Feb-2015 | CoA_Seeded_09-Mar-2015 | CoA_Seeded_28-Apr-2015 | CoA_Seeded_16-Mar-2015 |

*TEER and CBF are presented as average values from 12 culture inserts ± SEM. On the day of culture arrival, TEER was measured in randomly chosen inserts as a quality control retest. Abbreviations: CBF, ciliary beating frequency; hAEC, human airway epithelial cells; ID, identification; SEM, standard error mean; TEER, transepithelial electrical resistance.

### 7.3 Sample Generation

7.3.1 Experimental Repetitions: The Impact Assessment of THS2.2 Aerosol as Compared with 3R4F Smoke Exposure

The study to assess the biological impact of THS2.2 aerosol as compared with 3R4F smoke exposure on a human 3D nasal culture models comprised of five experimental repetitions. During each of the five experimental repetitions, the cultures were exposed to the reference item 3R4F smoke or test item THS2.2 aerosol at similar nicotine concentration in the 3R4F smoke/ THS2.2 aerosol (Table 5). Smoke from the reference item (3R4F) was generated using a 30-port-carousel smoking machine (SM)-2000 (Philip Morris International, Neuchâtel, Switzerland). Aerosol from the test item (THS2.2) was generated using a modified 30-port carousel smoking machine SM-2000 THS2.2 (Philip Morris International, Neuchâtel, Switzerland). Each of the smoking machines was connected to a Vitrocell® 24/48 exposure system (Vitrocell Systems GmbH, Waldkirch, Germany), where the culture inserts were exposed.

**Table 5. Target Nicotine Concentrations in the Smoke/Aerosol (mg nicotine/L smoke or aerosol) Applied in the Study**

| | Experiment Week | | | | | |
|---|---|---|---|---|---|---|
| | **Exp 1** | **Exp 2** | **Exp 3** | **Exp 4** | **Exp 5** | |
| | **07-Apr-2014** | **23-Jun-2014** | **23-Mar-2015** | **20-Apr-2015** | **15-Jun-2015** | |
| **Group name of 3R4F-exposed Cultures** | **mg nicotine/L smoke** | **mg nicotine/L smoke** | **mg nicotine/L smoke** | **mg nicotine/L smoke** | **mg nicotine/L smoke** | **Smoking Machine** |
| **Air Control (3R4F)** | 0.00 | 0.00 | 0.00 | 0.00 | 0.00 | SM-2000 |
| **3R4F (0.15)** | 0.15 | 0.15 | 0.15 | 0.15 | 0.15 | |
| **3R4F (0.20)*** | NA | 0.20* | NA | NA | NA | |
| **3R4F (0.25)** | 0.25 | 0.25 | 0.25 | 0.25 | 0.25 | |
| **Exposure Run Number** | 3 | 3 | 3 | 3 | 3 | |
| **Group name of THS2.2-exposed Cultures** | **mg nicotine/L aerosol** | **mg nicotine/L aerosol** | **mg nicotine/L aerosol** | **mg nicotine/L aerosol** | **mg nicotine/L aerosol** | **Smoking Machine** |
| **Air Control (THS2.2)** | 0.00 | 0.00 | 0.00 | 0.00 | 0.00 | SM-2000 THS2.2** |
| **THS2.2 (0.15)** | 0.15 | 0.15 | 0.15 | 0.15 | 0.15 | |
| **THS2.2 (0.27)** | 0.27 | 0.27 | 0.27 | 0.27 | 0.27 | |
| **THS2.2 (0.44)** | NA | 0.44 | 0.44 | 0.44 | 0.44 | |
| **Exposure Run Number** | 3 | 3 | 3 | 3 | 3 | |

* The medium concentration of 3R4F (at 0.20 mg/L smoke), refered to as group "3R4F (0.20)," was tested only in one experimental repetition. Therefore, the outcomes are not included in the Results sections but reported in Supplementary Table 9, Supplementary Figure 4, and Supplementary Figure 5. ** SM-2000 THS2.2 was also referred to as SM-2000 ZRH. Abbreviations: Exp, experiment; NA, not available (not tested during the indicated experimental repetition); SM, smoking machine.

The Vitrocell® 24/48 exposure system was equipped with a dilution system, which allows mixing of the smoke/aerosol with fresh air. To achieve the desired concentrations of nicotine, the smoke/aerosol stream was mixed with different rates of dilution airflow, while passing through the Vitrocell 24/48 exposure system (refered to as the Dilution/Distribution Module). From the Dilution/Distribution Module, diluted smoke/aerosol is conducted by negative pressure into the cultivation base module, which houses the tissue culture inserts during exposure. Figure 3 illustrates the set-up of the exposure system, which consists of a Dilution/Distribution Module (the top part) and Cultivation Base Module (underneath), and the set-up of the exposure runs for 3R4F and THS2.2 applying the nicotine concentrations described in Table 5.

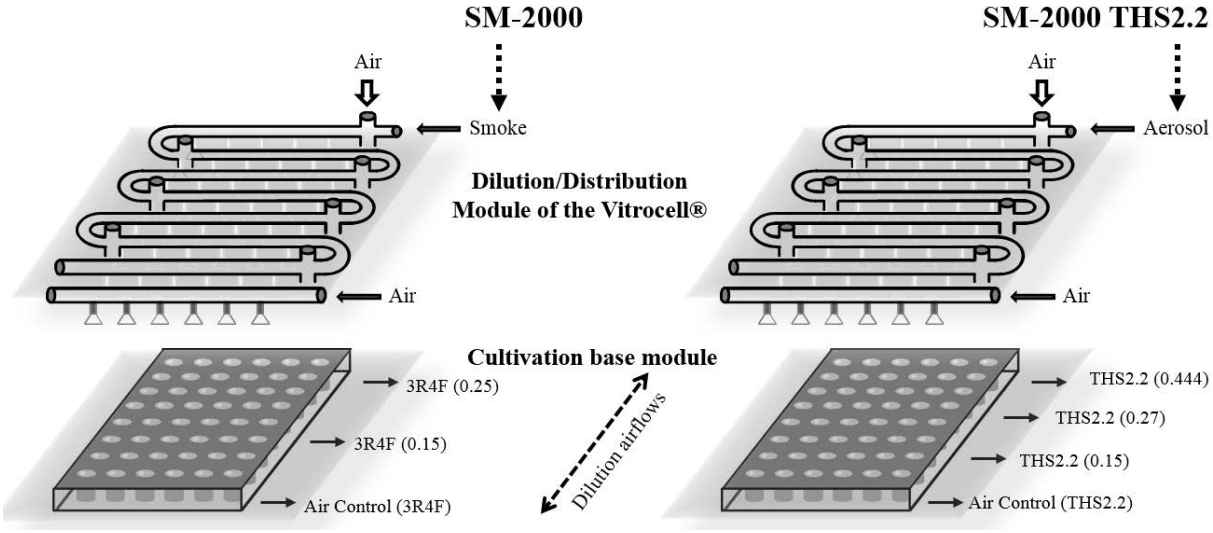



**Figure 3. Schematic representation of exposure runs for 3R4F and THS2.2.**

A Dilution/Distribution Module of the Vitrocell® 24/48 exposure system located on top of a cultivation Base Module is illustrated. Each of the Vitrocell® 24/48 exposure system was connected to a smoking machine (SM) ("SM-2000" for 3R4F smoke exposure and "SM-2000 THS2.2" for THS2.2 aerosol exposure). In the Base Module, up to 48 wells (culture inserts) can be simultaneously exposed in a single run. The delivery of the whole smoke/aerosols was achieved by delivering diluted smoke/aerosol through individual trumpets to each well. An exposure run consisted of the applied target concentration(s) paired with its air control (N =1 paired sample per run, for any given endpoint and post-exposure time point).

In each of the five experimental repetitions, various endpoints were measured at 4, 24, 48, and 72 h post-exposure, for each applied concentrations and air control (Table 6). The results reported in this document were calculated from the aggregated data obtained from experiments 1–5.

**Table 6. Post-Exposure Endpoints**

| | | Endpoint | | | | | | | | | | | | | | | | | | | |
|---|---|---|---|---|---|---|---|---|---|---|---|---|---|---|---|---|---|---|---|---|---|
| | | Cytotoxicity | | | | Gene Expression Microarray | | | | Secreted Pro-Inflammatory Mediators | | | | CYP1A1/1B1 Activity | | | | Histology and IHC | | | |
| | | Post-exposure (h) | | | | Post-exposure (h) | | | | Post-exposure (h) | | | | Post-exposure (h) | | | | Post-exposure (h) | | | |
| **Experimental Week** | | 4 | 24 | 48 | 72 | 4 | 24 | 48 | 72 | 4 | 24 | 48 | 72 | 4 | 24 | 48 | 72 | 4 | 24 | 48 | 72 |
| Exp 1 | **07-Apr-2014** | (3) | NA | (3) | (3) | (3) | NA | (3) | (3) | NA | NA | (3) | NA | NA | (3) | (3) | (3) | NA | NA | (3) | (3) |
| Exp 2 | **23-Jun-2014** | (3) | NA | (3) | (3) | (3) | NA | (3) | (3) | NA | NA | (3) | NA | NA | (3) | (3) | (3) | NA | NA | (3) | (3) |
| Exp 3 | **23-Mar-2015** | (3) | (3) | (3) | (3) | (3) | (3) | (3) | (3) | NA | (3) | (3) | (3) | NA | NA | (3) | NA | NA | NA | (3) | (3) |
| Exp 4 | **20-Apr-2015** | (3) | (3) | (3) | (3) | (3) | (3) | (3) | (3) | NA | (3) | (3) | (3) | NA | NA | (3) | NA | NA | NA | (3) | (3) |
| Exp 5 | **15-Jun-2015** | (3) | (3) | (3) | (3) | (3) | (3) | (3) | (3) | NA | (3) | (3) | (3) | NA | NA | (3) | NA | NA | NA | (3) | (3) |

Numbers in bracket indicate the total number of paired samples collected for the indicated endpoints per post-exposure time point at any given experimental repetition. One exposure run consisted of the applied target concentration(s) paired with its air control (N =1 paired sample per run, for any given endpoint and post-exposure time point). Abbreviations: CYP, cytochrome P450; Exp, experiment; h, hours; IHC, immunohistochemistry; NA, not available (i.e., endpoints were not generated/collected at the indicated experimental repetition).

### 7.3.2 Dose Range Assessment of THS2.2 Aerosol

For the dose range assessment of the test item, various dilutions of the aerosol from THS2.2 were generated using a SM-2000 THS2.2 machine (Table 7). For a given endpoint, three independent exposure runs were conducted with one replicate per run.

**Table 7. Concentrations of diluted Aerosol (%) Applied and Endpoints Assessed in the Dose Range Assessment of THS2.2**

| | Dose Range Assessment Experiment Week: 27-Apr-2015 | | | |
|---|---|---|---|---|
| **Group name of THS2.2-exposed Cultures** | **Aerosol Concentrations in the Dilution/Distribution Module of the Vitrocell® 24/48 exposure system** | **Endpoint Measured at 72 h Post-Exposure** | | **Smoking Machine** |
| | | **Cytotoxicity (N)** | **Histology (N)** | |
| **Air Control (THS2.2)** | - | (3) | (3) | SM-2000 THS2.2 |
| **THS2.2 Dilution 1** | 13% | (3) | (3) | |
| **THS2.2 Dilution 2** | 23% | (3) | (3) | |
| **THS2.2 Dilution 3** | 31% | (3) | (3) | |
| **THS2.2 Dilution 4** | 48% | (3) | (3) | |
| **THS2.2 Dilution 5** | 60% | (3) | (3) | |
| **THS2.2 Dilution 6** | 80% | (3) | (3) | |
| **THS2.2 Dilution 7** | 100% | (3) | (3) | |

Numbers in bracket indicate the total number of samples exposed for the indicated endpoints. Abbreviations: N, number of replicates; SM, smoking machine.

## 7.4 Testing Procedure

### 7.4.1 Aerosol/Smoke Generation and *in vitro* Exposure Regimens

Reference smoke was generated from 3R4F reference cigarettes (University of Kentucky, www.ca.uky.edu/refcig) using a 30-port carousel smoking machine SM-2000 (SM2000; Philip Morris, International) connected to the Vitrocell® 24/48 exposure system (Vitrocell Systems GmbH, Waldkirch, Germany). Another 30-port carousel smoking machine SM-2000 THS2.2 (also referred to as SM-2000 ZRH) was used to generate the test aerosol from the THS2.2. The 3R4F cigarettes and THS2.2 sticks were conditioned for at least 48 h and up to 21 days at 22 ± 1°C with a relative humidity of 60 ± 3% according to ISO standard 3402 (International Organization for Standardization). For the exposure experiments, each 3R4F cigarette was smoked to a standard butt length (approximately 35 mm), and each THS2.2 stick was aerosolized up to 12 puffs per stick. For a 28-min exposure experiment, ten 3R4F cigarettes were smoked and ten THS2.2 sticks were aerosolized using the dedicated smoking machines for a 55-mL puff over 2 sec, puffed twice per min with an 8-sec pump exhaust time (according to Health Canada smoking regimen).

### 7.4.2 Nicotine Determination in Whole Smoke/Aerosol

The nicotine concentration in whole smoke or test aerosol delivered to the *in vitro* exposure systems was determined routinely (during each *in vitro* exposure experiment) to ensure dosing of 3R4F smoke

and THS2.2 aerosol was standardized to have equal nicotine concentrations. For this, diluted whole 3R4F smoke or THS2.2 aerosol, was trapped at the exhaust of the Dilution/Distribution Module of the Vitrocell® 24/48 exposure system using EXtrelut® 3NT columns (Merck Millipore, Billerica, MA, USA) impregnated with 2 mL of 0.5 M $H_2SO_4$ solution (PMI_RD_WKI_001066). Whole smoke or aerosol from two sticks per item was trapped (10 puffs per stick, 5 minutes trapping duration), with each of them smoked/aerosolized by applying a modified Health Canada Intense puffing protocol of a 55-mL puff over 2 seconds, puffed twice per minute with an 8-second pump exhaust time. After trapping, EXtrelut® columns were either stored at 2–8°C for a maximum of 4 weeks or processed immediately by determining nicotine levels by gas chromatography–flame ionization detection (GC-FID) (PMI_RD_WKI_000409). Briefly, 250 µL of isoquinoline (4 mg/mL) used as an internal standard, was added to the top of the column and the trapped nicotine including the internal standard was eluted by adding 5 mL solution of 5% (v/v) triethylamine in N-butylacetate for a total of three cycles (total volume = 15 mL). This was mixed well, and 1 mL of the dilution was transferred to an amber glass vial for analysis. One µL of the eluent was injected into an Agilent 7890A gas chromatograph (Agilent Technologies, Santa Clara, CA, USA) in split mode using a split ratio of 1:20 and injector temperature of 220°C. The separation was performed at an oven temperature of 140°C in isothermal mode (runtime: 6 minutes) using a 15 m DB-5 fused silica capillary column (Agilent Technologies) with an internal diameter of 0.25 mm and 0.25 µm film thickness. Helium was used as the carrier gas, and the column flow was set to 2.25 mL/min. Peak detection, integration, and quantification of nicotine (according to an internal standard calibration curve) were performed automatically using the Agilent ChemStation software (Agilent Technologies).

### 7.4.3 Carbonyl Concentrations Deposited in the Vitocell Base Mocule Following Whole Smoke/Aerosol Exposure

Carbonyls were measured in phosphate buffered saline (PBS) following a 28-minute exposure to whole smoke or test aerosol (ten-twelve sticks per item, each of them was smoked/aerosolized by applying a modified Health Canada Intense puffing protocol of 55 mL puff over 2 seconds, twice per minute with an 8 seconds pump exhaust time) (PMI_RD_WKI_001094). Briefly, before exposure, each row in the Cultivation Base Module of the Vitrocell® 24/48 exposure system was filled with 18.5 mL PBS. Following exposure, an aliquot of 1.2 mL PBS-exposed sample (per row) was collected and mixed with 1.8 mL 2,4-dinitrophenylhydrazine solution (15 mM). Subsequently, 150 µL pyridine was added to quench the chemical derivatization. From this mixture, a 500 µL aliquot was taken and placed into a liquid chromatography–mass spectrometry (LC-MS) amber glass vial. After 30 min, 485 µL acetonitrile and 15 µL internal standard mixture (24 µg/mL acetone-d6 and 21 µg/mL methyl ethyl ketone-d5) were added to the mixture. Finally, 5 µL of the mixture was injected into a high-performance liquid chromatography (HPLC) instrument coupled with a tandem MS (HPLC-MS/MS) to determine the quantity of various carbonyls using an isotope dilution technique.

### 7.4.4 Maintenance of Nasal MucilAir™ 3D-organotypic Cultures (Air-Liquid Interface Cultures)

Upon arrival, human nasal MucilAir™ (Epithelix Sàrl, Geneva, Switzerland) cultures were placed into fresh culture medium (PMI_RD_WKI_001065). For this, 24-well culture plates containing 0.7 mL/well MucilAir™ culture medium (Epithelix Sàrl) were prepared and pre-warmed to 37°C before the MucilAir™ were transferred from the shipping plates to the fresh plates using sterile tweezers. For all *in vitro* exposure studies, MucilAir™ grown in 6.5-mm Transwell® inserts (Corning Incorporated,

Tewksbury, MA, USA) were used, in order to match the dimensions of the Vitrocell® 24/48 exposure system (Vitrocell GmbH, Waldkirch, Germany). MucilAir™ were maintained at 37°C (5% $CO_2$, 90% humidity) with medium changes every 2 days according to the supplier's instructions. Throughout the studies, the cultures were regularly inspected microscopically to check for potential morphological changes as well as for bacterial or fungal contamination.

### 7.4.5 Apical Wash of MucilAir™ 3D-organotypic Culture (Air-Liquid Interface Cultures)

Three days before exposure, the apical side of MucilAir™ (Epithelix Sàrl) inserts were washed gently by dropwise addition of 200 µL culture medium, which was pre-warmed to 37°C (PMI_RD_WKI_001087). No more than 12 culture inserts received medium at a time for the apical wash, to avoid prolong stress to the cultures. The medium was aspirated carefully using Pasteur pipette connected to a vacuum pump. Subsequently, the cultures were placed back in to the incubator. This apical wash was performed to remove accumulated mucus and to minimize the risk of a high mucus load on the apical side of the cultures interfering with the subsequent test exposure.

### 7.4.6 Adenylate Kinase (AK) Cytotoxicity Assay

AK activity was measured from the basolateral medium of cultures, using a Bioluminescence Cytotoxicity Assay Kit (BioVision Inc., Milpitas, CA, USA) (PMI_RD_WKI_001048). Briefly, 50 µL of basolateral medium was transferred to a well of a luminescence compatible 96-well microtiter-plate and mixed with 50 µL Reagent Working Solution (BioVision Inc.). After 5 min incubation, luminescence was measured using a FluoStar Omega reader (BMG Labtech GmbH, Ortenberg, Germany). Alternatively, a ToxiLight™ bioassay kit (Lonza, Rockland, MA, USA) was used to determine cytotoxicity upon aerosol exposure to cultures. For this, 20 µL of basolateral medium was transferred to a well of a luminescence compatible 96-well microtiter-plate and mixed with 100 µL AK detection reagent (Lonza). After 5 min of incubation, luminescence was measured using a FluoStar Omega reader (BMG Labtech GmbH). The kit used in each experiment is stated in Table 8. For normalization of the cytotoxicity level, AK assay was done in positive control samples. These positive controls were obtained from cultures treated with Triton X-100 at a 1% final concentration for 24 hours (added to the basolateral side) to induce complete lysis of the cells (= 100% cytotoxicity).

**Table 8. Cytotoxicity Kits Used in the Study**

| Experiment No. | Experimental Week | Kit |
|---|---|---|
| **Experiment 1** | **07-Apr-2014** | BioVision Kit |
| **Experiment 2** | **23-Jun-2014** | BioVision Kit |
| **Experiment 3** | **23-Mar-2015** | ToxiLight™ Kit |
| **Experiment 4** | **20-Apr-2015** | ToxiLight™ Kit |
| **Experiment 5** | **15-Jun-2015** | ToxiLight™ Kit |
| **Dose Range Assessment** | **27-Apr-2015** | ToxiLight™ Kit |

### 7.4.7 Measurement of Secreted Pro-Inflammatory Mediators

Multi-analyte profiling of pro-inflammatory mediators (MAP analysis) was carried out by collecting 200 µL of basolateral medium from cultures at different post-exposure times (i.e., 24, 48, and 72 h after whole smoke or aerosol exposure) (PMI_RD_SOP_000361; PMI_RD_WKI_001032; PMI_RD_WKI_001274; PMI_RD_FOR_000803). For the analysis, Luminex® xMAP® technology was employed (Luminex, Austin, TX, USA) using commercially available assay panels (Milliplex®, EMD Millipore Corp., Schwalbach, Germany), as outlined in Table 9 and according to the manufacturer's instructions. Briefly, 25 µL of diluted or non-diluted sample was used for each detection and the analysis was run on a Luminex® 200 or FLEXMAP 3D®, equipped with the xPONENT® software version 4.2 (Luminex). Data are represented as Median Fluorescent Intensity (MFI) using a 5-parameter logistic or spline curve-fitting method to calculate the analyte concentrations in the basal medium samples. As a positive control, MucilAir™ (Epithelix Sàrl), were treated (N=3) for 24 hours with tumor necrosis factor alpha (TNFA) and interleukin 1 beta (IL1B) (PMI_RD_FOR_000849)—each of them was added to the basolateral medium at a final concentration of 10 ng/mL—to induce (majority) mediators targeted by the MAP analysis. The analytes that were measured only once (in Experiment 1) were not reported because of the low sample number (as outlined in Table 9).

**Table 9. Summary of Milliplex® Kits used in the Experimental Repetitions**

| Experimental Repetition | Exp 1 | Exp 2 | Exp 3 | Exp 4 | Exp 5 |
|---|---|---|---|---|---|
| **Experiment Week** | **07-Apr-2014** | **23-Jun-2014** | **23-Mar-2015** | **20-Apr-2015** | **15-Jun-2015** |
| **Analyte/Mediator** | | | | | |
| CCL11/Eotaxin | A | - | - | - | - |
| CFS3/G-CSF | A | - | - | - | - |
| CSF2/GM-CSF | A | - | - | - | - |
| IL1A | A | - | - | - | - |
| IL1B | A | - | - | - | - |
| CXCL10/IP10 | A | - | - | - | - |
| CCL2/MCP1 | A | - | - | - | - |
| CCL5/RANTES | A | - | - | - | - |
| VEGFA | A | E | E | E | E |
| IL6 | A | E | E | E | E |
| CXCL8/IL8 | A | E | E | E | E |
| EGF | B | E | E | E | E |
| CXCL1/GROA | B | E | E | E | E |
| TNFA | B | E | E | E | E |
| IL10 | B | - | - | - | - |
| IL13 | B | - | - | - | - |
| TIMP1 | B | F | F | F | F |
| TLSP | C | - | - | - | - |
| CCL20/MIP-3A | C | G | G | G | G |
| sICAM1 | C | G | G | G | G |
| MMP1 | D | D | D | D | D |
| MMP9 | D | D | D | D | D |

Milliplex® kits were purchased from EMD Millipore Corp.: **A)** HCYTOMAG-60K custom panel 1; **B)** custom panel SPR505; **C)** custom panel SPR507; **D)** custom panel HMMP2MAG-55K; **E)** HCYTOMAG-60K custom panel 2; **F)** custom panel HTMP2MAG-54K; **G)** custom panel SPR550. Abbreviations: CCL, chemokine (C-C motif) ligand; CSF, colony-stimulating factor; CXCL, chemokine (C-X-C motif) ligand; EGF, epidermal growth factor; Exp, experiment; G-CSF, granulocyte colony-stimulating factor; GM-CSF, granulocyte-macrophage colony stimulating factor; GROA, growth related oncogene alpha; IL, interleukin; IP10, interferon gamma-induced protein 10; MCP, monocyte chemoattractant protein; MIP, macrophage inflammatory protein; MMP, matrix metalloproteinase; RANTES, regulated on activation, normal T expressed and secreted; sICAM1, soluble intercellular adhesion molecule;TIMP1, tissue inhibitor of metalloproteinase 1;TLSP, thymic stromal lymphopoietin; TNFA, tumor necrosis factor alpha; VEGFA, vascular endothelial growth factor alpha.

### 7.4.8 Culture Processing, Embedding, Sectioning, and Staining

Culture inserts were washed three times with PBS and fixed for 2 hours in freshly prepared 4% paraformaldehyde (PMI_RD_WKI_001242). Upon completion of the fixation, the fixative was aspirated and the fixed organotypic cultures were washed three times with PBS both apically and basally at room temperature. Following this process, the fixed cultures were separated from the inserts by detaching the membrane from the plastic using forceps and bisected at the mid-point prior to processing using a Leica ASP300 S tissue processor (Leica Biosystem Nussloch GmbH, Nussloch, Germany) (PMI_RD_WKI_001243). Subsequently, the two bisected pieces (per culture sample) were entirely placed in a cassette for embedding in paraffin (PMI_RD_WKI_001260). Microscopy sections of the paraffin block (5 µm-thick) were obtained using a microtome (PMI_RD_WKI_001262) and mounted on glass slides that were then transferred to a Leica ST5020 automated slide stainer (Leica Biosystem Nussloch GmbH) for staining with hematoxylin (Merck Millipore) and eosin (Sigma-Aldrich, St. Louis, MO, USA) (H&E)/Alcian blue (Sigma-Aldrich) (PMI_RD_WKI_001266). Digital images of each slide (comprised of the two bisected pieces per culture sample) were generated using a Hamamatsu NanoZoomer 2.0 (Hamamatsu Photonics, K.K., Japan) slide scanner (PMI_RD_WKI_001314).

### 7.4.9 Immunohistochemistry (IHC) Analysis

Automated immunostaining was performed using a Leica BOND-MAX autostainer (Leica Biosystem Nussloch GmbH) (PMI_RD_WKI_001309) with the following primary antibodies, a anti-Ki67 (Ready to use (RTU), Leica Biosystem-PA0230); anti-p63 (1:100µl, Abcam-ab735, Abcam, Cambridge, UK); anti-FoxJ1 (1:2000µl, Abcam-ab40869, Abcam). Digital images of each slide were generated using the Hamamatsu NanoZoomer 2.0 slide scanner (Hamamatsu Photonics, K.K.) (PMI_RD_WKI_001314). Quantification of the p63-, Ki67-, and FoxJ1-immunopositive cells was performed using Tissue Studio® and Image Miner® software (Definiens AG, Munich, Germany). The total number of positively stained and negatively stained nuclei was calculated using this application as follows: Digitized slides were transferred to a workstation (Definiens Tissue Studio 2.0, Munich, Germany). First, a preprocessing step was performed to classify and segment the culture, as well as to identify and discriminate the cellular compartments (nucleus, cilia, and cytoplasm) and the insert membrane. Second, positively and negatively stained areas were detected and classified using a combination of color threshold and morphology features. The algorithm segments pictures iteratively, recognizing groups of pixels as objects. Furthermore, for each of the markers, the objects are classified based on staining intensity and graded as weak, moderate, and strong staining. Third, the total count of strong staining was considered positive for Ki67 IHC; the total count of strong and moderate staining was considered positive for p63; and the total count of strong, moderate, and weak staining was considered positive for FoxJ1. Processed data (including number of total cells analyzed and number of nuclei per staining intensity) were exported into Excel files for statistical analysis. The relative proportion of positively stained cells for each specific marker was calculated, relative to the total cell number. Analysis and graphical display of data were performed using SAS v9.2 (SAS Institute, Cary, NC, USA).

### 7.4.10 Cytochrome P450 (CYP) 1A1/1B1 Activity Assay

The combined activity of CYP1A1/CYP1B1 was determined using the non-lytic P450-Glo™ assay (Promega, Madison, WI, USA), according to the manufacturer's instructions (PMI_RD_WKI_001049; PMI_RD_FOR_000846). Briefly, the luminogenic P450-Glo™ substrate luciferin-6′ chloroethyl ether (Luciferin-CEE), which is a substrate for both CYP1A1 and CYP1B1, was added to the basolateral medium 24 hours prior to sample collection. The luciferin product of the CYP reaction was detected by mixing 50 µL of the collected medium with 50 µL of Luciferin Detection Reagent. After 30 min incubation at room temperature, luminescence was measured in a FluoStar Omega reader (BMG Labtech GmbH). As a positive control for CYP1A1/B1 induction, three replicates of 3D-organotypic culture inserts were treated for 48 hours with 2,3,7,8-tetrachlorodibenzo-p-dioxin (TCDD) (Sigma-Aldrich, St. Louis, MO, USA), then added to a final concentration of 30 nM to the basolateral side. As a negative control, basolateral media from three replicates of untreated culture inserts were tested for CYP1A1/B1 activity.

### 7.4.11 RNA/microRNA Purification

Total RNA including microRNA (miRNA) was isolated after washing the 3D-organotypic culture inserts two times with cold (4°C) PBS at both the basal and apical sides. The cells were then disrupted in 700 µL QIAzol™ lysis buffer (Qiagen, Hilden, Germany) followed by RNA extraction using a Qiagen miRNeasy Mini Kit and a QIAcube robot (Qiagen) (PMI_RD_WKI_001117). The quantity of the purified RNA was determined using a NanoDrop™ ND8000 spectrophotometer (Thermo Fisher Scientific, Waltham, MA, USA), while the quality of the RNA was analyzed using an Agilent 2100 Bioanalyzer (Agilent Technologies) (PMI_RD_WKI_000978).

### 7.4.12 mRNA Profiling Analysis using GeneChips

The Target preparation workflow was performed using a liquid handling system Biomek FXP Target Prep Express (Beckman Coulter Pasadena, CA, USA). 100 ng of total RNA was reverse-transcribed to cDNA using an Affymetrix® HT 3' IVT PLUS kit (Affymetrix, Santa Clara, CA, USA) (PMI_RD_WKI_001109). The cDNA was labeled, and amplified to cRNA (complementary RNA, also referred to as amplified RNA), and the cRNA was purified using magnetic beads to remove unincorporated nucleotide triphosphates, salts, enzymes, and inorganic phosphates (PMI_RD_WKI_001109).

Purified cRNA (≥12 µg) was quantified, normalized, and quality checked using a Fragment Analyzer™ (Advanced Analytical, Ames, IA, USA) (PMI_RD_WKI_001125) and chemically fragmented (PMI_RD_WKI_001109). The completion of fragmentation was checked on a Agilent 2100 Bioanalyzer (Agilent Technologies). Then, 29.4 µL of fragmented and labeled cRNA was added to 190.6 µL of Hybridization Cocktail (PMI_RD_WKI_001126). After denaturation for 5 min at 95°C and 5 min at 45°C followed by centrifugation at Vmax (16,000 × g) for 1 minute, 200 µL of the cRNA cocktail was hybridized to a GeneChip® Human Genome U133 Plus 2.0 Array (Agilent Technologies) (PMI_RD_WKI_001126). The arrays were incubated in a GeneChip® Hybridization Oven 645 (Affymetrix) for 16 hours at 45°C with a rotation speed of 60 rpm. Arrays were washed and stained on a GeneChip® Fluidics Station FS450 DX (Affymetrix) using the Affymetrix® GeneChip® Command Console® Software (AGCC software v 3.2) with protocol FS450_0001.

Finally, the arrays were scanned using a GeneChip® Scanner 3000 7G (Affymetrix). Raw images from the scanner were saved as DAT files. The AGCC software automatically gridded the DAT file image and extracted probe cell intensities into a CEL file.

### 7.4.13 MiRNA profiling

A FlashTag™ Biotin HSR kit (Affymetrix) was used to label the miRNA (PMI_RD_WKI_001123). 200 ng of total RNA containing low molecular weight RNA was subjected to a brief tailing reaction followed by ligation of the biotinylated signal molecule to the target RNA sample. After denaturation for 5 min at 99°C and 5 min at 45°C followed by centrifugation at Vmax (16,000 × g) for 1 min, 21.5 µL of the biotin-labeled sample was mixed with 110.5 µL hybridization cocktail. The arrays (miRNA version 3.0) were incubated in a GeneChip® Hybridization Oven 645 (Affymetrix) for 16 hours at 48°C with a rotation speed of 60 rpm. Arrays were washed and stained on a GeneChip® Fluidics Station FS450 DX (Affymetrix) using the Affymetrix® GeneChip® Command Console™ Software (AGCC software v 3.2) with protocol FS450_0002. Finally, the arrays were scanned using a GeneChip® Scanner 3000 7G (Affymetrix). Raw images from the scanner were saved as DAT files. The AGCC software automatically gridded the DAT file image and extracted probe cell intensities into a CEL file.

# 8 STATISTICAL AND COMPUTATIONAL METHODS

## 8.1 Statistical Methods

The analysis and graphical display of the data were performed using SAS v9.2 (SAS Institute).

### 8.1.1 Experimental Unit

For the exposure experiments using human organotypic nasal culture models and the Vitrocell® 24/48 exposure system, the experimental unit was the smoke exposure run. If a particular endpoint was measured several times in the same culture insert or in different culture inserts exposed to the same experimental condition (e.g., a specific concentration of nicotine in the smoke/aerosol at a specific post-exposure time) during the same smoke exposure run, then all the average values of a given endpoint were calculated.

For the controls, endpoints were measured from culture inserts that were not exposed to smoke/aerosol in the Vitrocell® 24/48 exposure system but treated by reagents/chemicals. In this case, the experimental unit was the study phase, i.e., a single experimental repetition, and the average values of a given endpoint were calculated from the measurements performed on culture inserts that were treated identically with the specific corresponding reagent/chemical.

### 8.1.2 Derived Variables

#### 8.1.2.1 Normalized Cytotoxicity Levels

All values of the AK assay readout were normalized using the average of the positive control (Triton X-100-treated culture inserts) and negative control (PBS-treated or untreated culture inserts [unexposed, incubator control]) and percentage cytotoxicity was calculated as follows:

$$Cytotoxicity\ (\%) = \frac{AK_{Tissue} - AK_{Neg\ CTRL}}{AK_{Pos\ CTRL} - AK_{Neg\ CTRL}}\ x\ 100, \text{ where}$$

$$AK_{Pos\ CTRL} = \sum_{i=1}^{nbPhase} \frac{AK_{TX-100}}{nbPhase}$$

$$AK_{Neg\ CTRL} = \sum_{i=1}^{nbPhase} \frac{\sum_{j=1}^{nbCTRL^i} \frac{AK_{i,j}}{nbCTRL^i}}{nbPhase}$$

$$AK_{Tissue} = relative\ luminescence\ unit\ of\ a\ given\ sample$$

$$nbPhase = number\ of\ experimental\ phase$$

$$Neg = negative$$

$$Pos = positive$$

$$CTRL = control$$

8.1.2.2 Normalized CYP Activity Levels

All the measured activity of CYP1A1/CYP1B1 were normalized using the average of the positive control (TCDD-treated culture inserts) and negative control (luciferin substrate-treated, non-exposed culture inserts) as follows:

$$Normalized\ CYP\ activity\ (\%) = \frac{CYP_{Tissue} - CYP_{Neg\ CTRL}}{CYP_{Pos\ CTRL} - CYP_{Neg\ CTRL}}\ x\ 100, \text{ where}$$

$$CYP_{Neg\ CTRL} = \sum_{i=1}^{nbPhase} \frac{\sum_{j=1}^{nbCTRL^i} \frac{CYP_{i,j}}{nbCTRL^i}}{nbPhase}$$

$$CYP_{Pos\ CTRL} = \sum_{i=1}^{nbPhase} \frac{CYP_{TCDD}}{nbPhase}$$

$$CYP_{Tissue} = relative\ luminescence\ unit\ of\ a\ given\ tissue\ culture\ sample$$

$$nbPhase = number\ of\ experimental\ phase$$

$$Neg = negative$$

$$Pos = positive$$

$$CTRL = control$$

8.1.3 Data Transformation

All numerical values from the MAP analysis were transformed using the natural log transformation.

8.1.4 Statistical Comparisons

Continuous variables were compared as follows:

- The comparison of an exposed sample versus the corresponding air control (i.e., the paired samples from the same exposure run at a given experimental repetition) was done using a paired T-TEST.
- The comparison of 3R4F-exposed versus THS2.2-exposed samples was done after subtracting the values of the corresponding air controls (i.e., the paired sample). Then the comparison was done using a T-TEST corrected for non-equal variance (Satterthwaite correction).

*P*-values were not adjusted for multiple testing.

**8.2 Computational Methods: Affymetrix Gene Expression Analysis**

8.2.1 Processing and Quality Control (QC) of Raw CEL Files

The Affymetrix GeneChip® Human Genome U133 Plus 2.0 Array that was used for hybridization simultaneously probes the expression of thousands of genes. In accordance with PMI_RD_WKI_001228 and PMI_RD_SOP_000346, raw CEL files were background-corrected, normalized, and summarized using frozen Robust Microarray Analysis (fRMA) (McCall 2010).

Background correction and quantile normalization were performed to generate microarray expression values from all the arrays that passed the QC check, which was performed using the custom CDF environment HGU133Plus2_Hs_ENTREZG v16.0 (Dai 2005). A log-intensities plot, normalized-unscaled standard error (NUSE) plot, relative log expression (RLE) plot, median absolute value RLE (MARLE) plot, and pseudo as well as raw images were generated for quality checks using R packages (AffyPLM; Bioconductor, Seattle, WA, USA) (Bolstad 2005, Gautier 2004).

CEL files that fulfilled at least one of the quality metric rules described below were dropped from further analysis.

a) Pseudo-image displayed a spatial pattern covering approximately 10% of the pseudo-image.
b) Median NUSE >1.05
c) |Median RLE| >0.1
d) |(MARLE-median(MARLE))|/ (1.4826 *mad(MARLE)) >1/√0.01; (where mad is the median absolute deviation).

Subsequently, the RLE and NUSE-based metrics were recomputed, until no more CEL files were removed.

### 8.2.2 Gene-Level Analysis

For each experimental factor combination item, concentration and post-exposure, a model for estimating the treatment effect was fitted using the limma software (Smyth 2004) by including the covariate smoking run as a blocking variable to account for insert pairing during an exposure experiment. (An exposure run comprised samples exposed to a test item and air exposed controls, see Figure 3). The *p*-values for each computed effect were adjusted across genes using the Benjamini-Hochberg false discovery rate (FDR) method. The results were displayed as volcano plots (x-axis representing the estimated effect and y-axis representing the –log10(FDR) for each gene). Differentially expressed genes were defined as the set of genes with FDRs below 0.05.

The reproducibility was estimated by correlating the fold-changes (exposed samples vs. controls) across experimental repetitions. First, the gene expression data from experiments 1 and 2 were combined and the average of the fold-changes was computed for each of the genes in the dataset. Similarly, the combined data from experiments 3, 4, and 5 were used to compute the average of the fold-changes. Correlation plots of the fold-changes for all genes in the dataset were then generated for each comparison.

### 8.2.3 Statistical Analysis: Network-Level Analysis

#### 8.2.3.1 Network Perturbation Amplitude (NPA)

The collection of causal biological networks used in the study(s) was the human network suite CBN v1.3 (Boué 2015). These networks contain from a few dozen to 200 nodes. The relevant network models considered in this study are summarized in Table 10. The network models can be organized into four major families, representing global biological processes: cell stress (CST), cell proliferation (CPR), inflammatory process networks (IPN), and cell fate (CFA).

**Table 10. Network and Network Models Used in the Analysis**

| No | Abbreviated Network Family Name | Network Name |
|---|---|---|
| **1** | CFA | Apoptosis |
| **2** | CFA | Autophagy |
| **3** | CFA | Necroptosis |
| **4** | CFA | Response to DNA Damage |
| **5** | CFA | Senescence |
| **6** | CPR | Calcium |
| **7** | CPR | Cell Cycle |
| **8** | CPR | Cell Interaction |
| **9** | CPR | Clock |
| **10** | CPR | Epigenetics |
| **11** | CPR | Growth Factor |
| **12** | CPR | Hedgehog |
| **13** | CPR | Hox |
| **14** | CPR | Jak Stat |
| **15** | CPR | Mapk |
| **16** | CPR | Mtor |
| **17** | CPR | Notch |
| **18** | CPR | Nuclear Receptors |
| **19** | CPR | PGE2 |
| **20** | CPR | Wnt |
| **21** | CST | Endoplasmic Reticulum Stress |
| **22** | CST | Hypoxic Stress |
| **23** | CST | NFE2L2 Signaling |
| **24** | CST | Osmotic Stress |
| **25** | CST | Oxidative Stress |
| **26** | CST | Xenobiotic Metabolism Response |
| **27** | IPN | Epithelial Innate Immune Activation |
| **28** | IPN | Epithelial Mucus Hypersecretion |
| **29** | IPN | Tissue Damage |

Abbreviations: CFA, Cell Fate; CST, Cell Stress; CPR, Cell Proliferation; IPN, Inflammatory Process Networks; Jak Stat, Janus kinase/signal transducers and activators of transcription; Mapk, Mitogen-activated protein kinases; Mtor, mechanistic target of rapamycin; NFE2l2, nuclear factor, erythroid 2-like 2; PGE2, prostaglandin E2.

Network scoring exploits the network backbone nodes that are connected to downstream mRNA-abundance-nodes based on their known relationship reported in the literature. These signed relationships can be the backbone node increasing or decreasing the abundance of certain mRNAs and are used to infer the activation of a backbone node using transcriptomics data. Since not all backbone nodes have downstream mRNA nodes, the network models need to be prepared for scoring to improve the specificity and relevancy of the overall NPA score. Only backbone nodes that are on a directed path that starts and ends with a node that has downstream mRNA nodes are considered.

After removing the nodes that do not satisfy the above, the largest connected component is kept. Finally the edges "causesNoChange" are disregarded for the scoring.

The Network Perturbation Amplitude (NPA) methodology (Hoeng 2014, Martin 2014) aims at contextualizing the high dimensional transcriptomics data by combining gene expression ($\log_2$) fold-changes, β, into fewer differential node values (one value for each node of the network), *f*. The differential nodes values are determined by a fitting procedure that infers the values that best satisfy the directionality of the causal relationships (positive or negative signs) contained in the network model, while being constrained by the experimental data (the gene $\log_2$-fold-changes, which are described as downstream effects of the network itself):

$$f = L_3^{-1} L_2^T \beta$$

where *L* is the signed weighted Laplacian of the network and the extra edges and nodes describing the downstream effects (to gene expression nodes); $L_3$ is the sub-matrix of *L* for the nodes in the network; and $L_2$ is the sub-matrix corresponding to the edges connecting the network nodes to the downstream gene expression nodes. The differential node values are in turn summarized as a single positive number, referred to as the amplitude of perturbation (NPA scores).

$$NPA = \frac{1}{|E|} \sum_{e\ in\ E} (f(e_0) + \sigma(e) f(e_1))^2$$

where *E* is the set of edges in the network; $|E|$ is its size; and $e_0$ and $e_1$ denote the start and the end, respectively, of an edge *e*. The sum computing the NPA score can be expressed as $f^T Q f$, where *Q* is the signed Laplacian of the network when all of the edge signs have been reversed. All details of the methodology are described in a previous publication (Martin 2014).

For the NPA scores, a confidence interval accounting for experimental variation and associated *p*-values is computed. In addition, companion statistics, derived to inform on the specificity of the NPA score with respect to the biology described in the network model, are shown as *O and K* if their *p*-values are below the significance level (0.05). A network is considered to be significantly impacted if three values (the confidence interval, *O, and K* statistics) are below 0.05.

#### 8.2.3.2 Biological Impact Factor (BIF)

The methodology Biological Impact Factor (BIF) (Hoeng 2014, Thomson 2013) provides a unified, coherent framework for investigating mechanistic effects at each level of granularity of the biological processes represented in the network models. This methodology enables the derivation of the relative BIF, which is a measure of the overall biological impact across all network models. The BIF allows an assessment of the exposures in an objective, systematic, and quantifiable manner, computing a systems-wide and pan-mechanistic biological impact measure for a given substance, mixture, or test item.An aggregation of the NPA should satisfy the following criteria:

a) *Credibility*: The BIF should be an intuitive and logical aggregation scheme.
b) *Fairness*: All network families are equally important.
c) *Understandable*: Each decision or step should have a defined rationale.

To fulfil the first criterion, network scores are aggregated via a weighted sum (because every scoring in NPA is additive). In addition, only networks that have the *p*-values of the three statistics below 0.05 (*O, *, K*) are considered (denoted by $N_i^*$). BIF is defined as:

$$BIF = \sum_{N_i^*} \omega_i \, NPA(N_i) = \sum_{N_i^*} \omega_i \sum_{e \epsilon E(N_i)} (f(e_0) + \sigma(e) f(e_1))^2$$

where $f$ is the function of the network nodes that describe the differential node values; $E(N_i^*)$ is the network edges; and $e_0$ and $e_1$ are the start and the end, respectively, of an edge $e$.

For the second criterion, a *fair* BIF would represents the equality of the biological processes (networks) in a given system (e.g., 2D cultures of normal human bronchial epithelial cells, 3D organotypic cultures, or lung tissue samples from *in vivo* studies). If all the networks models were fitted perfectly by the gene expression data, the contribution of each network to the BIF is assumed to be equal. Therefore, the BIF methodology considers that all specific processes represented in the network models are equally involved and important for a given network family. A perfect fit of the network will maximize the NPA value and be smooth over the network. Using the notation defined above, a "perfect" network response (differential node values) would both maximize $f^T Q f$ with $||f||_2 = 1$ and minimize $f^T L_3 f$ (the NPA criteria (Martin 2014)). Additionally, there is a constraint that $L_3 f$ vanishes for network nodes that do not have direct downstream gene expression nodes (Hoeng 2014, Martin 2014), because they are expected to be in the image of $L^T_2$. Such nodes are denoted as *NH*. Therefore, the following optimization problem can be solved as:

$$argmax_{f \; s.t. (L_3 f)|_{NH}=0} \frac{f^T Q f}{f^T L_3 f}$$

To rebalance the network families, the average over the networks is considered.

For each edge $e = (e_0, \sigma(e), e_1)$, the number of occurrences of edge $e$ in the set of networks used in the BIF calculation is denoted by $o(e)$. Therefore, the maximum occurrence-corrected amplitude of a network $N_i$ can be defined as:

$$NPA_{max}(N_i) \doteq \sum_{e \epsilon E(N_i)} \frac{1}{o(e)} (f_{max}(e_0) + \sigma(e) f_{max}(e_1))^2$$

Finally, to normalize the NPAs, a correction factor of $|E(N_i)|/NPA_{max}(N_i)$ is applied. Considering all of these factors, the BIF is defined as the weighted sum ($F$ denotes the network families), as follows:

$$\sum_F \frac{1}{|F|} \sum_{N_i^* \in F} \frac{1}{NPA_{max}(N_i)} \sum_{e \epsilon E(N_i)} \frac{1}{o(e)} (f(e_0) + \sigma(e) f(e_1))^2$$

Therefore, the contribution of each network $F$ is:

$$\frac{\frac{1}{|F|} \sum_{N_i^* \in F} \frac{1}{NPA_{max}(N_i)} \sum_{e \epsilon E(N_i)} \frac{1}{o(e)} (f(e_0) + \sigma(e) f(e_1))^2}{BIF}$$

### 8.2.4 Gene-Set Analysis

Gene-set analysis (GSA) of transcriptomics data was performed using the *Piano* package in the R statistical environment (Varemo 2013). Pathway maps are obtained from the KEGG database (Kanehisa 2014) and exported as R objects into the package *graphite* (Sales 2012). Gene-set enrichment is assessed using over-representation analysis (ORA) and gene-set analysis. For the ORA, a one-tailed Fisher's exact test is employed. For the GSA, the fold-change is used as the gene-level statistic, the mean is used as the set statistic and sample permutation (Q2) is used to assess statistical significance (Ackermann 2009). For each test, the p-value is adjusted using the Benjamini-Hochberg procedure. The gene-set enrichment are the gene-set statistics mentioned before.

## 8.3 Computational Methods: Affymetrix miRNA Expression Analysis

### 8.3.1 Processing and Quality Control of Raw CEL Files

The raw array data in the CEL files were pre-processed through a standard pipeline based on the generic documents PMI_RD_WKI_001228 and PMI_RD_SOP_000346. CEL files were read using the *read.celfiles* function of the Oligo package in the Bioconductor suite of microarray analysis tools for the R statistical software environment (Carvalho 2010, Huber 2015, R Core Team 2013). The quality of the array data was controlled using the *arrayQualityMetrics* package in Bioconductor (Kauffmann 2009) and examined according to the following four metrics:

a) Distances between arrays at the raw data level
b) Distances between arrays at the normalized data level
c) NUSE
d) Array intensity distributions.

Arrays that were found to be outliers in at least two of these metrics were discarded. The quality was iteratively re-examined on the remaining arrays until all were accepted. For the experimental repetitions, the QC procedure for the miRNA expression analysis was applied separately on each miRNA processing batch (each processing batch was composed of samples obtained from two consecutive experimental repetitions). This approach was used to avoid batch effects on the QC. Subsequently, normalized probe-level data were obtained by applying robust multi-array (RMA) normalization and summarized using the median polish method at the probe set-level (Bolstad 2003, Irizarry 2003).

### 8.3.2 Probe Set Filtering

Affymetrix GeneChip® miRNA 3.0 arrays were used for the hybridization. These arrays probe the expression of 19,724 mature miRNAs relevant to 153 species, among them 1733 were human miRNAs (Affymetrix miRNA 3.0 Array). Using the annotation provided by Affymetrix and the latest miRNA nomenclature according to miRBase (21 June 2014 release) (Kozomara 2014), only the probe sets pertaining to human miRNAs were kept in the expression matrix.

Only the miRNA probe sets with significantly higher intensity values than their matched background probes (based on the GC content and sequence length) were considered to be "detected" (see the "Detection" section in (Affymetrix miRNA QCT Tool 2011). A *p*-value threshold of 0.01 was chosen to determine the detection calls based on Wilcoxon tests. If a miRNA probe set was detected in more than 50% of the samples in at least one sample group, then it was kept for further analysis, otherwise it was discarded. This pre-processing approach yielded 527 miRNA probe sets in the final expression matrix after exclusion of the control probe sets.

### 8.3.3 Determining a Differential miRNA Expression

According to the experimental design, the experiment unit consisted of a number of pairwise treatment vs. control comparisons (i.e., an exposure run comprised samples exposed to a test item and samples exposed to air (control), see section 8.1.1. Experimental Unit). For each comparison, a

submatrix was extracted from the global expression matrix by keeping only the samples that belonged to corresponding treatment or control groups, as well as the miRNA probe sets that were detected in more than 50% of the samples in at least one of these two groups. Linear models for differential expression were applied on all resulting submatrices using the moderated t-statistics implemented in the limma package (Ritchie 2015). The models included an additional variable that took into account the exposure runs, which improved the fitting procedure in limma. Subsequently, adjusted *p*-values were obtained following multiple testing corrections using the Benjamini-Hochberg FDR method (Benjamini 1995). The miRNAs below the FDR threshold of 0.05 were considered to be differentially expressed.

For a given comparison, the results were displayed as a volcano plot, where the x-axis represented the estimated treatment effect (differential expression) of each miRNA and the y-axis represented the corresponding statistical significances given by –log10(FDR). Moreover, for a given comparison, quantile-quantile (QQ) plots were generated by first sorting all miRNAs according to their unadjusted (raw) *p*-values in ascending order. Subsequently, the −log10 transformed raw *p*-values of the resulting quantiles (i.e. the rank divided by total number of miRNAs) were displayed on the x-axis and the corresponding, −log10 transformed raw *p*-values were displayed on the y-axis. For a given statistical significance threshold α, the "Z"-shaped boundaries of the plot correspond to raw *p*-values below α (lower horizontal line), the oblique line parallel to the diagonal x=y corresponds to the FDR values below α, and the upper horizontal line corresponds to the Bonferroni adjusted p-value below the threshold α.

# 9 RESULTS

## 9.1 Nicotine Concentrations in the Smoke/Aerosol

The Vitrocell® 24/48 exposure system is equipped with a dilution system (refered to as the Dilution/Distribution Module, Figure 3. To achieve the target concentrations of nicotine in the 3R4F smoke or THS2.2 aerosol, certain dilutions were applied during the exposure study using culture models. The actual nicotine concentrations in the smoke/aerosol were measured following trapping of smoke/aerosol in EXtrelut® 3NT columns; at least three independent samplings were collected per experimental repetition (Table 11). Because the whole smoke/aerosol are trapped in the EXtrelut® 3NT columns at the first row of the Dilution/Distribution Module, further dilutions of the smoke/aerosol cannot be applied (during trapping measurements). Therefore, trappings of whole smoke/aerosol in EXtrelut® 3NT columns to measure nicotine concentrations could not be done at the same time when the cultures were exposed to 3R4F smoke or THS2.2 aerosol. The trappings, were therefore, done within the same experimental week.

Table 11 shows that the higher the percentages of 3R4F smoke and THS2.2 aerosol applied within the Dilution/Distribution Module, the higher the concentration of nicotine in the smoke/aerosol, as expected. The actual nicotine concentrations in the smoke/aerosol for a given concentrations of 3R4F and THS2.2 were consistent among the experimental repetitions, except for those measured in the first experiment (the week of 07-Apr-2014). This lower levels of nicotine were attributed to the lower flow rate during the trapping experiment, making the observations inconsistent with the other trapping experiments.

Furthermore, according to the study design (Table 5), at least two concentrations of the test aerosol (THS2.2 aerosol) were applied at the comparable nicotine concentrations to those of the reference 3R4F smoke. Table 11 shows that to reach the comparable nicotine concentrations, the dilution of the THS2.2 aerosol was approximately 1.65 times that of the 3R4F smoke.

**Table 11. Target and Actual Nicotine Concentrations in the Smoke/Aerosol**

| Group | | Experiment Week | | | | |
|---|---|---|---|---|---|---|
| | | **Exp 1*** | **Exp 2** | **Exp 3** | **Exp 4** | **Exp 5** |
| | | **07-Apr-2014*** | **23-June-2014** | **23-Mar-2015** | **20-Apr-2015** | **15Jun-2015** |
| **3R4F Applied Concentration 1** | Target Nicotine (mg/L) | 0.15 | 0.15 | 0.15 | 0.15 | 0.15 |
| | Vitrocell Dilution (%) | 8.0 | 8.0 | 7.0 | 7.0 | 7.0 |
| | Actual Nicotine (mg/L) | 0.103 ± 0.004* (N = 3) | 0.139 ± 0.005 (N = 3) | 0.137 ± 0.007 (N = 3) | 0.155 ± 0.004 (N = 3) | 0.156 ± 0.007 (N = 3) |
| **3R4F Applied Concentration 2[§]** | Target Nicotine (mg/L) | NA | 0.20[§] | NA | NA | NA |
| | Vitrocell Dilution (%) | NA | 13 | NA | NA | NA |
| | Actual Nicotine (mg/L) | NA | 0.204 ± 0.004 (N = 4) | NA | NA | NA |
| **3R4F Applied Concentration 3** | Target Nicotine (mg/L) | 0.25 | 0.25 | 0.25 | 0.25 | 0.25 |
| | Vitrocell Dilution (%) | 15.0 | 15.0 | 13.0 | 13.0 | 13.0 |
| | Actual Nicotine (mg/L) | 0.176 ± 0.049* (N = 3) | 0.240 ± 0.013 (N = 4) | 0.247 ± 0.06 (N = 3) | 0.257 ± 0.004 (N = 3) | 0.263 ± 0.011 (N = 3) |
| **THS2.2 Applied Concentration 1** | Target Nicotine (mg/L) | 0.15 | 0.15 | 0.15 | 0.15 | 0.15 |
| | Vitrocell Dilution (%) | 12.8 | 12.8 | 13.0 | 13.0 | 13.0 |
| | Actual Nicotine (mg/L) | 0.096 ± 0.018* (N = 3) | 0.145 ± 0.04 (N = 3) | 0.148 ± 0.007 (N = 3) | 0.144 ± 0.001 (N = 3) | 0.154 ± 0.04 (N = 4) |
| **THS2.2 Applied Concentration 2** | Target Nicotine (mg/L) | 0.27 | 0.27 | 0.27 | 0.27 | 0.27 |
| | Vitrocell Dilution (%) | 22.6 | 22.6 | 24.0 | 24.0 | 24.0 |
| | Actual Nicotine (mg/L) | 0.165 ± 0.023* (N = 3) | 0.260 ± 0.042 (N = 3) | 0.279 ± 0.032 (N = 3) | 0.292 ± 0.006 (N = 3) | 0.266 ± 0.008 (N = 4) |
| **THS2.2 Applied Concentration 3** | Target Nicotine (mg/L) | NA | 0.44 | 0.44 | 0.44 | 0.44 |
| | Vitrocell Dilution (%) | NA | 31.0 | 31.0 | 31.0 | 31.0 |
| | Actual Nicotine (mg/L) | NA | 0.413 ± 0.017 (N = 3) | 0.437 ± 0.015 (N = 3) | 0.439 ± 0.009 (N = 3) | 0.452 ± 0.021 (N = 3) |

Actual nicotine concentrations are expressed as mean ± SEM. *During the sampling/trapping of smoke/aerosol in the in EXtrelut® 3NT columns, an unexpected decreased flow rate occurred in the tube, which resulted in the inaccurate measurement of the nicotine concentrations. [§]Medium concentration of 3R4F at 0.20 mg nicotine/L smoke (referred to as the 3R4F (0.20) group) was tested only in one experimental repetition. Abbreviations: N, number of samples (trapped in the EXtrelut® 3NT columns); NA, not available (the concentration was not tested in the experimental repetitions); SEM, standard error mean.

## 9.2 Histological Evaluation

The impact of exposure on culture morphology was evaluated by histological assessment and immunohistochemistry (IHC) at 48 and 72 h post-exposure.

### 9.2.1 Morphological Evaluation

Nasal organotypic cultures were embedded in paraffin at 48 and 72 h after exposure, sectioned, and stained with H&E and Alcian blue. Representative H&E/Alcian blue-stained sections are shown in Figure 4. The images show similar culture morphology at the 48 and 72 h post-exposure time points. At both post-exposure time points, the morphology of the cultures exposed to 3R4F smoke at the nicotine concentration of 0.15 mg nicotine/L smoke (refered to as the group 3R4F (0.15)) was comparable to the air control. However, for the cultures exposed to the higher concentration of 3R4F (at a nicotine concentration of 0.25 mg nicotine/L smoke, refered to as the group 3R4F (0.25)), thinning of the epithelium was observed. In contrast, thinning of the epithelium was not observed in the cultures exposed to THS2.2 aerosol at the comparable nicotine concentration (0.27 mg nicotine/L aerosol, refered to as the group THS2.2 (0.27)). Moreover, the morphology of the cultures exposed to THS2.2 aerosol at all concentrations tested (i.e. 0.15, 0.27, and 0.44 mg nicotine/L aerosols; referred to as the groups THS2.2 (0.15), THS2.2 (0.27), and THS2.2 (0.44), respectively) were not different than the air control, at both 48 and 72 h post-exposure time points.

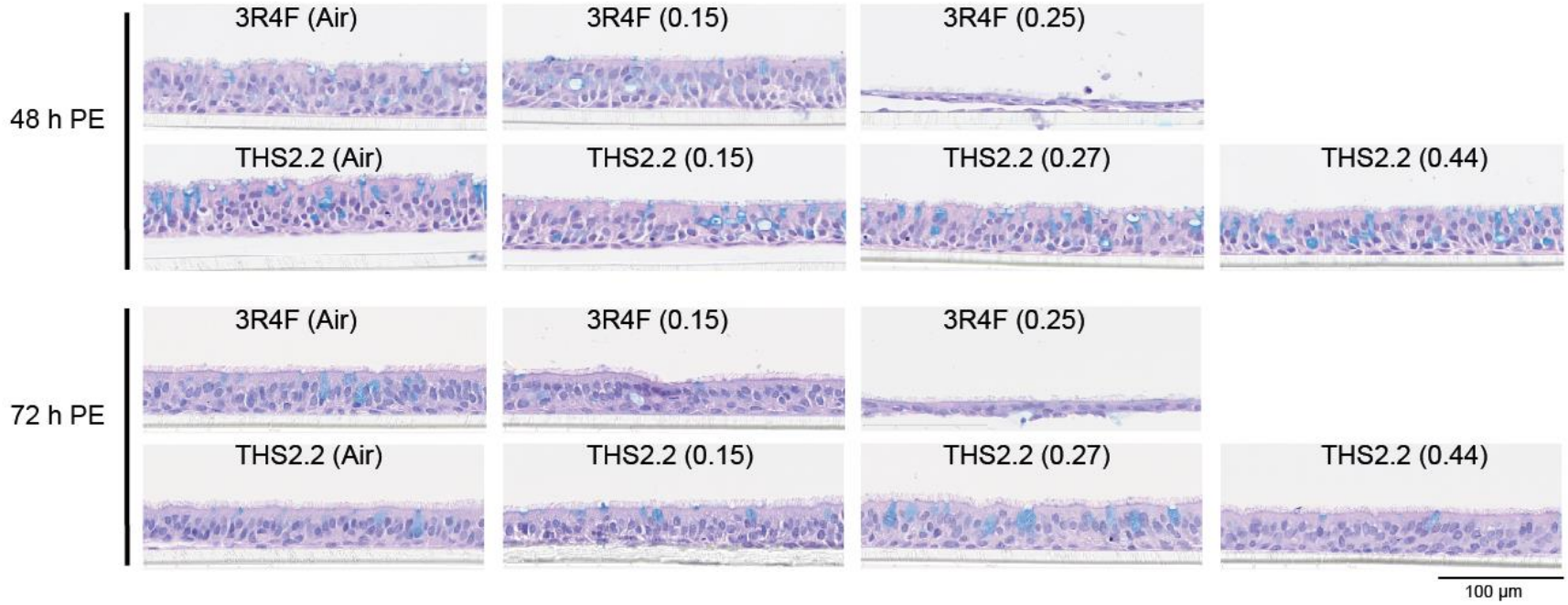



**Figure 4. Histology following exposure of the human organotypic 3D nasal cultures to 3R4F smoke/THS2.2 aerosol.**

Representative images (63 × magnification) of organotypic nasal culture sections stained with H&E/Alcian Blue, 48 and 72 h after exposure to 3R4F cigarette smoke or THS2.2 aerosol at the indicated nicotine concentrations (mg nicotine/L 3R4F smoke, or mg nicotine/L THS2.2 aerosol). Abbreviations: H&E, haematoxylin and eosin; h, hour.

### 9.2.2 Immunohistochemistry (IHC) Analysis

IHC analysis was performed to detect the expression of FoxJ1, Ki67, and p63 in ciliated cells, proliferating cells, and basal cells, respectively, of culture sections 48 and 72 h following exposure. Quantification of the markers was subsequently conducted to assess the impact of the exposures relative to the corresponding air controls. Figure 5 shows representative images of the stained culture sections at 48 and 72 h after exposure.

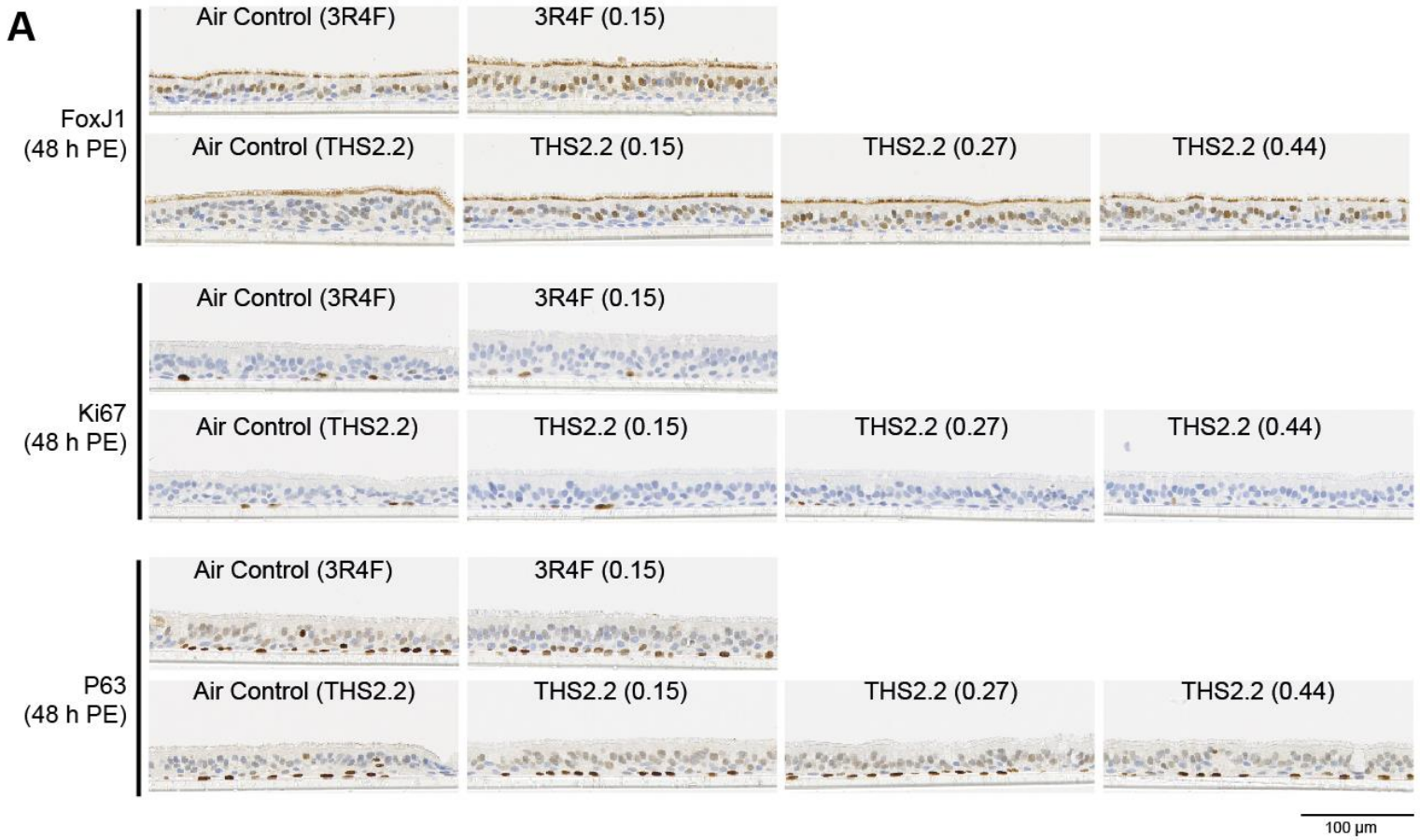



Figure continues

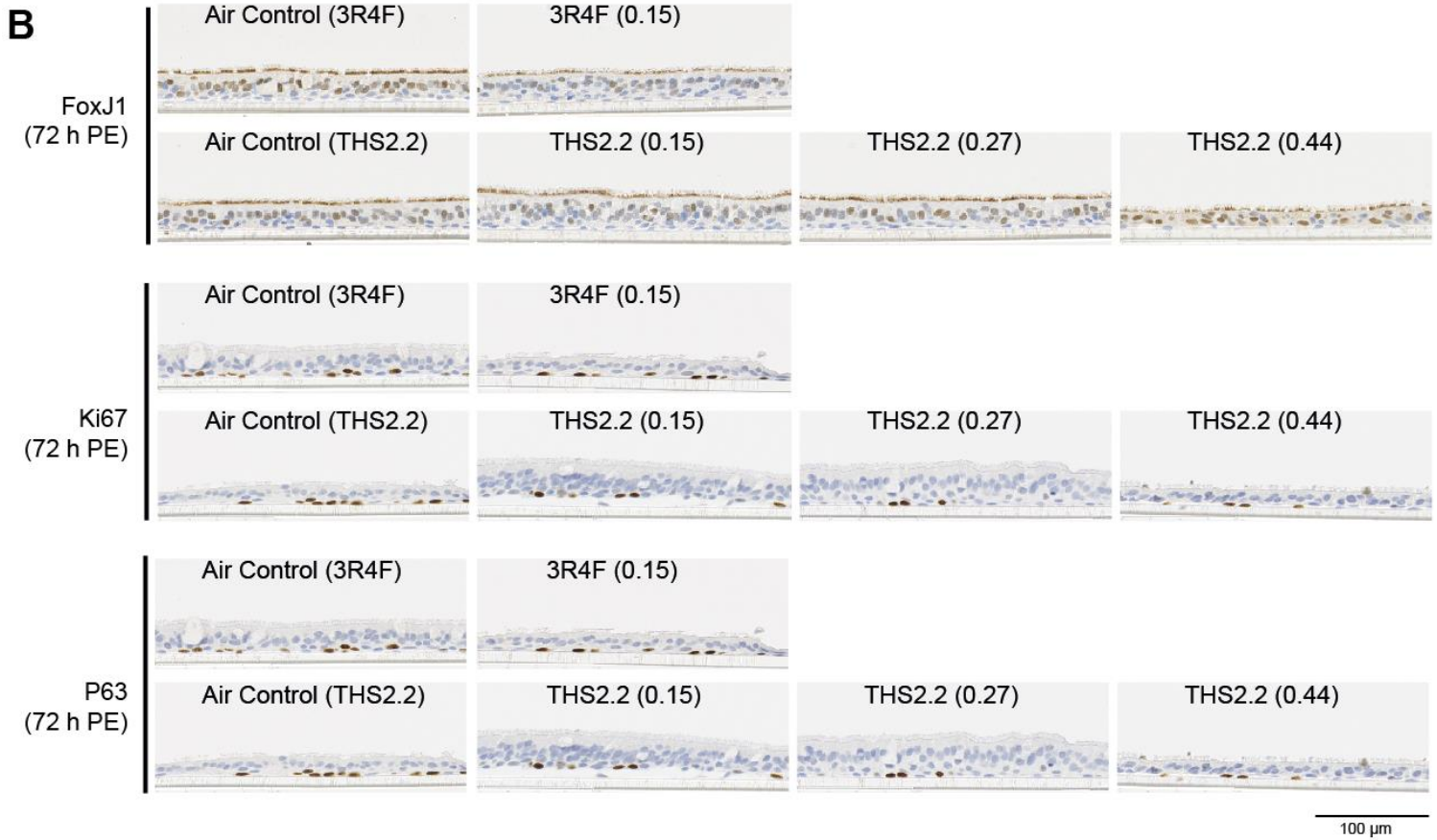



**Figure 5. IHC images of FoxJ1, Ki67, and p63 immunostaining.**

Representative images (63 × magnification) of organotypic nasal culture sections stained with anti-FoxJ1, anti-Ki67, and anti-p63 antibodies 48 (**A**) and 72 h (**B**) after 3R4F smoke or THS2.2 aerosol exposure at the indicated nicotine concentrations (mg/L).

A quantification analysis showed that 3R4F (0.15)-exposed cultures had a lower proportion of FoxJ1-positive cells 72 h after exposure, while THS2.2-exposed cuttures had a lower proportion of Ki67-positive cells 48 and 72 h after exposure (Figure 6). Furthermore, both 3R4F and THS2.2 exposure did not impact the proportion levels of p63-stained cells. In addition, at comparable nicotine concentrations (0.15) in the smoke/aerosol, among the three markers, only the proportion levels of FoxJ1-stained cells were found to be significantly lower in the THS2.2-exposed compared with the 3R4F-exposed cultures (Figure 6**)**. Descriptive statistics are reported in Supplementary Table 10–Supplementary Table 12.

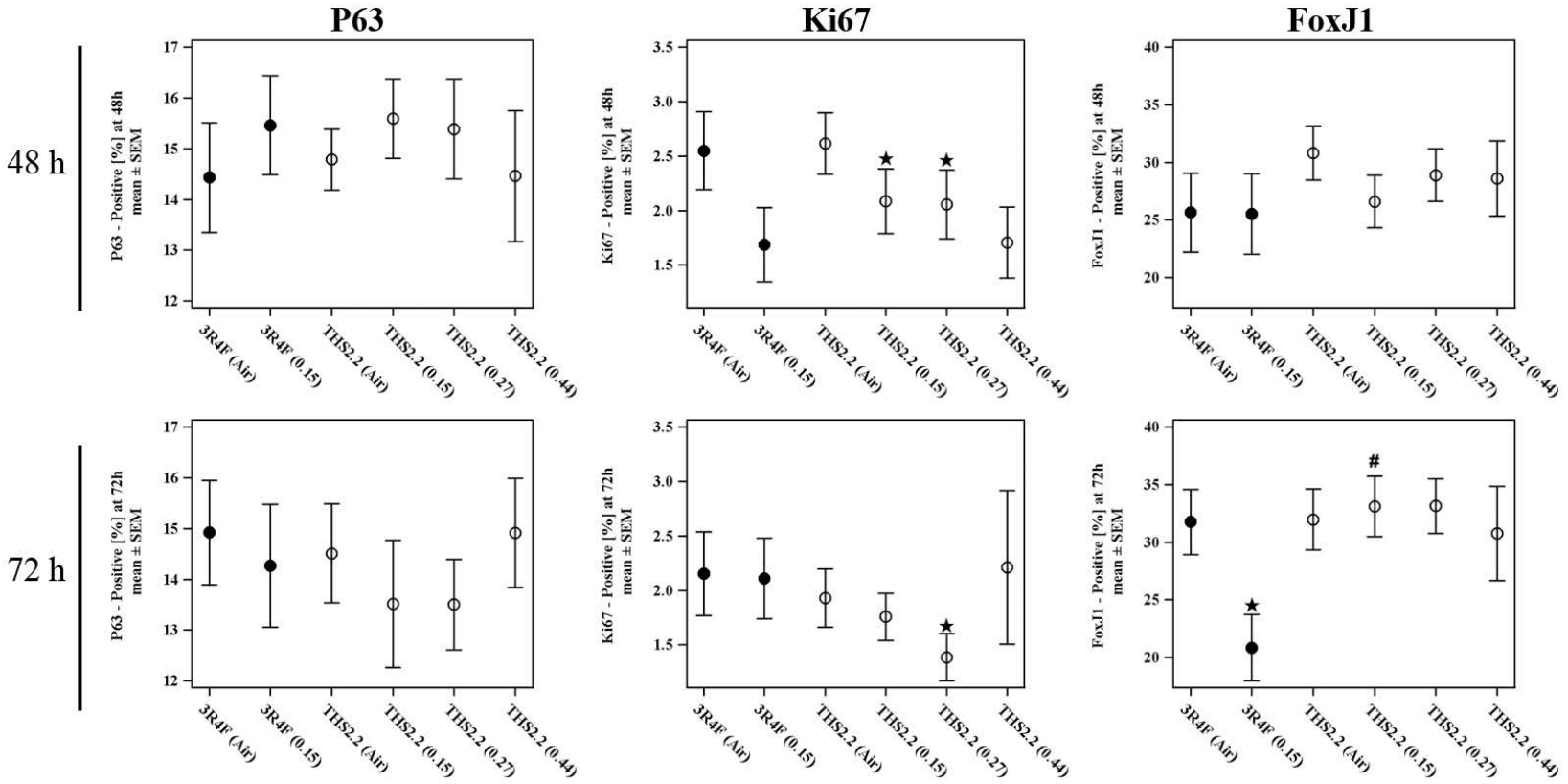



**Figure 6. Quantitative analysis of FoxJ1, Ki67, and p63 immunostaining of exposed organotypic nasal cultures**

Shown is the mean ± SEM of the fold-changes of the proportion of the immunopositive-stained cells in sections of culture exposed to 3R4F smoke or THS2.2 aerosol at the indicated nicotine concentrations (mg/L) for 28 min at 48 and 72 h post-exposure (N = 12–15, from five experimental repetitions with three exposure runs/repetition). Staining was digitally quantified and expressed as the proportion of positive cells with respect to the total number of cells. ★ indicates a significant difference compared with the corresponding air controls (*p*-values <0.05). # indicates a significant difference as compared with 3R4F (*p*-values <0.05): THS2.2 (0.15) vs. 3R4F (015), or THS2.2 (0.27) vs. 3R4F (0.25), or THS2.2 (0.44) vs. 3R4F (0.25).Abbreviations: SEM, standard error mean.

### 9.3 Cytotoxicity

Cytotoxicity following 3R4F smoke or THS2.2 aerosol exposure was assessed by measuring the levels of adenylate kinase (AK) released from the cultures into the basolateral media. Figure 7 shows that at the 4 h post-exposure time point, 3R4F exposure was not associated with marked cytotoxicity. However, as the post-exposure time was prolonged, a substantial increase of cytotoxicity was observed in 3R4F-exposed cultures. In contrast, no noticeable cytotoxicity was observed in THS2.2-exposed cultures at any of the tested concentrations, irrespective of the post-exposure time points and concentrations of nicotine in the THS2.2 aerosols. Descriptive statistics of these results are reported in Supplementary Table 13.

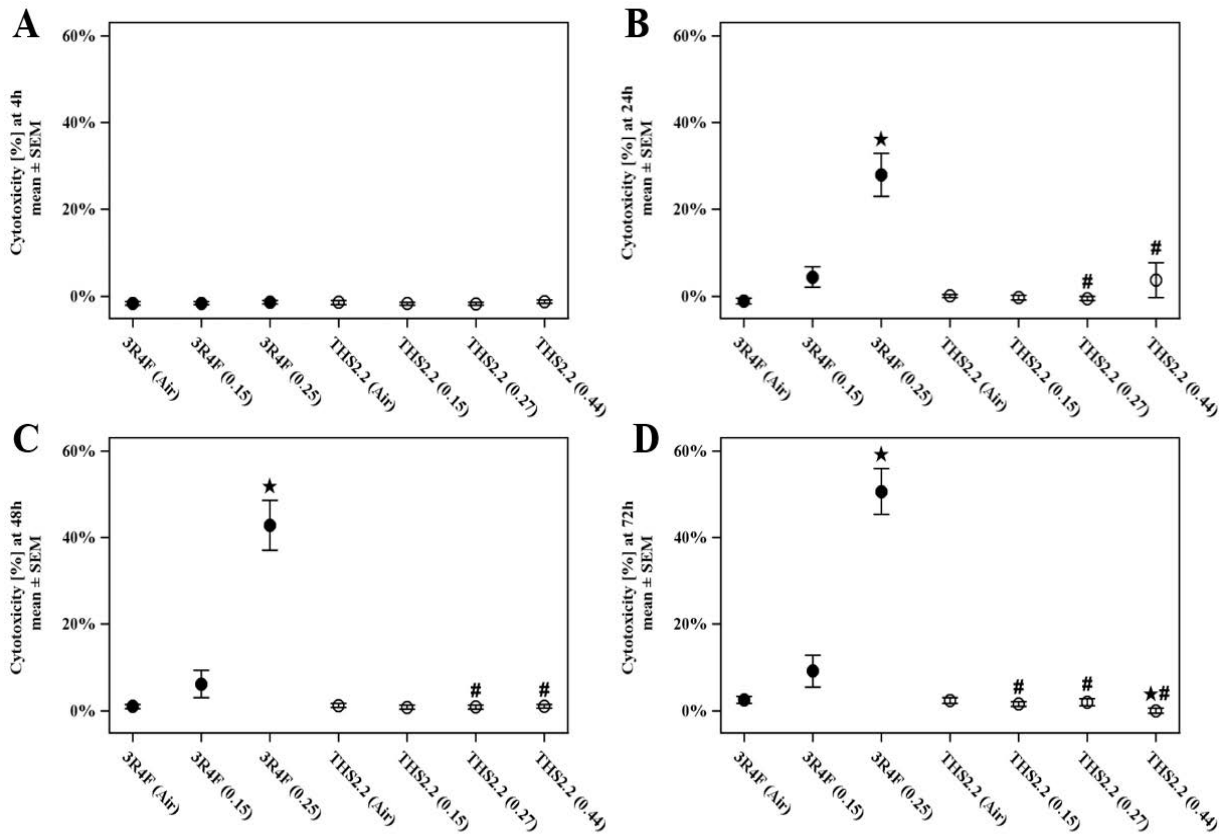



**Figure 7 Cytotoxicity in organotypic cultures following 3R4F and THS2.2 exposure.**

The release of adenylate kinase (AK) into the basolateral media of the cultures was measured 4, 24, 48, and 72 h after exposure to 3R4F smoke or THS2.2 aerosol at the indicated nicotine concentrations (mg/L) for 28 min (**A**–**D**). Data are presented as mean of the normalized cytotoxicity relative to the positive control (Triton X-100 treated culture was taken as 100% cytotoxicity) ± SEM (N = 9–15, from five experimental repetitions with three exposure runs/repetition) ★ indicates a significant difference compared with the corresponding air controls ($p$-values <0.05). # indicates a significant difference as compared with 3R4F ($p$-values <0.05): THS2.2 (0.15) vs. 3R4F (015), or THS2.2 (0.27) vs. 3R4F (0.25), or THS2.2 (0.44) vs. 3R4F (0.25).

### 9.4 Cytochrome P450 (CYP) 1A1/1B1 Activity

The combined CYP1A1 and CYP1B1 activity was measured in the organotypic nasal cultures following exposure. At the 24 h post-exposure time point, neither 3R4F smoke nor THS2.2 aerosol were associated with substantial changes in the CYP1A1/1B1 activity (Figure 8A). At 48 and 72 h post-exposure (Figure 8B-C), 3R4F (0.15)-exposed samples had greater CYP1A1/1B1 activity than the air controls (approximately 12 % increase); however, the CYP1A1/1B1 activity in the 3R4F (0.25)-exposed group was similar to that of the controls. At 48 h post-exposure (Figure 8B), a slight increase of CYP1A1/1B1 activity was detected in the THS2.2-exposed groups compared with the air control (2–6 % increases). At 72 h post-exposure, negligible increases of CYP1A1/1B1 activity were detected in the THS2.2 (0.15)- and (0.27)-exposed cultures regardless of the statistically significant differences (Figure 8C). Descriptive statistics of these results are reported in Supplementary Table 14.

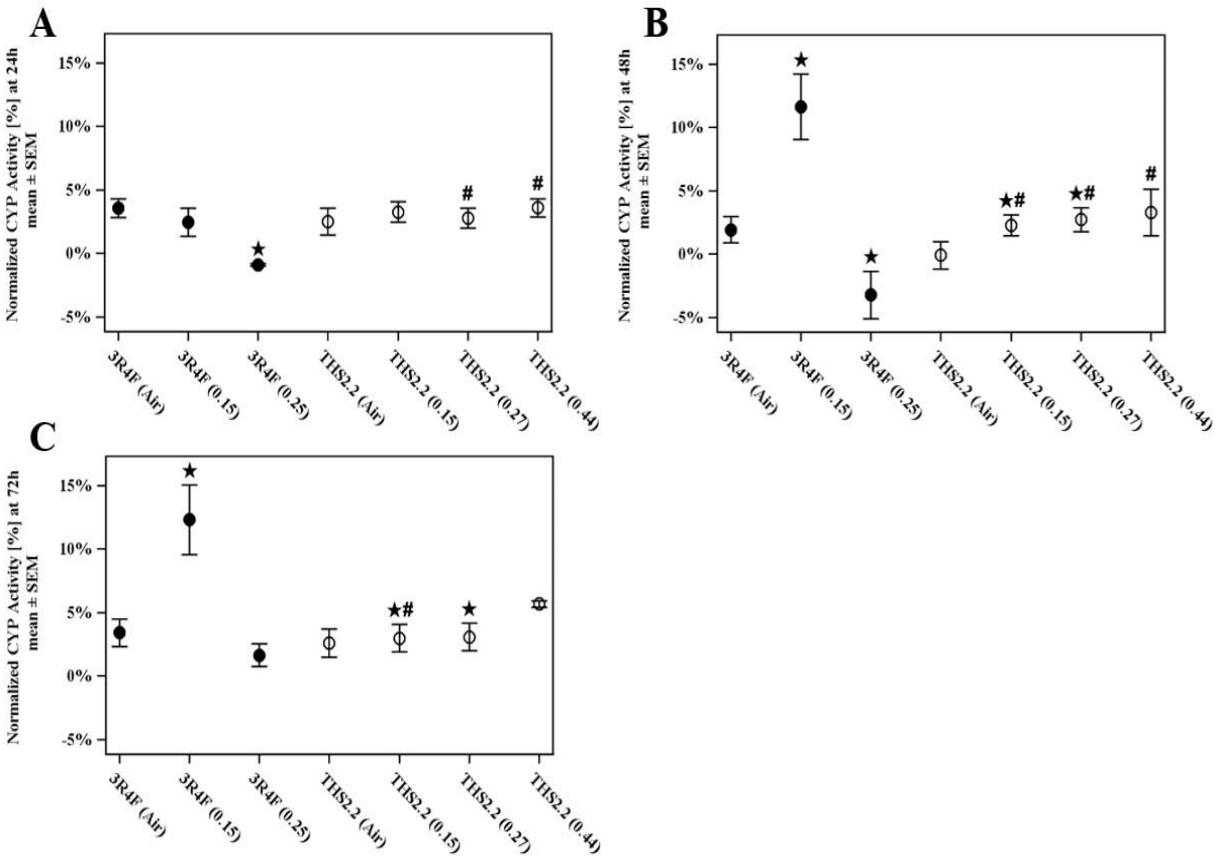



**Figure 8. CYP1A1/CYP1B1 activity following 3R4F and THS2.2 exposure in the organotypic nasal cultures.**

The combined CYP1A1/1B1 activity was measured 24, 48, and 72 h after cultures were exposed to 3R4F smoke or THS2.2 aerosol at the indicated nicotine concentrations (mg/L) for 28 min (**A**–**C**). Data are presented as the mean ± SEM (N = 3–12, from five experimental repetitions with three exposure runs/repetitions) of the normalized activity relative to the positive control (TCDD-treated culture was considered as 100% induction). ★ indicates a significant difference compared with the corresponding air controls (*p*-values <0.05). # indicates a significant difference as compared with 3R4F (*p*-values <0.05): THS2.2 (0.15) vs. 3R4F (015), or THS2.2 (0.27) vs. 3R4F (0.25), or THS2.2 (0.44) vs. 3R4F (0.25).

### 9.5 Secretion of Pro-Inflammatory Mediators

The inflammatory response of the organotypic nasal cultures to exposure was assessed by measuring mediators secreted into the basolateral media of the cultures at 24, 48, and 72 h post-exposure (from different cultures as cross-sectional data). From the 3R4F-exposed cultures, the levels of TIMP1, VEGFA, MMP1, CXCL8, and EGF secreted into the media were greater compared with the air controls (significant fold-changes are highlighted in the heatmap in Figure 9A). These increases in secretion were observed at all post-exposure time points, except for VEGFA. At 72 h post-exposure, VEGFA levels had decreased following 3R4F (0.25) exposure. In contrast, in THS2.2 (0.15)-exposed cultures, VEGFA was the only mediator that was altered (i.e., reduced at 72 h post-exposure, Figure 9A). Moreover, following higher concentrations of THS2.2 aerosol, increased levels of VEGFA were observed (statistically significant increases were found in the THS2.2 (0.44) group at all post-exposure time points measured). Furthermore, the levels of MMP1 and TIMP1 were higher in the THS2.2 groups compared with the corresponding air controls. However, the increased fold-changes of MMP1 and TIMP1 levels in THS2.2-exposed cultures (1.2–1.8-fold increases compared with the controls) was lower than those in 3R4F-exposed cultures (2.1–6.6-fold increases compared with the controls).

A statistical analysis assessing whether the 3R4F-induced levels of the mediators were different from the THS2.2-induced levels, showed that levels of VEGFA TIMP1, MMP1, and CXCL8 in the 3R4F-exposed cultures (in both concentraions tested) remained higher than those in the THS2.2-exposed cultures. The fold-change differences are listed in Figure 9B with the statistically significant difference highlighted. Descriptive statistics of these results are reported in Supplementary Table 15–Supplementary Table 25 and the individual representations of the mediators are reported in Supplementary Figure 1. Additional analytes that were only measured in one experimental repetition (see Table 9) are reported in Supplementary Table 26–Supplementary Table 36).

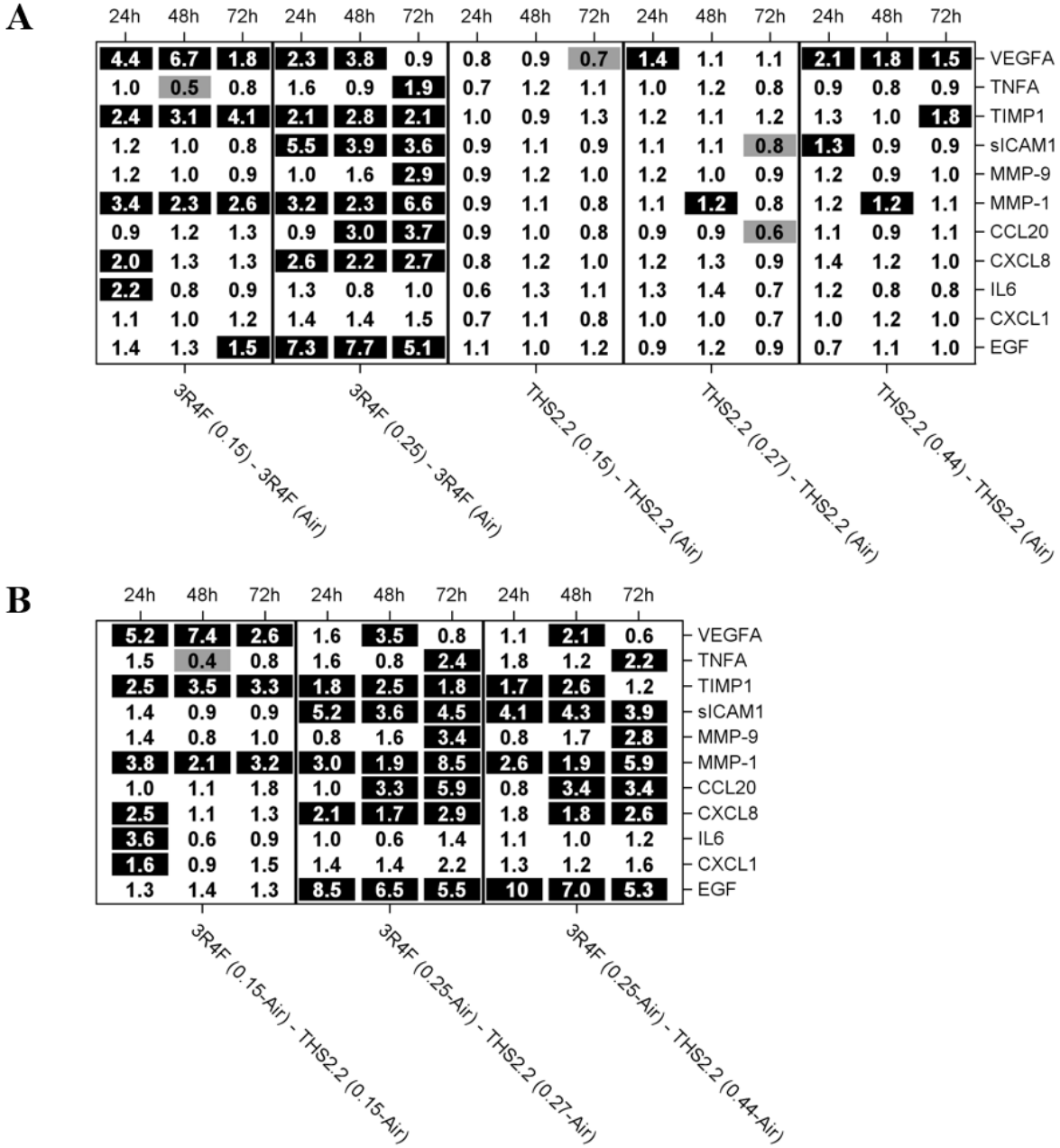



**Figure 9. Fold changes of secretion levels of pro-inflammatory mediators into the basolateral medium of the organotypic nasal cultures following exposure.**

Fold-changes of the concentrations of mediators (listed on the y-axis, right) were measured in the basolateral media of the organotypic nasal cultures 24, 48, and 72 h after they were exposed to 3R4F smoke or THS2.2 aerosol at the indicated nicotine concentrations (mg/L) for 28 min. The fold-changes are expressed relative to the corresponding air controls (N = 9–15, from five experimental repetitions with three exposure runs/repetition) (**A**). Differences between 3R4F- and THS2.2-induced mediator levels are reported as the ratio of the fold-changes (**B**). Dark and light gray shading indicates significant increase and decrease, respectively, between the comparisons ($p$-values <0.05).

## 9.6 Transcriptome of Nasal Epithelial Cultures

### 9.6.1 Differentially Expressed Genes

The investigation of possible toxicity-specific mechanisms associated with 3R4F and THS2.2 exposure was conducted in cultures that exhibited minimal damage. This choice was made to assess toxicity-related mechanisms in surviving cells, instead of reflecting morphological alterations associated only with severely damaged tissue (Haschek 2013) and (Davis 2013). Substantial cytotoxicity (Figure 7) and culture damage (Figure 4) were observed in cultures exposed to the higher nicotine concentration in 3R4F smoke (i.e., 3R4F (0.25)). Consequently, gene expression was evaluated using the transcriptomic data from the 3R4F (0.15), THS2.2 (0.15), THS2.2 (0.27), and THS2.2 (0.44) groups. The gene expression profiles of all these groups are reported in Supplementary Figure 2.

Figure 10 shows the global gene expression changes of the cultures from the four groups collected 4, 24, 48, and 72 h after exposure compared with the corresponding air controls. In all contrasts, the shorter the duration of the post-exposure, the higher the number of genes altered significantly. In addition 3R4F (0.15) smoke exposure was associated with more gene expression changes than THS2.2 (0.15) aerosol exposure at all post-exposure time points. Moreover, at 24, 48, and 72 h post-exposure, the impact of THS2.2 (0.27) and THS2.2 (0.44) aerosols on the gene expression profiles was less than the impact of 3R4F (0.15). Further, at the 4 h post-exposure time point, the number of genes that were altered following THS2.2 exposure (at all concentrations) was less than the number altered following 3R4F (0.15) exposure.

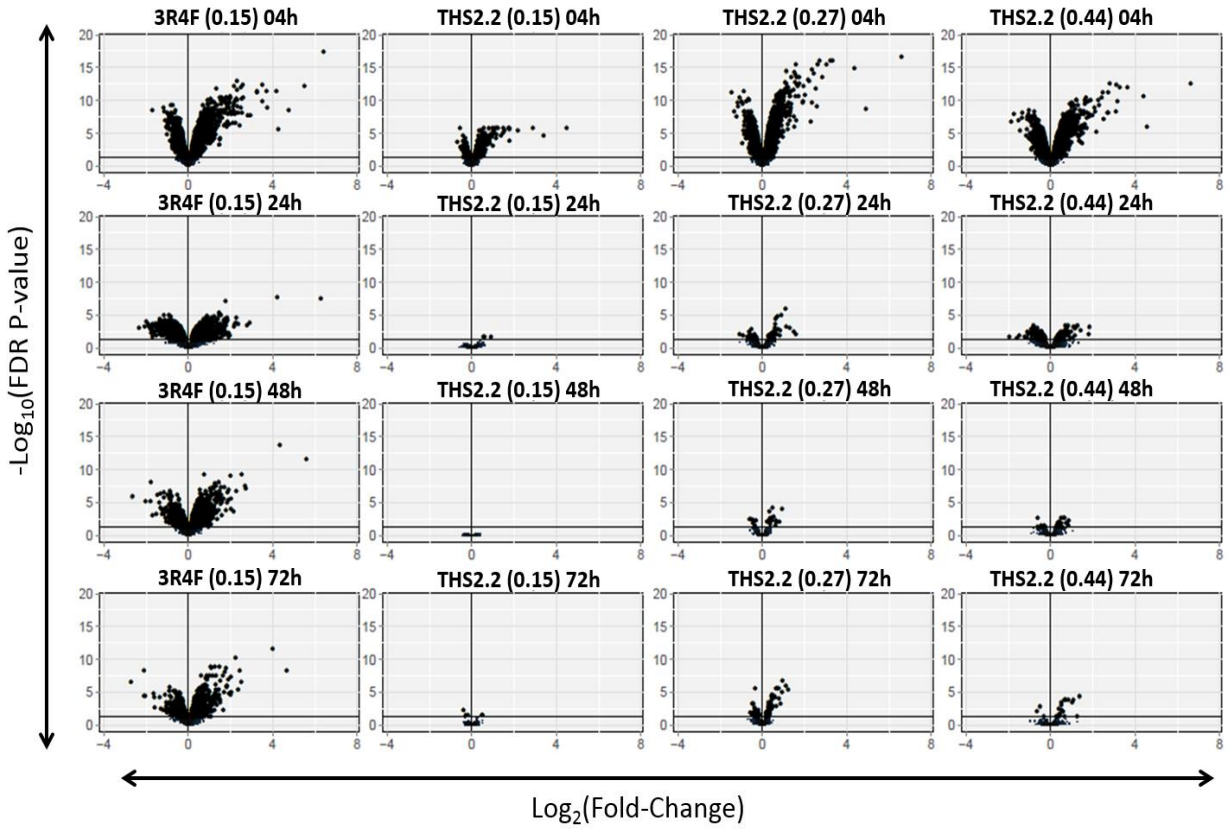



**Figure 10. Volcano plots of the differentially expressed genes in nasal epithelial cultures following exposure.**

Each dot in a plot represents a gene. Gene expression changes (x-axis) are expressed as $\log_2(fold - change)$; increased when >0 and decreased when <0 as compared with the corresponding air controls. The statistical significance (y-axis) is represented as −log10 (adjusted *p*-value FDR) (N = 9–15 from the total of five experimental repetitions with three exposure runs/repetition). The horizontal line represents statistical significance ($-\log_{10}(0.05)$).

### 9.6.2 Biological Impact Factor

The framework used to quantify the impact of exposure on the biological processes leverages the transcriptomic data using a network-based systems biology approach (Hoeng 2014). The approach uses biological network models, which comprise a series of cause-and-effect relationships, representing biological processes involved in Cell Proliferation (CPR), Cell Fate (CFA), Cell Stress (CST), and inflammatory response (IPN, Inflammatory Process Networks) (Boué 2015). The edges of the networks carry a causal directionality (increase or decrease) between two nodes based on information extracted from scientific literature (Martin 2014). The nodes of the networks correspond to biological entities (e.g., protein abundances, protein activities, chemical compounds, or biological processes described as molecular entities) and are referred to as "backbone nodes", which form the functional layer of the network models (Martin 2014).

For many of the backbone nodes, literature-derived knowledge about the ability of that node to regulate the expression of particular genes is included in the network model. Hence, in addition to the model backbone, each model can have a measurable layer consisting of mRNA nodes; the abundance of the mRNA transcripts can vary in transcriptomic data. Thus, The transcriptomic data from the four groups collected 4, 24, 48, and 72 h after exposure (exposed vs. control samples) were used quantitatively to computationally predict the activity/functionality of the functional layer of the network using the Network Perturbation Amplitude (NPA) algorithm (Martin 2014). The algorithm is based on backward reasoning, by which changes in the gene expression are considered as the consequence of the activity of an upstream backbone node. The predicted activation or inhibition of the backbone nodes and the causality of the network edges permit inference and computation on the network as a whole (Martin 2014).

The overall systems impact (the aggregation of the network perturbations) is referred to as the biological impact factor (BIF) (Thomson 2013). Figure 11 shows the overall biological impact, in the context of the biology covered in the network models, for each exposure condition compared with the corresponding air controls. At the 4 h post-exposure time point, 3R4F (0.15) smoke exposure produced the highest impact on the cultues; thus, the relative BIF was set to 100% as the reference (REF). The impact of 3R4F (0.15) exposure decreased with increasing duration of the post-exposure. At the comparable nicotine concentration, the impact of THS2.2 (0.15) aerosol on the cultures at 4 h post-exposure was comparable to that of 3R4F (0.15) at 72 h post-exposure. The impact of the THS2.2 (0.15) aerosol then decreased with increasing duration of the post-exposure.

Moreover, when higher nicotine concentrations of THS2.2 were tested (0.27 and 0.44 mg/L), the greatest impact on the cultures was still observed at the 4 h post-exposure time point. The pattern of BIF—which was decreasing with the duration of post-exposure—was similarly observed across all exposure conditions—however, the degree of impact attributed to THS2.2 exposure (at any of the tested concentrations) was considerably lower than that attributed to 3R4F exposure.

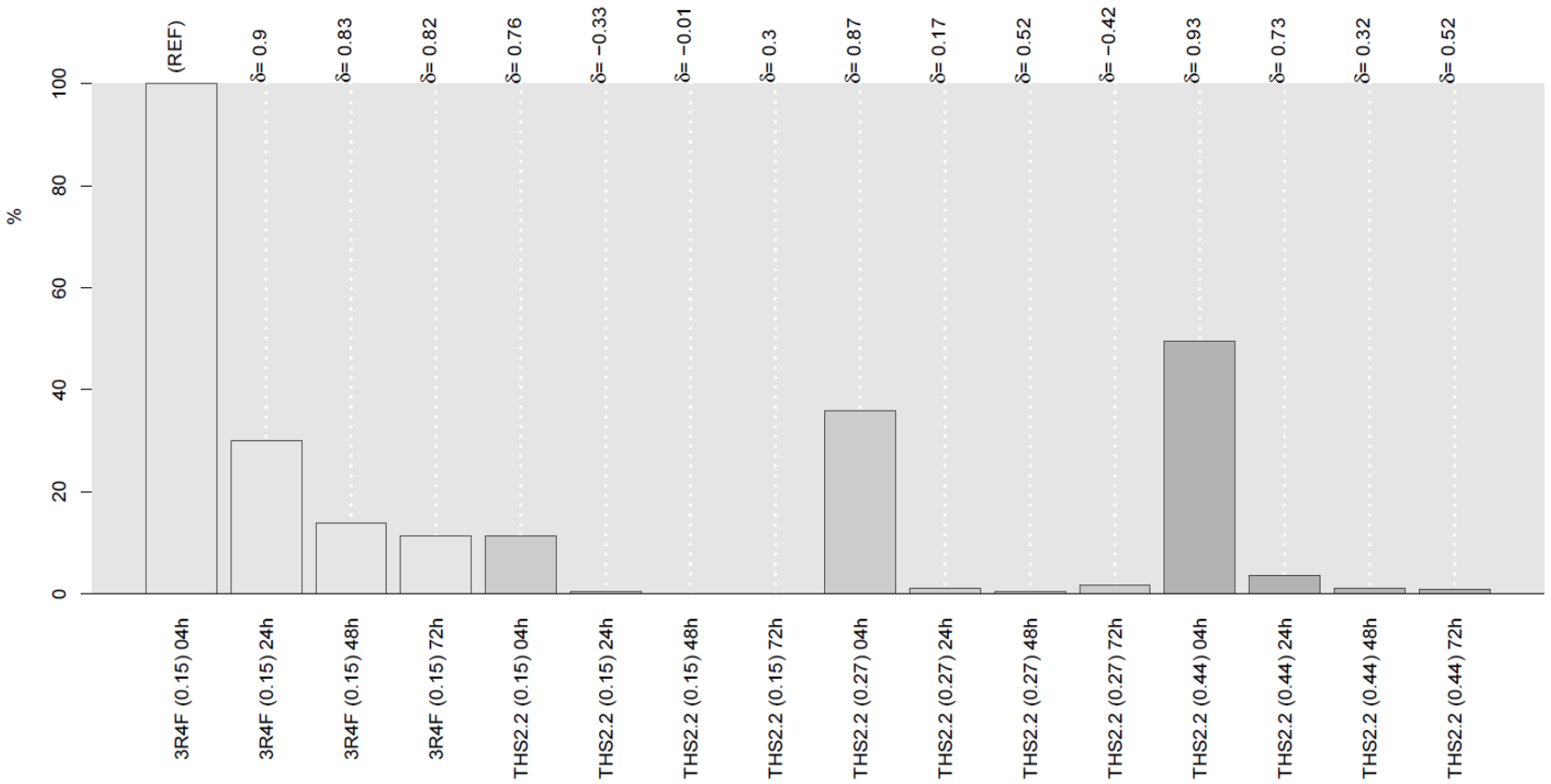



**Figure 11. Relative biological impact factor (BIF) derived from cumulated network perturbations impacted by 3R4F and THS2.2 exposure compared with the air controls.**

The relative BIF (in percent) is plotted on the *y*-axis. The highest BIF is labelled REF and was used as the 100% point. The δ values (δ in [-1,1]) given above the plot indicate how similar the underlying networks that were perturbed in a particular test were to the underlying networks in the REF, δ = 0 indicating no similarity, δ = 1 indicating identical underlying networks were perturbed, and δ = −1 indicating completely opposite underlying networks were perturbed.

An overview of the different biological processes represented as network families that contributed to the overall BIF for each exposure is given in Figure 12. Pie charts are used to show the contribution of the perturbation of each network family to the BIF. Among the network families, the impact of 3R4F (0.15) smoke and THS2.2 aerosol (at all tested concentrations) was highest on the Cell Stress (CST) network family at all post-exposure time points.




**Figure 12. Contribution of individual network perturbations to the biological impact factor (BIF) analysis.**

Each pie chart represents the corresponding bar in the BIF plot in Figure 11. The charts show the subdivision of BIF into the different network families for each comparison. A pie slice indicates one of the CFA, CST, CPR, and IPN network families. The area of the slices indicates the relative contribution of each network perturbation to the BIF for a given comparison. The pie chart of the REF (the comparison with the highest BIF taken as 100%) is outlined with a thick black line. The relative BIF and the δ value for each comparison are given above each plot The δ values (δ in [-1,1]) indicate the similarity between the underlying networks that were perturbed in the test and the networks that were perturbed in the REF, δ = 0 indicating no similarity, δ = 1 indicating identical networks were perturbed, and δ = −1 indicating exactly opposite networks were perturbed. Abbreviations: CFA, Cell Fate; CST, Cell Stress; CPR, Cell Proliferation; IPN, Inflammatory Process Networks; RBIF, relative BIF.

### 9.6.3 Network Perturbation Amplitude

Each network family consists of a set of network models and the BIF can be decomposed down to the network level. Figure 13 shows the perturbation of each network across the comparisons. The highest BIF in the 3R4F (0.15) at 4 h post-exposure time point (100% BIF) is reflected in the heatmap; at 4 h post-exposure, 3R4F (0.15) produced the highest network perturbation amplitude (NPA) score in the majority of the networks compared with the other comparisons. Mirroring the trend of the BIF pattern, the impact of 3R4F (0.15) on the perturbation of the networks also decreased with increasing duration of post-exposure, with the exception of the Notch and Hedgehog networks (however, their perturbations were not statistically significant). Furthermore, the heatmap shows that all of the networks in the IPN (i.e., Tissue Damage, Epithelial Mucus Hypersecretion, and Epithelial Innate Immune Activation) were impacted by 3R4F (0.15) at all post-exposure time points. The impact of 3R4F (0.15) on Cellular Stress (within the Cell Stress network family) at all post-exposure time points was reflected by perturbations in the Xenobiotic Metabolism Response, Oxidative Stress, and NFE2L2 Signaling networks. Further, the Senescence, Response to DNA Damage, and Apoptosis networks (within the Cell Fate network family), were impacted by 3R4F (0.15) exposure at all post-exposure time point. Within the Cell Proliferation network family, 3R4F (0.15) exposure impacted mainly the MAPK, Jak Stat, and Growth Factor networks at all post-exposure time points.

In contrast, at the comparable nicotine concentration, THS2.2 (0.15) aerosol exposure did not result in substantial perturbations of these networks; the exposure had minimal impact on the cultures, but was most pronounce at 4 h post-exposure. Exceptions were observed for the Apoptosis, Xenobiotic Metabolism Response, and Oxidative Stress networks, which were impacted at 72 h post-exposure. However, the NPA scores were relatively lower than those observed in cultures exposed to 3R4F (0.15) smoke at 72 h post-exposure. Moreover, it was only at the higher nicotine concentrations (0.27 and 0.44 mg/L) that the THS2.2 aerosol-exposed cultures were impacted at all post-exposure time points, as indicated by the NPA scores for the Senescence, Apoptosis, Xenobiotic Metabolism Response, and NFE2L2 signaling networks. Nevertheless, the degree of impact (i.e., their NPA scores) was lower compared with the impact of 3R4F (0.15) at the corresponding post-exposure time points.

A gene-set analysis was also conducted and the results are reported as a heatmap of the enrichment scores (Supplementary Figure 3). The heatmap shows that the gene expression data from the cultures exposed to 3R4F (0.15) had higher enrichment scores for the various biological annotations compared with the data from the cultures exposed to all three nicotine concentrations of THS2.2 aerosol at any given post-exposure time-point. This finding is consistent to the results obtained based on the NPA scores, where higher signals (i.e., enrichment scores) were observed with the shorter post-exposure duration.

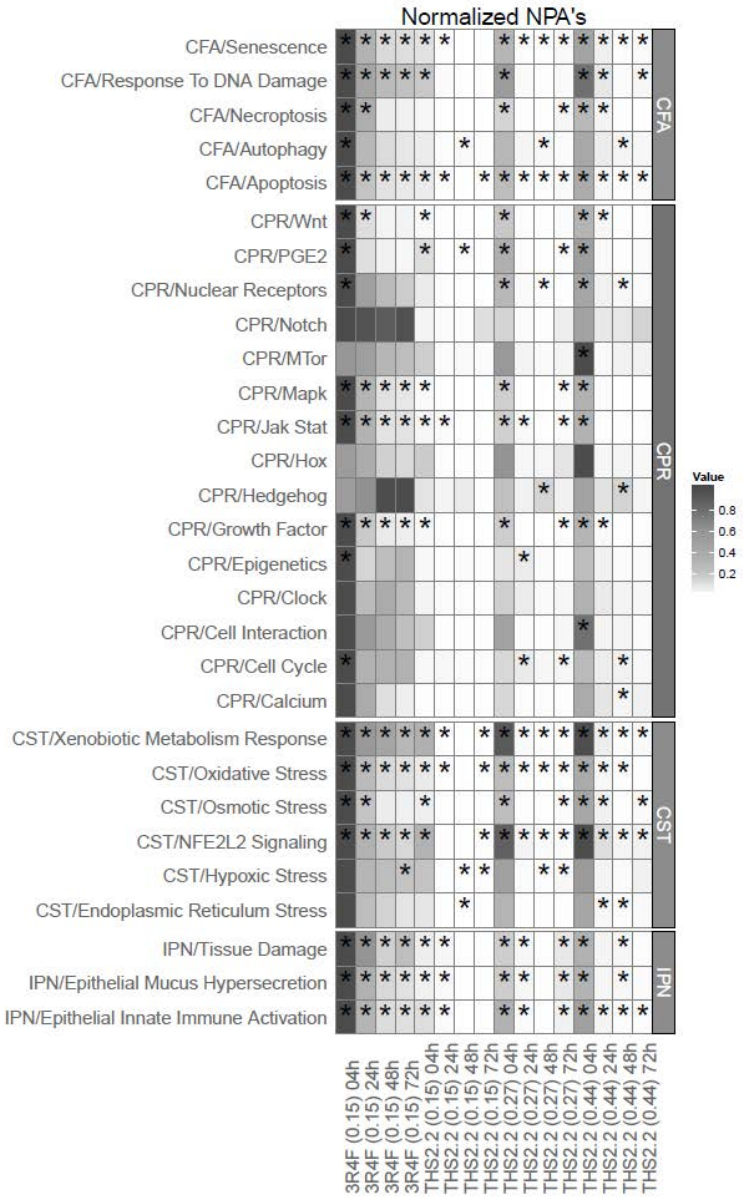



**Figure 13. Heatmap of network perturbation amplitude (NPA) scores of biological networks impacted by 3R4F and THS2.2 exposure.**

The network names are listed on the left side of the heatmap with the corresponding network family on the right side of the heatmap. All networks that were significantly impacted in at least one comparison are listed. The shading gradient of the NPA score was normalized to the maximum NPA score per network. A network was considered significantly perturbed if the NPA score was significant after accounting for experimental variations and if the companion statistics O and K were significant ($p$-values <0.05). The O and K statistics indicate the specificity of the NPA score with respect to the biology represented by each network. *indicates significant NPA scores with respect to the experimental variation and with significant O and K statistics. Abbreviations: CFA, Cell Fate; CST, Cell Stress; CPR, Cell Proliferation; and IPN, Inflammation Process Networks.

### 9.6.4 Alterations of the Expression Levels of Genes Regulating Cell Stress and Inflammation

In addition to the network analysis, alterations of relevant genes known to regulate oxidative stress and inflammation processes are displayed in Figure 14 and Figure 15, respectively.

Increased expression of many of the genes regulating oxidative stress was observed in 3R4F (0.15)-exposed cultures at all post-exposure time points: *SLC7A11*, *HMOX1*, *FTL*, *FTH1*, *GSR*, *GCLC*, *NQO1*, *GPX2*, *TXNRD1*, *GCLM*, *SQSTM1*, and *GPX3*, as well as *MAFG* and *MAFF* (Figure 14, upper right panel). The majority of these genes are regulated by the NRF2 transcription factor (also known as NFE2L2); whereas, MAFG and MAFF play roles in regulating the intracellular location of NRF2, thus contributing to its transcriptional activity. The expressions of the majority of these genes increased only at the earlier post-exposure time points in THS2.2-exposed cultures.

Furthermore, the expressions of many genes involved in the Xenobiotic Stress network (Figure 14, lower right panel) increased in 3R4F (0.15)-exposed cultures. At all post-exposure time points, the expression levels of *CYP1A1* and *CYP1B1* increased more than the expression levels of the genes listed above following 3R4F (0.15) smoke exposure. Additionally, 3R4F (0.15)-exposed cultures had increased levels of *TIPARP*, *AHRR*, *ALDH3A1*, *AKR1C3*, and *AKR1B10* at all post-exposure time points. In contrast, at the comparable nicotine concentration, THS2.2 (0.15), the expression levels of these genes increased at 4 and 24 h post-exposure; however, the increased expression levels of these genes in the THS2.2-exposed cultres (at all concentrations) were lower than those in 3R4F (0.15).

The expression levels of genes related to DNA damage, ER stress, heat shock, and hypoxic stress (Figure 14, left panels) were altered in 3R4F (0.15)-exposed cultres at different post-exposure time points. In THS2.2 (0.15)-exposed cultures, the expression of only a few of these genes was altered, and it was only at the higher nicotine concentrations, THS2.2 (0.27) and THS2.2 (0.44), mostly at 4 h post-exposure. In addition, both 3R4F smoke and THS2.2 aerosol (at all tested concentrations) did not majorly affect the genes regulating Osmotic stress (Figure 14, lower left panel).

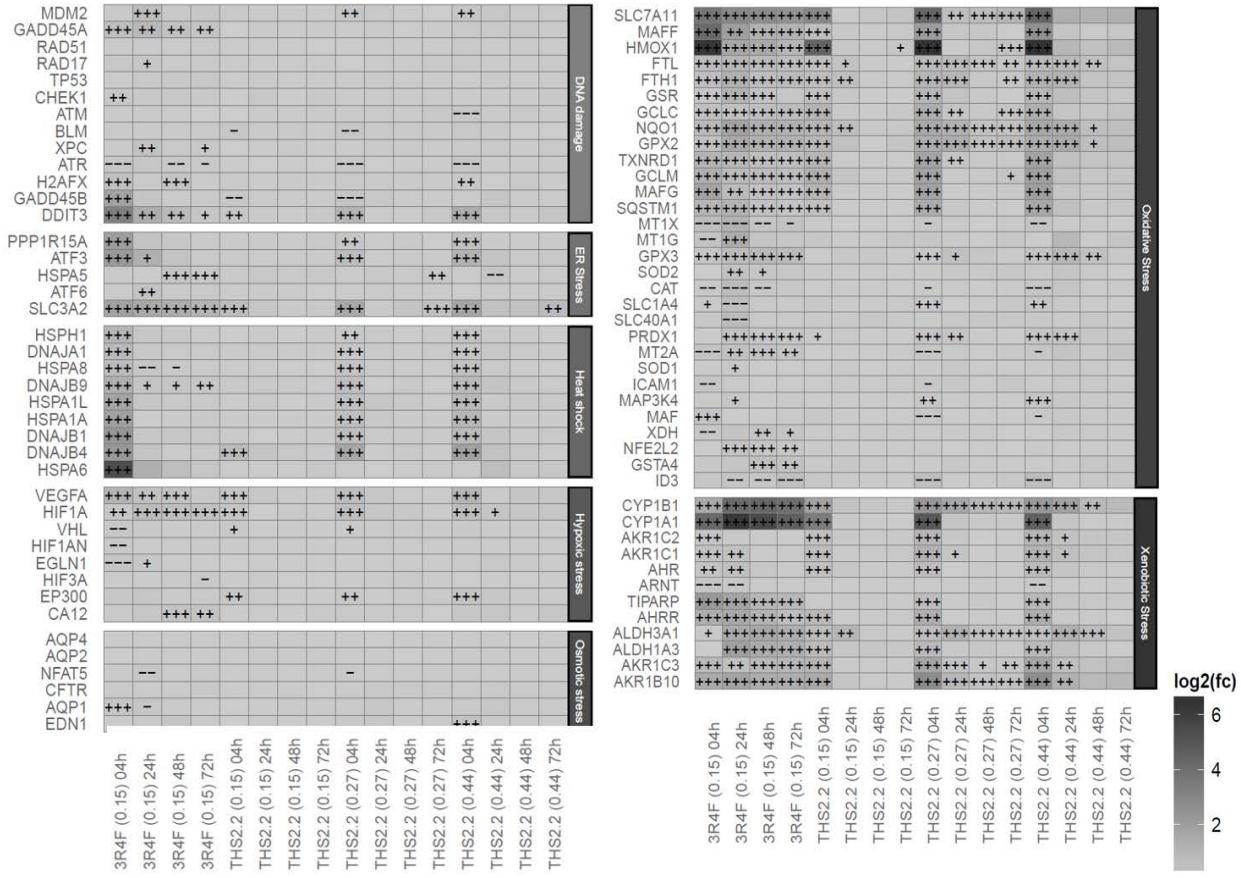



**Figure 14. Altered expression levels of genes regulating cellular stress after 3R4F and THS2.2 exposure.**

The heatmap shows changes in gene expression expressed as $\log_2(fold-change)$. Up- and down-regulated gene expression levels compared with the corresponding air controls are marked with + and − signs, respectively (+++ and −−− indicate adjusted *p*-values <0.01; ++ and −− indicate adjusted *p*-values <0.05; and + and − indicate adjusted *p*-values <0.1). Gene symbols are listed on the left of the heatmap. Stress-related processes are marked on the right of the heatmap. Abbreviation: fc, fold change.

3R4F (0.15)-exposure substantially altered the expression levels of genes important for the culture inflammatory response (Figure 15). At the comparable nicotine concentration, THS2.2 (0.15) minimally influenced the expression of these genes, if at all; and significant changes were observed only for *CEBPB*, *NFKBIA*, *TNF*, and *FOS* only at the 4 h post-exposure time point. Moreover, although more genes were altered after exposure to THS2.2 (0.27) and THS2.2 (0.44), the majority of these changes were observed only at the 4 h post-exposure time-point.

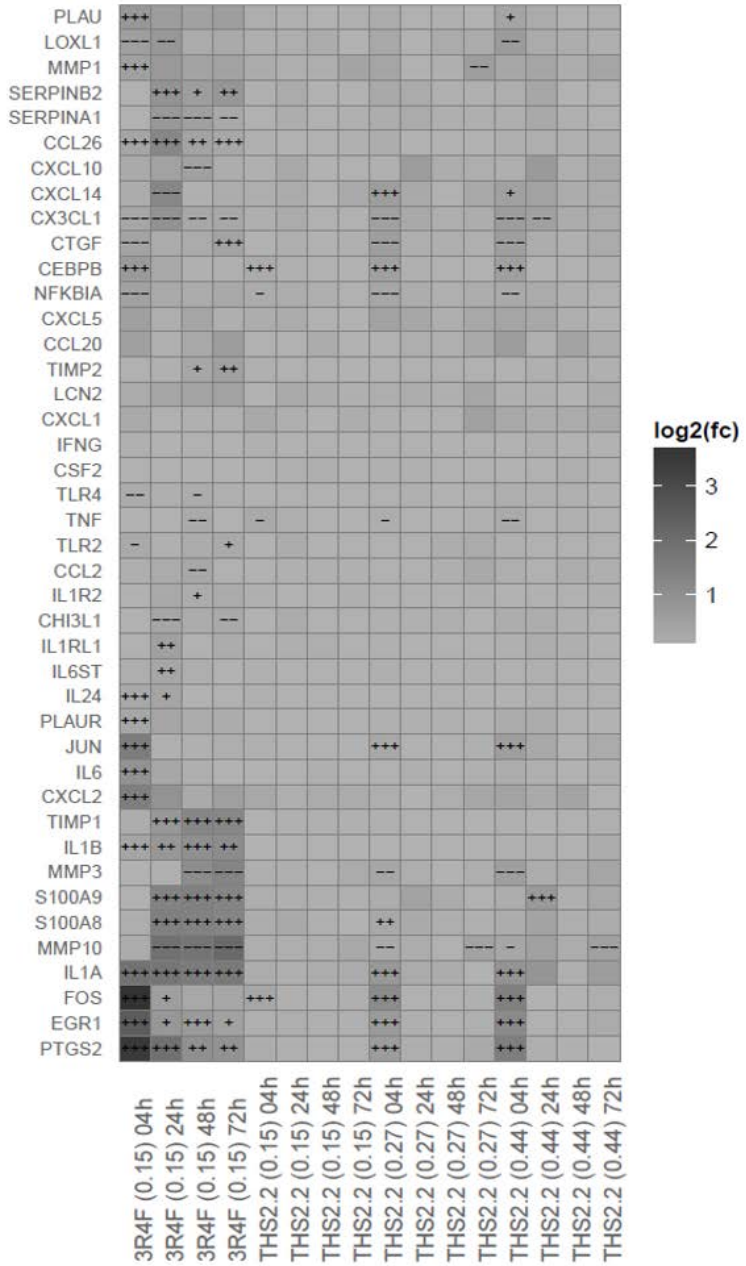



**Figure 15. Altered expression levels of genes regulating inflammation after 3R4F and THS2.2 exposure.**

The heatmap shows the changes in gene expression expressed as $\log_2(fold-change)$. Up- and down-regulated gene expression levels compared with the corresponding air controls are marked with + and − signs, respectively (+++ and −−− indicate adjusted *p*-values <0.01; ++ and −− indicate adjusted *p*-values <0.05; and + and − indicate adjusted *p*-values <0.1). Gene symbols are listed on the left of the heatmap. Abbreviations: fc, fold change.

### 9.7 MiRNA Transcriptome of the Nasal Epithelial Cultures

MiRNAs regulate gene expression and influence many biological processes (Pritchard 2012). Possible mechanisms associated with the 3R4F and THS2.2 exposure responses were further inferred from the miRNA transcriptome data from the nasal epithelial cultures exposed to 3R4F (0.15) and THS2.2 (0.15), THS2.2 (0.27), and THS2.2 (0.44), relative to the corresponding air controls. The profiles of the differentially expressed miRNAs from all exposure groups are reported in Supplementary Figure 4.

The changes in miRNA expression levels following the exposures are shown in Figure 16. Compared with the corresponding air controls, the expression levels of more miRNAs were altered following 3R4F (0.15) exposure than the following THS2.2 aerosol exposure at all the concentrations tested. The longer the post-exposure duration after 3R4F exposure, the higher the number of the miRNAs that were altered. In contrast, the longer the post-exposure duration after THS2.2 aerosol exposure, the lower the number of the altered miRNAs.

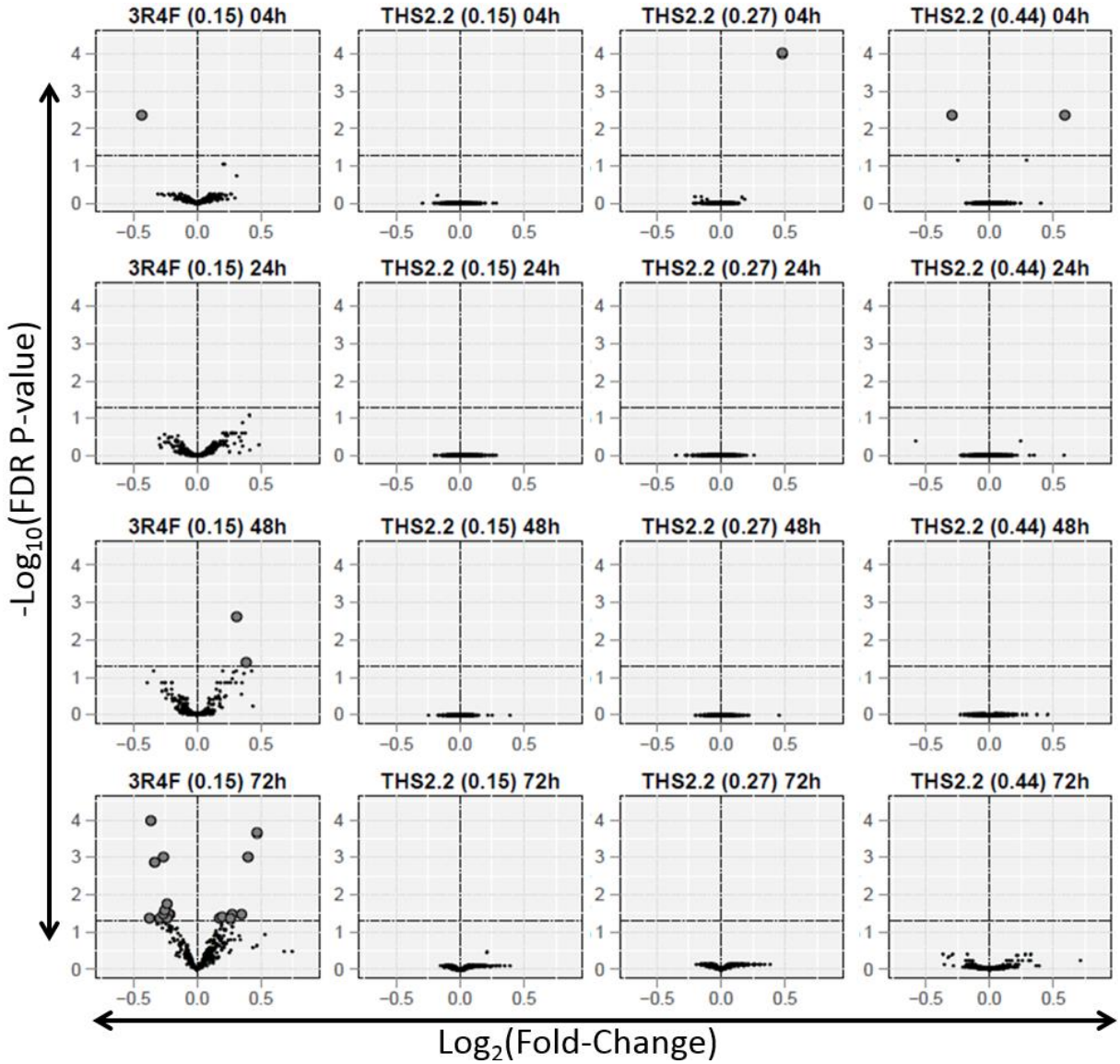



**Figure 16. Volcano plots of the differentially expressed miRNAs in nasal epithelial cultures following exposure.**

Each dot in a plot represents a miRNA. The change in miRNA expression (x-axis) is expressed as $\log_2(fold-change)$; increased when >0 and decreased when <0. The statistical significance (y-axis) is expressed as the $-\log_{10}(adjusted\ p-value)$ (N = 9–15 from the total of five experimental repetitions with three exposure runs/repetition). The threshold line of the statistical significance ($-\log_{10}(0.05)$) is drawn as a solid line (y-axis = 1.3).

Another representation of the global miRNA changes is illustrated as quantile-quantile (QQ) plots (Supplementary Figure 5, for all comparisons). When differentially expressed miRNAs were not markedly visible (as in the volcano plots of the adjusted *p*-values in Figure 16), the QQ plots can provide additional depiction of the miRNA alterations by displaying the similarity of the detected miRNA changes to those of randomly permuted miRNA expression matrices. The QQ plots suggested that 3R4F (0.15) exposure may be related to significant global effects on miRNA expression levels,

which increased with the duration of post-exposure. In contrast to the impact of 3R4F (0.15), THS2.2 exposure at all concentrations tested had a reduced impact on the miRNA expression profiles, and the impact decreased with the duration of post-exposure.

The miRNAs that were significantly altered in at least one comparison are listed in Figure 17. At the comparable nicotine concentration, THS2.2 (0.15) did not impact the expression levels of these miRNAs. However, THS2.2 (0.27)-exposed cultures had increased expression of miR-4521 at 4 h post-exposure, and only at the highest nicotine concentration, was THS2.2 (0.44) exposure associated with reduced expression of miR-27b-5p.

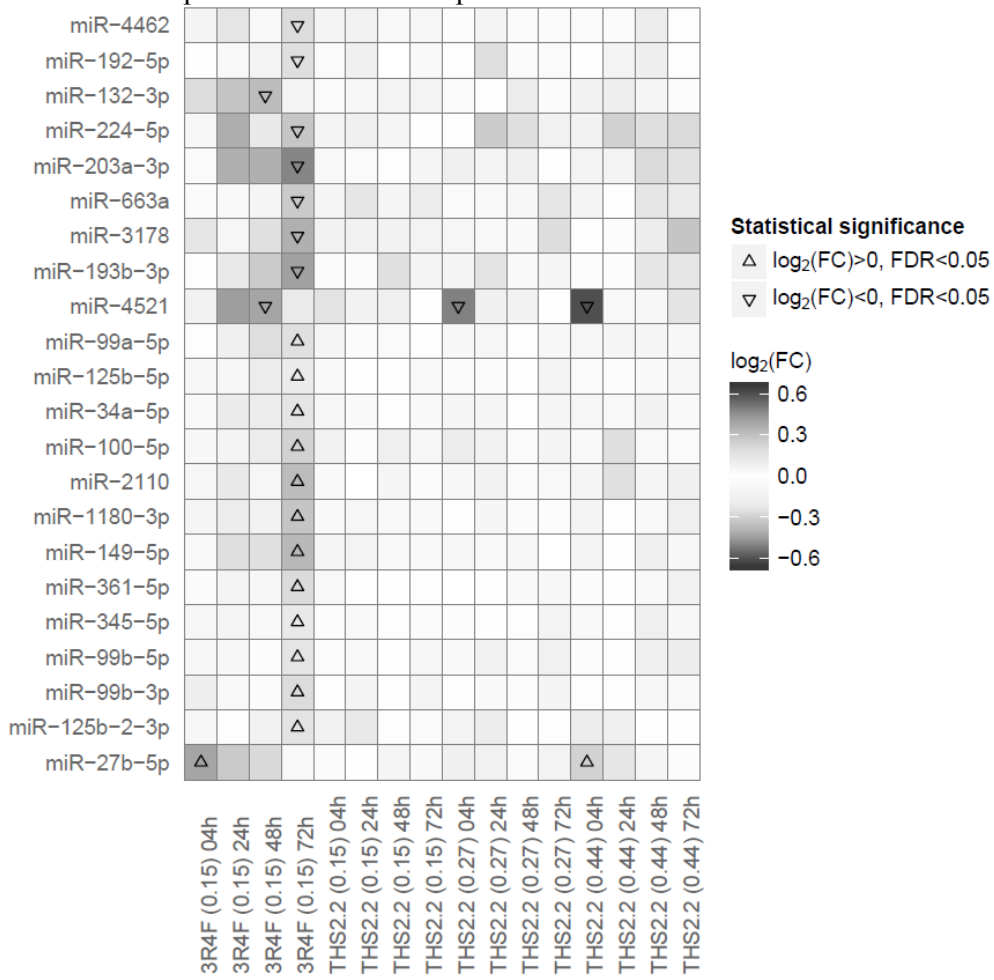



**Figure 17. Heatmap of differentially expressed miRNAs after 3R4F smoke and THS2.2 aerosol exposure.**

The heatmap shows changes in miRNA expression levels expressed as $\log_2(fold-change)$; increased expression when >0 and decreased when <0, compared with the corresponding air controls. The △ and ▽ signs indicate increased and decreased expression levels, respectively (N = 9–15/group from the total of five experimental repetitions with three exposure runs/repetition). The miRNAs that were significantly altered in at least one comparison are listed on the left of the heatmap. The shading indicates the extent of the absolute fold changes compared with the controls.

## 9.8 Correlation of the Outcomes across the Experimental Repetitions

### 9.8.1 Correlation of Immunohistochemistry, Cytotoxicity, CYP1A1/1B1 Activity, and Pro-Inflammatory Mediators across the Experimental Repetitions

To assess the variability of the observation across the experimental repetitions, a correlation of the endpoint values from various functional assays (i.e. immunohistochemistry scores [proportion of the positive stained cells]; normalized cytotoxicity level [based on AK assays]; normalized CYP1A1/1B1 activity level; and the concentrations of the secreted pro-inflammatory mediators [the logarithmic base 10 of the concentration]) were computed. For this, for each of these endpoints and post-exposure time points, the difference (Δ) between the exposed and air control was calculated (i.e. the pair sample, see Statistical Comparisons). Subsequently, we computed the average of these differences; i.e. those obtained in experimental repetitions 1 and 2 (the x-axis, Figure 18) and those obtained in experimental repetitions 3, 4, and 5 (the y-axis, Figure 18). The plots are separated into stimulus exposure type. They illustrate that these averaged values obtained from the experimental repetition 1 and 2, were correlated to those obtained from the experimental repetition 3, 4, and 5. Greater correlations were observed for 3R4F smoke exposure as compared with THS2.2 aerosol exposure. This is consistent with the greater biological impact upon 3R4F exposure (greater cytotoxicity, greater alteration of CYP1A1/1B1 activity, and greater secretion of pro-inflammatory mediators) than upon THS2.2 exposure.

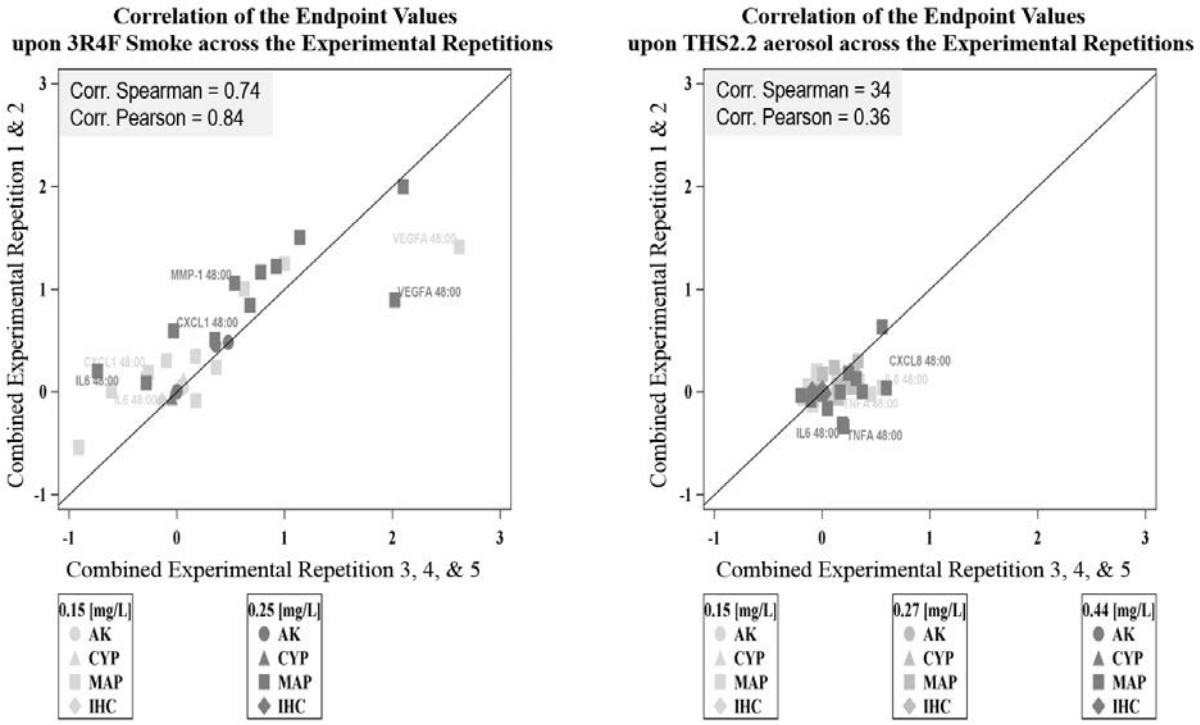



**Figure 18. Correlation plots of the immunohistochemistry, cytotoxicity, CYP1A1/1B1 activity, and pro-inflammatory mediators across the experimental repetitions.**

The average of the differences of the endpoint values (exposed vs. control), which were obtained from the experimental repetition 1 and 2 (x-axis), were correlated to those obtained from the experimental repetition 3, 4 and 5 (y-axis). Different symbols are used to highlight the different endpoints: AK (the normalized cytotoxicity measurement), CYP (the normalized activity of CYP1A1/1B1), and MAP (the logarithm based 10 of the concentration measured using Luminex based analyses of pro-inflammatory mediators), as well as IHC (the proportion of the p63, Ki67, and FoxJ1 positive stained cells). A 45-degree line is drawn to ease the visualization. A Spearman and Pearson correlations were computed. Abbreviations: AK, adenylate kinase; Cor, correlation; CYP, cytochrome P450; Exp; experimental repetition; IHC, immunohistochemistry; MAP, multianalyte profiling.

9.8.2 Correlation of the Gene Expression Fold-Changes across the Experimental Repetitions

Correlation plots were generated to assess the reproducibility of the gene-expression changes obtained from the different experimental repetitions. We first combined the gene expression data from experiments 1 and 2 and generated the average of the fold-changes for each gene in the dataset. Similarly, we combined the combined the gene expression data from experiments 3, 4, and 5 and generated the average of the fold-changes for each gene in the dataset. Finally, correlation plots for the different comparisons were generated with each dot in the correlation plots representing an individual gene (Figure 19).

The plots show that at the different post-exposure time points, the gene expression changes in cultures exposed to 3R4F (0.15) and 3R4F (0.25) were correlated between those obtained in experiments 1 and 2 and those obtained in experiments 3, 4, and 5 (the correlation values were between 0.73 and 0.89). Furthermore, relatively high correlations were observed at 4 h post-exposure following THS2.2 (0.15), THS2.2 (0.27), and THS2.2 (0.44) (their correlation values were between 0.58 and 0.80). However, the correlations were lower between the fold-changes of the gene expression at 24, 48, and 72 h post-exposure to THS2.2 at all concentrations tested, as compared with those at 4 h post-exposure; this is expected because of the minimal following THS2.2 exposure (see Figure 10).

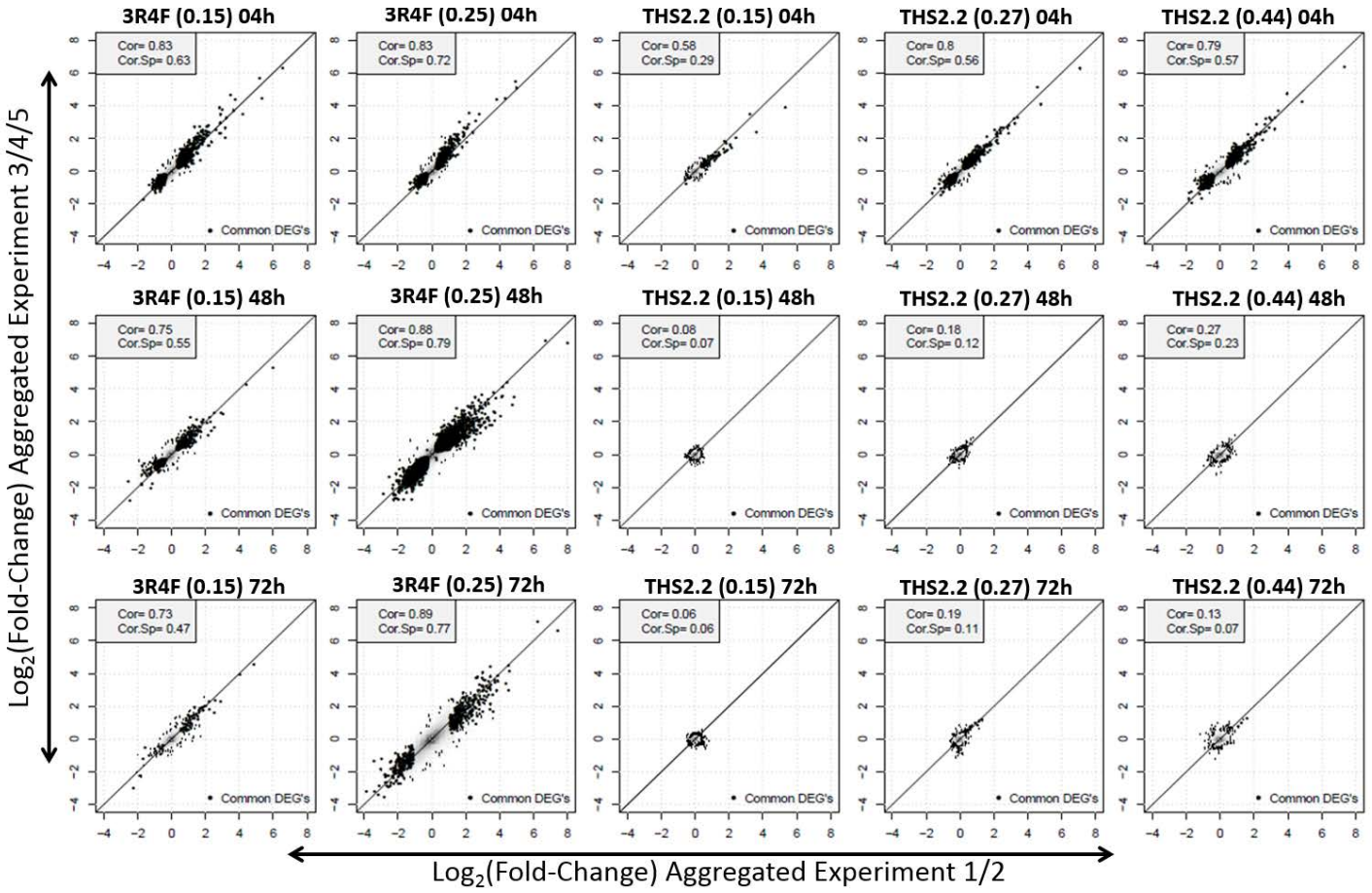



**Figure 19. Correlation plots of gene fold-changes generated from the microarray analysis.**

Each dot represents a gene. The fold-change of a given gene from the combined experiments 1 and 2 (x-axis) was compared with the fold-change of the same gene from the combined experiment 3, 4, and 5 (y-axis). Abbreviations: Corr, correlation; Sp, Spearman correlation; DEG, differentially expressed gene.

### 9.8.3 Correlation of the miRNA Expression Fold-Changes across the Experimental Repetitions

A similar approach (to the one for assessing the reproducibility of the mRNA changes) was used to assess the reproducibility of the miRNA expression changes obtained from the different experimental repetitions. The miRNA expression data from experiments 1 and 2 were combined and used to compute a single value of fold-changes for each of the detected miRNAs. Similarly, the combined data from experiments 3, 4, and 5 were used to compute a single value of the fold-changes of the miRNA. Finally, correlations between the fold-changes for all detected miRNA in the datasets were computed for each comparison (Figure 20).

Good correlations of the miRNA fold-changes were obtained across the experimental repetitions from the cultures exposed to 3R4F (0.25 compared with the air controls, at 48 and 72 h post-exposure (the correlations values were between 0.81 and 0.86). The correlation for 3R4F (0.15) at 72 h post-exposure also was relatively high compared with the others. The correlation data show that the altered miRNA expression levels following the exposures were highly reproducible across the experimental repetitions, especially when the number of the altered miRNAs was high.

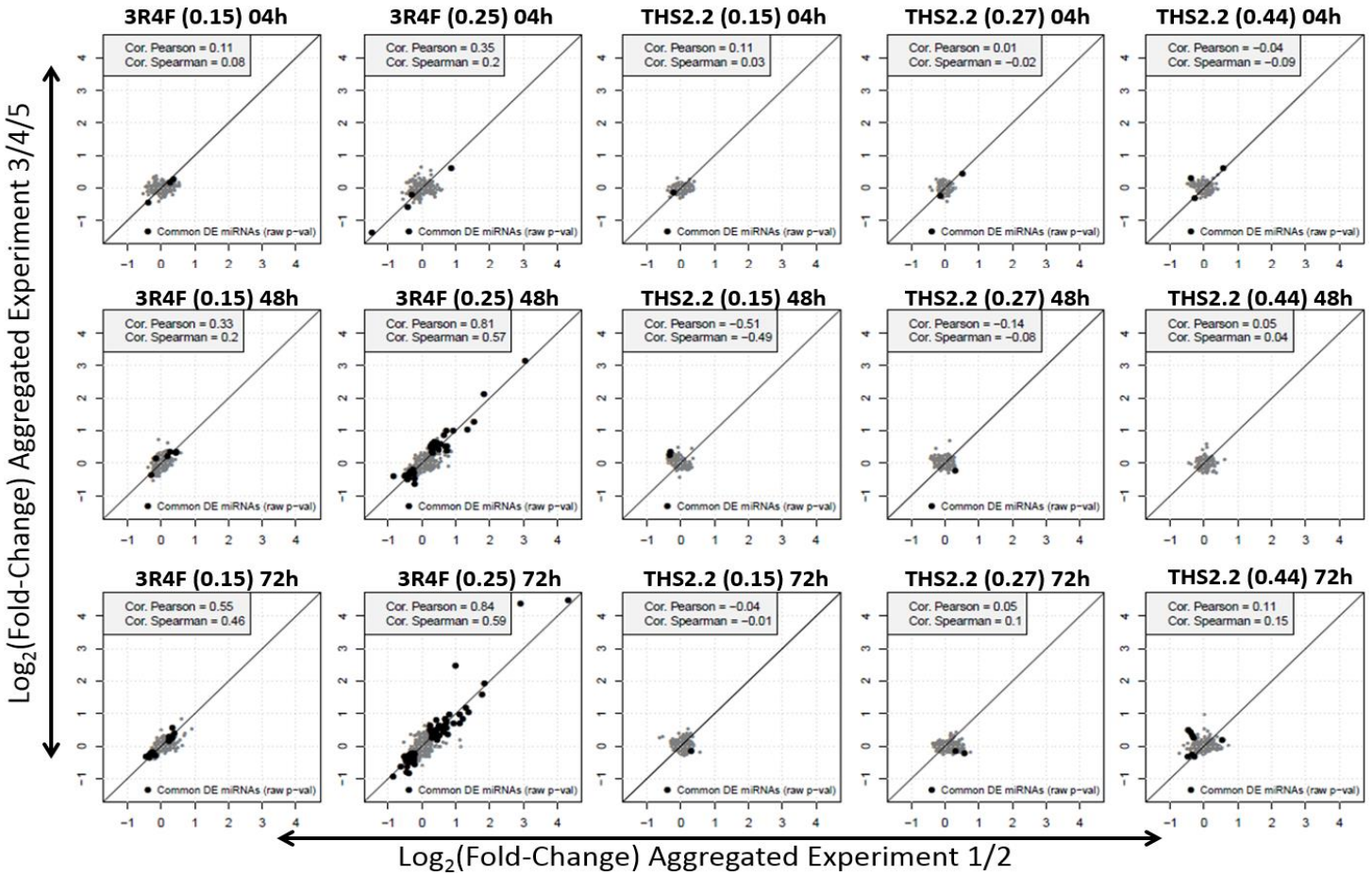



**Figure 20. Correlation plots of miRNA fold-changes generated from the miRNA array analysis.**

Each dot represents a miRNA. The fold-change of a given miRNA from the combined experiments 1 and 2 (x-axis) was compared with the fold-change of the same gene from the combined experiments 3, 4, and 5 (y-axis). Abbreviations: Corr, correlation; Sp, Spearman correlation; DE, differentially expressed.

### 9.9 Dose Range Assessment of THS2.2 Based on the Cytotoxicity and Culture Histology

In addition to the concentrations of the THS2.2 aerosol used in the above experiments, the impact of a wider range of THS2.2 concentrations on cytotoxicity and culture morphology was examined. We assessed the impact at 72 h post-exposure, because the greatest impact on cytotoxicity and overt alterations of the culture morphology were hypothesized to occur at the later time point.

Various dilutions of the THS2.2 aerosol were applied within the Dilution/Distribution Module of the Vitrocell® 24/48 exposure system to assess the impact of the aerosols. Table 12 shows the actual nicotine concentrations measured in the aerosol at the various dilutions that were tested in the dose range assessment. Three independent exposure runs were conducted for this dose range assessment.

**Table 12. Actual Nicotine Concentrations in the THS2.2 Aerosol from the Various Dilutions Applied for the Dose Range Assessment of THS2.2**

| | Dose Range Assessment Experiment Week: 27-Apr-2015 | |
|---|---|---|
| **Group** | **Aerosol Concentrations in the Dilution/Distribution Module of the Vitrocell® 24/48 Exposure System** | **Actual Nicotine Concentrations in the THS2.2 Aerosol** |
| | | **Mean (mg/L) ± SEM** |
| **Air Control (THS2.2)** | - | NA |
| **THS2.2 Dilution 1** | 13% | 0.137 ± 0.009 (N = 3) |
| **THS2.2 Dilution 2** | 23% | 0.223 ± 0.007 (N = 3) |
| **THS2.2 Dilution 3** | 31% | 0.369 ± 0.035 (N = 3) |
| **THS2.2 Dilution 4** | 48% | 0.547 ± 0.066 (N = 3) |
| **THS2.2 Dilution 5** | 60% | 0.766 ± 0.024 (N = 3) |
| **THS2.2 Dilution 6** | 80% | 1.024 ± 0.148 (N = 3) |
| **THS2.2 Dilution 7** | 100% | 1.786 ± 0.055 (N = 3) |

The actual nicotine concentrations for a given aerosol dilutions were obtained from three independent samplings (shown as the mean ± SEM). Abbreviations: SEM, standard error mean; THS, tobacco heating system.

Figure 21 shows the increases of cytotoxicity at 72 h post-exposure in cultures exposed to THS2.2 aerosol at nicotine concentrations above 1 mg/L. The marked cytotoxicity levels were observed following the exposure of THS2.2 (1.02) and THS2.2 (1.79). Descriptive statistics for the cytotoxicity are reported in Supplementary Table 37.

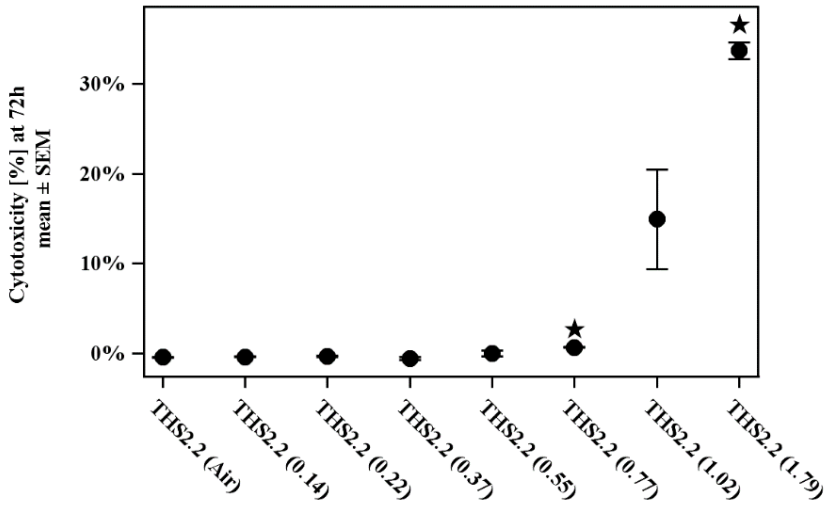



**Figure 21. Cytotoxicity following exposure to various dilutions of THS2.2 aerosol.**

The release of adenylate kinase (AK) into the basolateral media at 72 h post-exposure to THS2.2 aerosol at the indicated nicotine concentrations (mg/L) for 28 min was measured to determine cytotoxicity. The mean cytotoxicity (normalized cytotoxicity relative to the positive control (Triton X-100 treated culture taken as 100% cytotoxicity)) ± SEM (N = 2-3 independent exposure runs; one replicate per exposure run) is shown. ★ indicates a significant difference compared with the corresponding air controls (*p*-values <0.05).

Alterations in the culture morphology, consistent with the levels of cytotoxicity, were observed in the histological sections of THS2.2 (1.02 and 1.79)-exposed cultures collected 72 h after exposure (Figure 22).

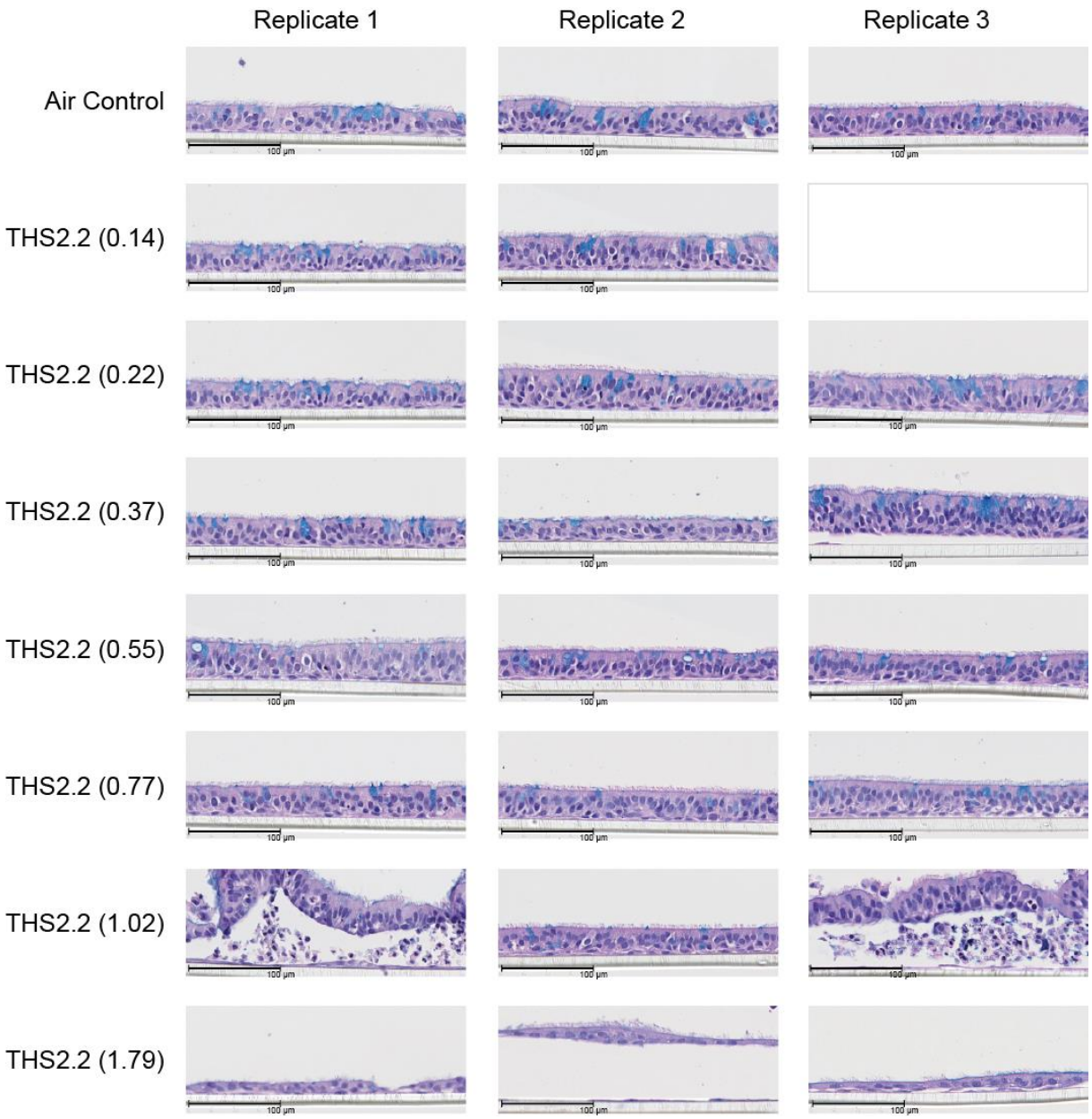



**Figure 22. Histology following exposure to various dilutions of THS2.2 aerosol.**

Culture sections stained with H&E/Alcian blue at 72 h post-exposure to THS2.2 aerosol at the indicated nicotine concentrations (mg/L) for 28 min. One sample is not reported (problem with the sample integrity). Abbreviations: H&E, haematoxylin and eosin.

## 10 DISCUSSION AND CONCLUSION

This study examined the biological effects of exposure to THS2.2 aerosol compared with exposure to 3R4F smoke at comparable nicotine concentrations on the human organotypic nasal epithelial cultures. To minimize the variabilities and increase the robustness of the assessment, this study comprised five experimental repetitions. Within each of the experimental repetitions, three independent exposure runs were performed. The repetitions were performed within approximately a twelve month period. For each of the repetitions, a new batch of nasal cultures was obtained from the supplier. The nasal epithelial cultures used in this study were reconstituted from primary nasal epithelial cells of a single donor: a nonsmoker, 30 year-old male. The choice of using one donor is to reduce the donor-to-donor variability. The results reported here are the aggregated data collected throughout the study period. For each of the exposure run performed using the Vitrocell® 24/48 exposure system, air-exposed cultures were always included (referred to as the air control in this study). The air control is used to isolate the effect of the experimental exposure. Moreover, the study was designed such that the batch effect could be reduced; for example, the variability of the culture batch, operator, reagent, and day of the exposure run and sample collection. These variabilities may lead to improper biological conclusions, because observations due to the batch effect cannot be distinguished from the real biological effects. To explore the associations across the experimental repetitions, the correlation analyses of the various endpoint values were reported. The correlation analyses suggest that the results obtained from the different experimental repetitions were correlated, although we acknowledge that additional sources of variabilities might exist. The correlation analyses suggested that most of the observations were correlated across the experimental repetitions, indicating that the design of the study was considerably robust.

The generation of 3R4F smoke and THS2.2 aerosol was done using two independent smoking machines connected to two different Vitrocell® 24/48 exposure system (each is a dedicated system for 3R4F or THS2.2). The Vitrocell® 24/48 exposure system has a Cultivation Base Module, in which the organotypic nasal cultures were exposed to smoke or aerosol at the air-liquid interface. The suitability of the Vitrocell® 24/48 exposure system for the assessment of smoke exposure has been reported previously (Adamson 2013, Majeed 2014). Because the exposure was done in an air-liquid interface, the set-up permitted exposures that are physiologically relevant to an actual smoking situation. The Vitrocell® 24/48 exposure system also has a Dilution/Distribution Module in which various dilutions of 3R4F smoke or THS2.2 aerosol can be administered. To compare the biological impact of the test aerosol relative to the reference smoke, two of the tested concentrations of THS2.2 aerosol were set at nicotine concentrations that were comparable to those of 3R4F smoke. Moreover, to assess the reproducibility of delivering target nicotine concentrations following the dilutions of smoke/aerosol within the Vitrocell® 24/48 exposure system, samples of the smoke/aerosols (trapped in EXtrelut® 3NT columns) were collected within the same weeks that the experimental repetitions were performed. The data obtained from these samplings revealed that effective adjustments of the dilutions of the smoke/aerosol had reached the target nicotine concentrations.

The impact of 3R4F smoke on cytotoxicity was greater than that of THS2.2 aerosol exposure at any of the concentrations tested. At the comparable nicotine concentrations in the smoke/aerosol (approximately 0.15 and 0.25 mg nicotine/L), the AK release-based cytotoxicity assays showed greater toxicity levels in 3R4F-exposed cultures as compared with THS2.2-exposed cultures at 24, 48, and 72 h post-exposure. This observation was consistent with the histological evaluation, in which

the morphology of the 3R4F (0.25)-exposed cultures displayed some degree of damage (i.e. epithelial thinning) at 48 and 72 h post-exposure. The observed damage following continuous exposure (28 min) to 3R4F smoke at 0.25 mg nicotine/L (equivalent to a dilution of approximately 14% smoke) was consistent with our previously reported observations in bronchial organotypic cultures where, following 15% CS exposure, bronchial epithelial monoculture cultures and bronchial epithelial co-culture with fibroblast both had thinner epithelium than the air-exposed cultures (Iskandar 2015). Thinning of the epithelium was also not observed in the bronchial cultures exposed to a lower concentration of CS (i.e., 8% 3R4F smoke) (Iskandar 2015). Conversely, exposure to THS2.2 aerosol at 0.27 mg nicotine/L was not associated with damage (epithelium thinning), and the morphology of the THS2.2 (0.27)-exposed cultures was similar to that of the air controls. This was also the case for the THS2.2 (0.44)-exposed cultures.

A dose-range assessment of THS2.2 aerosol was conducted to evaluate the likelihood and severity of adverse effects in nasal cultures. The dose range assessment aimed to evaluate the toxicity related to a larger range of THS2.2 aerosol concentrations than was used in the series of experimental repetitions. The assessment showed overt cytotoxicity in the nasal cultures exposed to THS2.2 aerosol with nicotine concentration higher than 1 mg/L aerosol.

A higher number of secreted pro-inflammatory mediators were detected in the basolateral media of nasal cultures exposed to 3R4F smoke than in those exposed to THS2.2 aerosol. We observed increased levels of VEGFA, TIMP1, and MMP1 in 3R4F (0.15 and 0.25)-exposed samples compared with the air controls at 24, 48, and 72 h post-exposure. Moreover, in the higher concentration of 3R4F smoke-exposed samples (i.e., 3R4F containing 0.25 mg nicotine/L, which is equivalent to approximately 14% smoke), increased levels of not only VEGFA and MMP1, but also CXCL8, were observed in the basolateral media. This observation was consistent with our previous finding in organotypic nasal epithelial cultures that were subjected to repeated exposures of 16% CS (Talikka 2014). Talikka et al. reported increased levels of VEGFA, MMP1, and CXCL8 in the basolateral media of nasal cultures following four repeated exposures to 16% CS. Furthermore, Mathis et al. reported increased levels of MMP1 in the basolateral media of organotypic bronchial cultures following various durations of exposure to 15% CS (Mathis 2013). Additionally, in contrast to the effects of 3R4F smoke, we found that at the comparable nicotine concentrations, THS2.2 (0.15 and 0.27) aerosol only minimally altered the levels of VEGFA and MMP1 secreted in the basolateral media. Moreover,. THS2.2 (0.15 and 0.27) aerosol exposure did not significantly impact the levels of secreted CXCL8.

The activity of the xenobiotic metabolizing enzymes CYP1A1 and CYP1B1, which are involved in the metabolism of tobacco smoke constituents (Anttila 2011, Port 2004), were examined in the nasal cultures following 3R4F smoke or THS2.2 aerosol exposure. CYP-mediated reactions contribute to the generation of toxic metabolites that can bind to DNA and form DNA adducts, which can interfere with normal DNA replication resulting in gene mutations that can lead to malignant transformation (Anttila 2011, Port 2004). CYP1A1 and CYP1B1 are the major enzymes metabolizing nitrosamines and PAHs abundant in CS (Hukkanen 2002). CS exposure is linked to the increased CYP1A1/CYP1B1 activity (Hukkanen 2002, Hussain 2014). The results further indicated that the prominent 3R4F (0.25)-induced toxicity (thinning of the nasal epithelium cultures and increased cytotoxicity level) also impacted the metabolic capacity of the cultures, i.e. the culture capability to metabolize nitrosamines and polycyclic aromatic hydrocarbons, which are abundant in CS (Hukkanen

2002). It was observed that, at 48 and 72 h post-exposure, the activity of CYP1A1/CYP1B1 in the 3R4F (0.25)-exposed cultures were comparable to the air control. This finding is consistent with our previous observation in human 3-D bronchial culture models (Iskandar 2015). Moreover, in 3R4F (0.15)-exposed cultures, where the epithelium remained intact (no thinning), an increased level of CYP1A1/CYP1B1 activity was detected in 3R4F (0.15) group at 48 and 72 h post-exposure. In contrast, the levels of CYP1A1/CYP1B1 activity in THS2.2-exposed culture (at all concentrations tested) were nearly comparable to the air control. This results could infer a lower presence of nitrosamines and polycyclic aromatic hydrocarbons in THS2.2 aerosol, as compared with that in 3R4F smoke (at all concentrations tested).

Furthermore, the present study further aimed to deduce the exposure-related mechanisms associated with 3R4F smoke and THS2.2 aerosol by evaluating the expressions of global mRNA and miRNA of the cultures. Because substantial damage was observed in cultures exposed to 3R4F (0.25) smoke — as was evident in the histological sections and reflected by the greater degree of cytotoxicity (AK release) as well as the lack of CYP1A1/CYP1B1 activity — the molecular changes detected in these cultures could not be used to evaluate the exposure impact on the toxicity-related mechanisms. Any changes would simply have reflected the damage that had already occurred (Davis 2013). Therefore, exposure-related mechanisms were investigated from the mRNA and miRNA expression profiles of the cultures with minimal damage: 3R4F (0.15 mg nicotine/L), and THS2.2 (0.15, 0.27, and 0.44 mg nicotine/L). A network-based systems biology approach, which leveraged the gene expression data, was used to reveal the biological impact of the exposures. This approach has been used successfully to deduce the impact of CS exposure on various organotypic epithelial culture models (Iskandar 2015, Schlage 2014, Talikka 2014). The analysis indicated that the impact of the exposures was more pronounced at the earlier post-exposure time points for all exposure groups. The impact on the network perturbations of 3R4F smoke containing 0.15 mg nicotine/L (equivalent to approximately 8% CS) decreased with the longer post-exposure times; this observation was similar to our previous finding in organotypic nasal and bronchial cultures (Iskandar 2015, Talikka 2014). The present study further demonstrated that greater perturbation of various biological networks occurred in the 3R4F (0.15)-exposed cultures compared with the THS2.2-(0.15)-exposed cultures. Additionally, the degree of network perturbations in the cultures exposed to THS2.2 (0.27 and 0.44) were lower than in the cultures exposed to 3R4F (0.15) at all post-exposure time points.

The overall findings show a greater impact of 3R4F smoke exposure on the nasal cultures compared with THS2.2 aerosol exposure at comparable nicotine concentrations, although a donor-specific factors cannot be excluded. Such donor-specific attributes could influence the nasal culture responses (e.g., undetected genetic variations may have influenced the outcome of the experiment). Future studies using a larger number of donors could be done to confirm the observations reported here.

## 11 ARCHIVING

After completion of the study, the study plan with any amendment, the test and reference item retention samples, all raw data, the report with any amendment, and all study-related records needed to reconstruct the study will be archived. They will be retained for at least 10 years according to the applicable archiving procedures. Paper records will be archived in the archive at Philip Morris Products S.A., Research & Development, PMI Product Testing, Neuchâtel Switzerland and electronic records will be managed by PMI Product Testing e-archivist on the central archiving server at Philip Morris S.A., Lausanne, Switzerland.

# 12 REFERENCES

## 12.1 Literature

Ackermann M, Strimmer K. A general modular framework for gene set enrichment analysis. BMC Bioinformatics. 2009;10(1):47. doi: 10.1186/1471-2105-10-47. PubMed PMID: doi:10.1186/1471-2105-10-47.

Adamson J, Thorne D, Dalrymple A, Dillon D, Meredith C. Assessment of cigarette smoke particle deposition within the Vitrocell(R) exposure module using quartz crystal microbalances. Chem Cent J. 2013;7:50. Epub 2013/03/19. doi: 10.1186/1752-153X-7-50
1752-153X-7-50 [pii]. PubMed PMID: 23497606; PubMed Central PMCID: PMC3635897.

Affymetrix miRNA 3.0 Array. GeneChip miRNA 3.0 Array: 902019. Available at: //affymetrix.com/catalog/131473/AFFY/miRNA-Array#1_1.

Affymetrix miRNA QCT Tool. Affymetrix miRNA QCTool: User's Guide. Available at: //media.affymetrix.com/support/downloads/manuals/mirna_qctool_user_manual.pdf. 2011.

Anttila S, Raunio H, Hakkola J. Cytochrome P450-mediated pulmonary metabolism of carcinogens: regulation and cross-talk in lung carcinogenesis. Am J Respir Cell Mol Biol. 2011;44(5):583-90. Epub 2010/11/26. doi: 10.1165/rcmb.2010-0189RT
2010-0189RT [pii]. PubMed PMID: 21097654.

Bascom R, Kesavanathan J, Fitzgerald TK, Cheng KH, Swift DL. Sidestream tobacco smoke exposure acutely alters human nasal mucociliary clearance. Environmental Health Perspectives. 1995;103(11):1026-30. PubMed PMID: PMC1519197.

Benjamini Y, Hochberg Y. Controlling the False Discovery Rate: A Practical and Powerful Approach to Multiple Testing. Journal of the Royal Statistical Society Series B (Methodological). 1995;57(1):289-300. doi: 10.2307/2346101.

Benninger MS. The impact of cigarette smoking and environmental tobacco smoke on nasal and sinus disease: a review of the literature. Am J Rhinol. 1999;13(6):435-8. Epub 2000/01/13. PubMed PMID: 10631398.

Bolstad B, Collin F, Brettschneider J, Simpson K, Cope L, Irizarry R, et al. Quality assessment of Affymetrix GeneChip data. Bioinformatics and computational biology solutions using R and bioconductor: Springer; 2005. p. 33-47.

Bolstad BM, Irizarry RA, Astrand M, Speed TP. A comparison of normalization methods for high density oligonucleotide array data based on variance and bias. Bioinformatics. 2003;19(2):185-93. Epub 2003/01/23. PubMed PMID: 12538238.

Boué S, Talikka M, Westra JW, Hayes W, Di Fabio A, Park J, et al. Causal biological network database: a comprehensive platform of causal biological network models focused on the pulmonary and vascular systems. Database. 2015;2015. doi: 10.1093/database/bav030.

Carvalho BS, Irizarry RA. A framework for oligonucleotide microarray preprocessing. Bioinformatics. 2010;26(19):2363-7. Epub 2010/08/07. doi: 10.1093/bioinformatics/btq431. PubMed PMID: 20688976; PubMed Central PMCID: PMC2944196.

Dai M, Wang P, Boyd AD, Kostov G, Athey B, Jones EG, et al. Evolving gene/transcript definitions significantly alter the interpretation of GeneChip data. Nucleic Acids Res. 2005;33(20):e175. Epub 2005/11/15. doi: 10.1093/nar/gni179. PubMed PMID: 16284200; PubMed Central PMCID: PMC1283542.

Davis MA, Eldridge S, Louden C. Chapter 10 - Biomarkers: Discovery, Qualification and Application. In: Wallig WMHGRA, editor. Haschek and Rousseaux's Handbook of Toxicologic Pathology (Third Edition). Boston: Academic Press; 2013. p. 317-52.

Dimova S, Brewster M, Noppe M, Jorissen M, Augustijns P. The use of human nasal in vitro cell systems during drug discovery and development. Toxicology in vitro. 2005;19(1):107-22.

Gautier L, Cope L, Bolstad BM, Irizarry RA. affy--analysis of Affymetrix GeneChip data at the probe level. Bioinformatics. 2004;20(3):307-15. Epub 2004/02/13. doi: 10.1093/bioinformatics/btg405. PubMed PMID: 14960456.

Goldkorn T, Filosto S, Chung S. Lung Injury and Lung Cancer Caused by Cigarette Smoke-Induced Oxidative Stress: Molecular Mechanisms and Therapeutic Opportunities Involving the Ceramide-Generating Machinery and Epidermal Growth Factor Receptor. Antioxidants & Redox Signaling. 2014;21(15):2149-74. doi: 10.1089/ars.2013.5469. PubMed PMID: PMC4215561.

Harkema JR, Carey SA, Wagner JG. The nose revisited: a brief review of the comparative structure, function, and toxicologic pathology of the nasal epithelium. Toxicologic pathology. 2006;34(3):252-69.

Harvey BG, Heguy A, Leopold PL, Carolan BJ, Ferris B, Crystal RG. Modification of gene expression of the small airway epithelium in response to cigarette smoking. Journal of molecular medicine. 2007;85(1):39-53. doi: 10.1007/s00109-006-0103-z. PubMed PMID: 17115125.

Haschek WM, Rousseaux CG, Wallig MA. Haschek and Rousseaux's handbook of toxicologic pathology: Academic Press; 2013.

Hoeng J, Talikka M, Martin F, Sewer A, Yang X, Iskandar A, et al. Case study: the role of mechanistic network models in systems toxicology. Drug discovery today. 2014;19(2):183-92. Epub 2013/08/13. doi: 10.1016/j.drudis.2013.07.023. PubMed PMID: 23933191.

Huber W, Carey VJ, Gentleman R, Anders S, Carlson M, Carvalho BS, et al. Orchestrating high-throughput genomic analysis with Bioconductor. Nat Methods. 2015;12(2):115-21. Epub 2015/01/31. doi: 10.1038/nmeth.3252. PubMed PMID: 25633503; PubMed Central PMCID: PMC4509590.

Hukkanen J, Pelkonen O, Hakkola J, Raunio H. Expression and regulation of xenobiotic-metabolizing cytochrome P450 (CYP) enzymes in human lung. Critical reviews in toxicology. 2002;32(5):391-411. Epub 2002/10/23. doi: 10.1080/20024091064273. PubMed PMID: 12389869.

Hussain T, Al-Attas OS, Al-Daghri NM, Mohammed AA, De Rosas E, Ibrahim S, et al. Induction of CYP1A1, CYP1A2, CYP1B1, increased oxidative stress and inflammation in the lung and liver tissues of rats exposed to incense smoke. Molecular and cellular biochemistry. 2014;391(1-2):127-36. Epub 2014/02/22. doi: 10.1007/s11010-014-1995-5. PubMed PMID: 24557852.

Huvenne W, Pérez-Novo CA, Derycke L, De Ruyck N, Krysko O, Maes T, et al. Different regulation of cigarette smoke induced inflammation in upper versus lower airways. Respiratory research. 2010;11(1):100.

International Organization for Standardization. ISO 3402: 1999Tobacco and tobacco products -- Atmosphere for conditioning and testing. Available at: //iso.org/iso/home/store/catalogue_tc/catalogue_detail.htm?csnumber=28324.

Irizarry RA, Bolstad BM, Collin F, Cope LM, Hobbs B, Speed TP. Summaries of Affymetrix GeneChip probe level data. Nucleic Acids Res. 2003;31(4):e15. Epub 2003/02/13. PubMed PMID: 12582260; PubMed Central PMCID: PMC150247.

Iskandar AR, Martin F, Talikka M, Schlage WK, Kostadinova R, Mathis C, et al. Systems approaches evaluating the perturbation of xenobiotic metabolism in response to cigarette smoke exposure in nasal and bronchial tissues. BioMed research international. 2013;2013:512086. Epub 2013/11/14. doi: 10.1155/2013/512086. PubMed PMID: 24224167; PubMed Central PMCID: PMCPMC3808713.

Iskandar AR, Xiang Y, Frentzel S, Talikka M, Leroy P, Kuehn D, et al. Impact assessment of cigarette smoke exposure on organotypic bronchial epithelial tissue cultures: a comparison of mono-culture and co-culture model containing fibroblasts. Toxicological Sciences. 2015. doi: 10.1093/toxsci/kfv122.

Jaspers I. Cigarette smoke effects on innate immune mechanisms in the nasal mucosa. Potential effects on the microbiome. Ann Am Thorac Soc. 2014;11 Suppl 1:S38-42. Epub 2014/01/21. doi: 10.1513/AnnalsATS.201306-154MG. PubMed PMID: 24437404.

Jorissen M, Jaspers M. Cilia, Ciliary Movement, and Mucociliary Transport. In: Önerci TM, editor. Nasal Physiology and Pathophysiology of Nasal Disorders: Springer Berlin Heidelberg; 2013. p. 15-25.

Kanehisa M, Goto S, Sato Y, Kawashima M, Furumichi M, Tanabe M. Data, information, knowledge and principle: back to metabolism in KEGG. Nucleic Acids Res. 2014;42(Database issue):D199-205. Epub 2013/11/12. doi: 10.1093/nar/gkt1076. PubMed PMID: 24214961; PubMed Central PMCID: PMC3965122.

Kauffmann A, Gentleman R, Huber W. arrayQualityMetrics--a bioconductor package for quality assessment of microarray data. Bioinformatics. 2009;25(3):415-6. Epub 2008/12/25. doi: 10.1093/bioinformatics/btn647. PubMed PMID: 19106121; PubMed Central PMCID: PMC2639074.

Kentucky Tobacco Research & Development Center. 3R4F Preliminary Analysis. Available at: //ctrp.uky.edu/resources/pdf/webdocs/3R4F%20Preliminary%20Analysis.pdf.

Kern R, Decker J. Functional Defense Mechanisms of the Nasal Respiratory Epithelium. In: Önerci TM, editor. Nasal Physiology and Pathophysiology of Nasal Disorders: Springer Berlin Heidelberg; 2013. p. 27-45.

Kim D-D. In vitro cellular models for nasal drug absorption studies. Drug Absorption Studies: Springer; 2008. p. 216-34.

Kim JS, Rubin BK. Nasal and sinus inflammation in chronic obstructive pulmonary disease. Copd. 2007;4(2):163-6. Epub 2007/05/29. doi: 10.1080/15412550701341228. PubMed PMID: 17530509.

Kozomara A, Griffiths-Jones S. miRBase: annotating high confidence microRNAs using deep sequencing data. Nucleic Acids Res. 2014;42(Database issue):D68-73. Epub 2013/11/28. doi: 10.1093/nar/gkt1181
gkt1181 [pii]. PubMed PMID: 24275495; PubMed Central PMCID: PMC3965103.

Lee HS, Kim J, editors. Cigarette smoke inhibits nasal airway epithelial cell growth and survival. International forum of allergy & rhinology; 2013: Wiley Online Library.

Lieu JE, Feinstein AR. Confirmations and surprises in the association of tobacco use with sinusitis. Archives of otolaryngology--head & neck surgery. 2000;126(8):940-6. Epub 2000/08/02. PubMed PMID: 10922224.

Majeed S, Frentzel S, Wagner S, Kuehn D, Leroy P, Guy PA, et al. Characterization of the Vitrocell(R) 24/48 in vitro aerosol exposure system using mainstream cigarette smoke. Chem Cent J. 2014;8(1):62. Epub 2014/11/21. doi: 10.1186/s13065-014-0062-3
62 [pii]. PubMed PMID: 25411580; PubMed Central PMCID: PMC4236458.

Martin F, Sewer A, Talikka M, Xiang Y, Hoeng J, Peitsch M. Quantification of biological network perturbations for mechanistic insight and diagnostics using two-layer causal models. BMC Bioinformatics. 2014;15 (1):238. doi: 10.1186/1471-2105-15-238.

Mathis C, Gebel S, Poussin C, Belcastro V, Sewer A, Weisensee D, et al. A systems biology approach reveals the dose- and time-dependent effect of primary human airway epithelium tissue culture after exposure to cigarette smoke in vitro. Bioinform Biol Insights. 2015;9:19-35. Epub 2015/03/20. doi: 10.4137/BBI.S19908 bbi-9-2015-019 [pii]. PubMed PMID: 25788831; PubMed Central PMCID: PMC4357630.

Mathis C, Poussin C, Weisensee D, Gebel S, Hengstermann A, Sewer A, et al. Human bronchial epithelial cells exposed in vitro to cigarette smoke at the air-liquid interface resemble bronchial epithelium from human smokers. American Journal of Physiology - Lung Cellular and Molecular Physiology. 2013;304(7):L489-L503. doi: 10.1152/ajplung.00181.2012. PubMed PMID: PMC3627940.

Maunders H, Patwardhan S, Phillips J, Clack A, Richter A. Human bronchial epithelial cell transcriptome: gene expression changes following acute exposure to whole cigarette smoke in vitro. Am J Physiol Lung Cell Mol Physiol. 2007;292(5):L1248-56. Epub 2007/01/16. doi: 10.1152/ajplung.00290.2006. PubMed PMID: 17220372.

McCall MN, Bolstad BM, Irizarry RA. Frozen robust multiarray analysis (fRMA). Biostatistics. 2010;11(2):242-53. doi: 10.1093/biostatistics/kxp059.

McDougall CM, Blaylock MG, Douglas JG, Brooker RJ, Helms PJ, Walsh GM. Nasal epithelial cells as surrogates for bronchial epithelial cells in airway inflammation studies. American journal of respiratory cell and molecular biology. 2008;39(5):560-8.

Moller W, Haussinger K, Ziegler-Heitbrock L, Heyder J. Mucociliary and long-term particle clearance in airways of patients with immotile cilia. Respir Res. 2006;7:10. doi: 10.1186/1465-9921-7-10. PubMed PMID: 16423294; PubMed Central PMCID: PMCPMC1363720.

Nelson HS. Advances in upper airway diseases and allergen immunotherapy. J Allergy Clin Immunol. 2004;113(4):635-42. Epub 2004/04/22. doi: 10.1016/j.jaci.2004.01.741 S0091674904006050 [pii]. PubMed PMID: 15100666.

Port JL, Yamaguchi K, Du B, De Lorenzo M, Chang M, Heerdt PM, et al. Tobacco smoke induces CYP1B1 in the aerodigestive tract. Carcinogenesis. 2004;25(11):2275-81. Epub 2004/08/07. doi: 10.1093/carcin/bgh243 bgh243 [pii]. PubMed PMID: 15297370.

Pritchard CC, Cheng HH, Tewari M. MicroRNA profiling: approaches and considerations. Nat Rev Genet. 2012;13(5):358-69. doi: http://www.nature.com/nrg/journal/v13/n5/suppinfo/nrg3198_S1.html.

R Core Team. R: A language and environment for statistical computing. R Foundation for Statistical Computing, Vienna, Austria. Available at: http://www.R-project.org/. 2013.

Ritchie ME, Phipson B, Wu D, Hu Y, Law CW, Shi W, et al. limma powers differential expression analyses for RNA-sequencing and microarray studies. Nucleic acids research. 2015. doi: 10.1093/nar/gkv007.

Sales G, Calura E, Cavalieri D, Romualdi C. graphite - a Bioconductor package to convert pathway topology to gene network. BMC Bioinformatics. 2012;13(1):20. doi: 10.1186/1471-2105-13-20 PubMed PMID: doi:10.1186/1471-2105-13-20.

Schamberger AC, Mise N, Jia J, Genoyer E, Yildirim AO, Meiners S, et al. Cigarette Smoke-Induced Disruption of Bronchial Epithelial Tight Junctions is Prevented by Transforming Growth Factor-Beta. Am J Respir Cell Mol Biol. 2013. Epub 2013/12/24. doi: 10.1165/rcmb.2013-0090OC. PubMed PMID: 24358952.

Schlage WK, Iskandar AR, Kostadinova R, Xiang Y, Sewer A, Majeed S, et al. In vitro systems toxicology approach to investigate the effects of repeated cigarette smoke exposure on human buccal and gingival organotypic epithelial tissue cultures. Toxicology mechanisms and methods. 2014;24(7):470-87. Epub

2014/07/22. doi: 10.3109/15376516.2014.943441. PubMed PMID: 25046638; PubMed Central PMCID: PMCPMC4219813.

Smyth GK. Linear models and empirical bayes methods for assessing differential expression in microarray experiments. Stat Appl Genet Mol Biol. 2004;3:Article3. Epub 2006/05/02. doi: 10.2202/1544-6115.1027. PubMed PMID: 16646809.

Soyka MB, Wawrzyniak P, Eiwegger T, Holzmann D, Treis A, Wanke K, et al. Defective epithelial barrier in chronic rhinosinusitis: the regulation of tight junctions by IFN-gamma and IL-4. J Allergy Clin Immunol. 2012;130(5):1087-96 e10. Epub 2012/07/31. doi: 10.1016/j.jaci.2012.05.052
S0091-6749(12)00958-X [pii]. PubMed PMID: 22840853.

Sridhar S, Schembri F, Zeskind J, Shah V, Gustafson AM, Steiling K, et al. Smoking-induced gene expression changes in the bronchial airway are reflected in nasal and buccal epithelium. BMC genomics. 2008;9(1):259. doi: 10.1186/1471-2164-9-259.

Talikka M, Kostadinova R, Xiang Y, Mathis C, Sewer A, Majeed S, et al. The response of human nasal and bronchial organotypic tissue cultures to repeated whole cigarette smoke exposure. Int J Toxicol. 2014;33(6):506-17. Epub 2014/10/10. doi: 10.1177/1091581814551647. PubMed PMID: 25297719.

Thomson TM, Sewer A, Martin F, Belcastro V, Frushour BP, Gebel S, et al. Quantitative assessment of biological impact using transcriptomic data and mechanistic network models. Toxicology and Applied Pharmacology. 2013;272(3):863-78. doi: http://dx.doi.org/10.1016/j.taap.2013.07.007.

Varemo L, Nielsen J, Nookaew I. Enriching the gene set analysis of genome-wide data by incorporating directionality of gene expression and combining statistical hypotheses and methods. Nucleic Acids Res. 2013;41(8):4378-91. Epub 2013/02/28. doi: 10.1093/nar/gkt111. PubMed PMID: 23444143; PubMed Central PMCID: PMC3632109.

Virgin FW, Azbell C, Schuster D, Sunde J, Zhang S, Sorscher EJ, et al. Exposure to Cigarette Smoke Condensate Reduces Calcium Activated Chloride Channel Transport in Primary Sinonasal Epithelial Cultures. The Laryngoscope. 2010;120(7):1465-9. doi: 10.1002/lary.20930. PubMed PMID: PMC3763501.

Werner U, Kissel T. In-vitro cell culture models of the nasal epithelium: a comparative histochemical investigation of their suitability for drug transport studies. Pharmaceutical research. 1996;13(7):978-88. Epub 1996/07/01. PubMed PMID: 8842033.

Yaghi A, Zaman A, Cox G, Dolovich MB. Ciliary beating is depressed in nasal cilia from chronic obstructive pulmonary disease subjects. Respiratory Medicine. 2012;106(8):1139-47. doi: http://dx.doi.org/10.1016/j.rmed.2012.04.001.

Yoo J-W, Kim Y-S, Lee S-H, Lee M-K, Roh H-J, Jhun B-H, et al. Serially passaged human nasal epithelial cell monolayer for in vitro drug transport studies. Pharmaceutical research. 2003;20(10):1690-6.

### 12.2 List of Standard Operating Procedures (SOP) and Work Instructions (WKI)

The procedures and instructions followed to perform the study are listed below:

PMI_RD_WKI_001066. Title: EXtrelut trapping for Nicotine measurement

PMI_RD_WKI_000409. Title: Perform Analysis: Determination of Nicotine in diluted aerosol

PMI_RD_WKI_001094. Title: Sample preparation for Carbonyl measurements

PMI_RD_WKI_001065. Title: Placing Epithelix tissues in culture and maintenance

PMI_RD_WKI_001087. Title: Apical wash of 3D cultures

PMI_RD_WKI_001048. Title: Adenylate kinase assay for 3D cultures

PMI_RD_SOP_000361. Title: Luminex

PMI_RD_WKI_001032. Title: Calibration and Maintenance of LMX200

PMI_RD_WKI_001274. Title: Procedure for Luminex assay (FM3D)

PMI_RD_FOR_000803. Title: Luminex Assay Working Sheet

PMI_RD_FOR_000849. Title: Treatment with controls for MAP analysis

PMI_RD_WKI_001242. Title: Histology Fixation procedure

PMI_RD_WKI_001243. Title: Tissue Processing using LEICA ASP300S

PMI_RD_WKI_001260. Title: Tissue Paraffin Embedding

PMI_RD_WKI_001262. Title: Sectioning Paraffin Blocks using Microtome

PMI_RD_WKI_001266. Title: Haematoxylin & Eosin with or without Alcian Blue Staining Procedure for Formalin- Fixed Paraffin Embedded and Frozen Tissues Sections

PMI_RD_WKI_001314. Title: Slides scanning with Nanozoomer

PMI_RD_WKI_001309. Title: Immunohistochemistry Procedure on Leica Bond-Max Autostainer

PMI_RD_WKI_001049. Title: CYP assay for 3D cultures

PMI_RD_FOR_000846. Title: Treatment and substrate preparation for CYP1A1/1B1 activity assay

PMI_RD_WKI_001117. Title: Isolation of total RNA including microRNAs from Tissue and Organotypic tissue inserts using miRNeasy mini kit protocol

PMI_RD_WKI_000978. Title: Quality controls following RNA extractions

PMI_RD_WKI_001109. Title: Affymetrix IVT PLUS Protocol

PMI_RD_WKI_001125. Title: Quality controls assessment of the Affymetrix IVT and Nugen amplification products using the Fragment Analyzer

PMI_RD_WKI_001126. Title: Affymetrix-3'array-Cartridge-Hybridization (IVT_PLUS, NugenWB, PicoV2)

PMI_RD_WKI_001123. Title: MiRNA labeling using the FlashTag Biotin HSR kits

PMI_RD_WKI_001228. Title: Computational Practices for Omics (mRNA and miRNA) Analyses

PMI_RD_SOP_000346. Title: Computational Processing for mRNA and miRNA Affymetrix Data

### 12.3 Philip Morris International (PMI) Internal Documents

1722_Organotypic_Nasal_SP. PMI Internal Document. Study Plan Translational Organotypic Acute Human Nasal Tissues Study (THS2.2). Study Plan Number S172200.

PMI Internal Document. Unpublished data. Email Correspondence Regarding the Batch Issue. Stored at: \\rd-bsrdata.app.pmi\BSR_Data\Cellular Systems Biology\Acute human nasal - ZRH-S172200\02_Main phase 1_CW48_2013\Planning_MP1\Correspondences_with_Epithelix_Culture_Batch_Issue.msg

PMI Internal Document. Unpublished data. Folder of 00_S172200_Study_Documents. Stored at: \\rd-bsrdata.app.pmi\BSR_Data\Cellular Systems Biology\Acute human nasal - ZRH-S172200\00_S172200_Study_Documents

PMI Internal Document. Unpublished data. Certificate of THS2.2 Batch B-08163. Stored at: \\rd-bsrdata.app.pmi\BSR_Data\Cellular Systems Biology\Batch_Certificates_CellSB_activities\P1_Certificate_No_045_StickBatchNo_B-08163_Manufactured_Oct_2013.pdf

PMI Internal Document. Unpublished data. Certificate of THS2.2 Batch B-11433. Stored at: \\rd-bsrdata.app.pmi\BSR_Data\Cellular Systems Biology\Batch_Certificates_CellSB_activities\P1_Certificate_No_055_StickBatchNo_B-11433_Manufactured_Mar_2014.pdf

PMI Internal Document. Unpublished data. Certificate of THS2.2 Batch B-13055. Stored at: \\rd-bsrdata.app.pmi\BSR_Data\Cellular Systems Biology\Batch_Certificates_CellSB_activities\P1_Certificate_No_072_StickBatchNo_B-13055_Manufactured_Jun_2014.pdf

PMI Internal Document. Unpublished data. Certificate of Device THS2.2 B-06050. Stored at: \\rd-bsrdata.app.pmi\BSR_Data\Cellular Systems Biology\Batch_Certificates_CellSB_activities\P1_Device_Information_B-06050_Release_Date_Sep_2013.pdf

PMI Internal Document. Unpublished data. Certificate of Device THS2.2 No. B-18731. Stored at: \\rd-bsrdata.app.pmi\BSR_Data\Cellular Systems Biology\Batch_Certificates_CellSB_activities\P1_Device_Information_B-18731_Release_Date_Feb_2015.pdf

PMI Internal Document. Unpublished data. Certificate of Nasal MucilAir™ CoA_Seeded_25-Feb-2014. Stored at: \\rd-bsrdata.app.pmi\BSR_Data\Cellular Systems Biology\Acute human nasal - ZRH- S172200\03_Main phase 2_CW15_2014\Epithelix_QC_and_CoA\MucilAir_Nasal_CoA_MD041701_Seeded_25-Feb-2014.pdf

PMI Internal Document. Unpublished data. Certificate of Nasal MucilAir™ CoA_Seeded_05-May-2014. Stored at: \\rd-bsrdata.app.pmi\BSR_Data\Cellular Systems Biology\Acute human nasal - ZRH- S172200\04_Main phase 3_CW26_2014\Epithelix_QC_and_CoA\MucilAir_Nasal_CoA_MD04170_Seeded_05-May-2014.pdf

PMI Internal Document. Unpublished data. Certificate of Nasal MucilAir™ CoA_Seeded_05-Feb-2015. Stored at: \\rd-bsrdata.app.pmi\BSR_Data\Cellular Systems Biology\Acute human nasal - ZRH- S172200\05_Main phase 4_CW13_2015\Epithelix_QC_and_CoA\MucilAir_Nasal_CoA_MD04170_Seeded_05-Feb-2015.pdf

PMI Internal Document. Unpublished data. Certificate of Nasal MucilAir™ CoA_Seeded_09-Mar-2015. Stored at: \\rd-bsrdata.app.pmi\BSR_Data\Cellular Systems Biology\Acute human nasal - ZRH- S172200\06_Main phase 5_CW17_2015\Epithelix_QC_and_CoA\MucilAir_Nasal_CoA_MD04170_Seeded_09-Apr-2015.pdf

PMI Internal Document. Unpublished data. Certificate of Nasal MucilAir™ CoA_Seeded_28-Apr-2015. Stored at: \\rd-bsrdata.app.pmi\BSR_Data\Cellular Systems Biology\Acute human nasal - ZRH- S172200\07_Main phase 6_CW25_2015\Epithelix_QC_and_CoA\MucilAir_Nasal_CoA_MD04170_Seeded_28-Apr-2015.pdf

PMI Internal Document. Unpublished data. Certificate of Nasal MucilAir™ CoA_Seeded_16-Mar-2015. Stored at: \\rd-bsrdata.app.pmi\BSR_Data\Cellular Systems Biology\Acute human nasal - ZRH-S172200\01_DRF[DRA]_CW18_2015\Epithelix_QC_and_CoA\MucilAir_Nasal_CoA_MD041701_Seeded_16-Mar-2015.pdf

## 13 ABBREVIATIONS

| Abbreviation/Term | |
|---|---|
| AK | Adenylate Kinase |
| BIF | Biological Impact Factor |
| CBF | Cilia Beat Frequency |
| CCL | Chemokine (C-C motif) ligand |
| cDNA | Complementary DNA |
| CFA | Cellular Fate |
| COPD | Chronic Obstructive Pulmonary Disease |
| Corr | Correlation |
| CPR | Cellular Proliferation |
| cRNA | Complementary RNA |
| CS | Cigarette Smoke |
| CSF | Colony-Stimulating Factor |
| CST | Cellular Stress |
| CYP | Cytochrome P450 |
| CXCL | Chemokine (C-X-C motif)Ligand |
| DEG | Differentially Expressed Gene |
| DNA | Deoxyribonucleic Acid |
| EGF | Epidermal Growth Factor |
| Exp | Experiment |
| FC | Fold Change |
| FDR | False Discovery Rate |
| fRMA | Frozen-Robust Microarray Analysis |
| GC-FID | Gas Chromatograph-Flame Ionization Detector |
| G-CSF | Granulocyte Colony-Stimulating Factor |
| GLP | Good Laboratory Practice |

| | |
|---|---|
| GM-CSF | Granulocyte-Macrophage Colony-Stimulating Factor |
| GRO | Growth Related Oncogene |
| H&E | Hematoxylin & Eosin |
| HCN | Hydrogen Cyanide |
| HPLC | High-performance liquid chromatography |
| IHC | Immunohistochemistry |
| IL | Interleukin |
| IP10 | Interferon γ-induced Protein 10 |
| IPN | Inflammation Pulmonary Network |
| ISO | International Organization for Standardization |
| LCLM | Lower Confidence Limit for the Mean |
| LC-MS | Liquid chromatography–mass spectrometry |
| Limma | Linear Models for Microarray |
| MAP | Multi Analyte Profiling |
| MARLE | Median Absolute Value RLE |
| MCP | Monocyte Chemoattractant Protein |
| MFI | Median Fluorescent Intensity |
| MIP | Macrophage Inflammatory Protein |
| miRNA | MicroRNA |
| MMP | Matrix Metalloproteinase |
| mRNA | messenger RNA |
| MRTP | Modified Risk Tobacco Product |
| MS/MS | Mass Spectrometry/Mass Spectrometry (also referred as Tandem Mass Spectrometry) |
| NA | Not Available |
| NAB | N-nitrosoanabasine |
| NAT | N-nitrosoanatabine |
| NFDPM | Nicotine-Free Dry Particulate Matter |

| | |
|---|---|
| NH3 | Ammonia |
| NNK | 4-(N-nitrosomethylamino)-1-(3-pyridyl)-1-butanone |
| NNN | N-nitrosonornicotine |
| NO | Nitrogen Oxide |
| NOx | Mono-Nitrogen Oxide (Generic Term) |
| NPA | Network Perturbation Amplitude |
| NUSE | Normalized-Unscaled Standard Error |
| PAH | Polycyclic Aromatic Hydrocarbon |
| PBS | Phosphate-Buffered Saline |
| pMRTP | prototype Modified Risk of Tobacco Products |
| PE | Post-Exposure |
| RANTES | Regulated on Activation, Normal T Expressed and Secreted |
| RLE | Relative Log Expression |
| QC | Quality Control |
| QQ | Quantile-Quantile |
| RNA | Ribonucleic Acid |
| SD | Standard Deviation |
| SEM | Standard Error Mean |
| sICAM1 | Soluble InterCellular Adhesion Molecule 1 |
| SM | Smoking Machine |
| SOP | Standard Operating Procedure |
| TCDD | 2,3,7,8-Tetrachlorodibenzodioxin |
| TEER | Transepithelial Electrical Resistance |
| THS | Tobacco Heating System (also referred to as ZRH) |
| TIMP | Tissue Inhibitor of Metalloproteinase |
| TLSP | Thymic Stromal Lymphopoietin |
| TNFA | Tumor Necrosis Factor Alpha |

| | |
|---|---|
| TPM | Total Particulate Matter |
| UCLM | Upper Confidence Limit for the Mean |
| VEGFA | Vascular Endothelial Growth Factor Alpha |
| WKI | Work Instructions |
| ZRH | See THS |

# 14 TABLES AND SUPPLEMENTARY FIGURES

## 14.1 Supplementary Tables

### 14.1.1 **Supplementary Table 1**. Descriptive Statistics of Formaldehyde Levels Deposited in the Cultivation Base Module of the Vitrocell® 24/48 exposure system

| Descriptive Statistics: Formaldehyde (µg/mL) | | | | | | | | | | | | | | |
|---|---|---|---|---|---|---|---|---|---|---|---|---|---|---|
| Year. Calendar Week | 3R4F (Air) | | 3R4F (0.15) | | 3R4F (0.25) | | THS2.2 (Air) | | THS2.2 (0.15) | | THS2.2 (0.27) | | THS2.2 (0.44) | |
| | M | SEM | M | SEM | M | SEM | M | SEM | M | SEM | M | SEM | M | SEM |
| **2014.14** | 0.03 | 0.01 | 0.07 | 0.03 | 0.22 | 0.09 | 0.18 | 0.06 | 0.16 | 0.04 | 0.28 | 0.07 | NA | NA |
| **2014.19** | 0.00 | 0.00 | 0.00 | 0.00 | 0.03 | 0.00 | 0.00 | 0.00 | 0.00 | 0.00 | 0.00 | 0.00 | NA | NA |
| **2014.25** | 0.00 | 0.00 | 0.00 | 0.00 | 0.05 | 0.00 | 0.00 | 0.00 | 0.00 | 0.00 | 0.00 | 0.00 | 0.00 | 0.00 |
| **2015.11** | 0.02 | 0.00 | 0.07 | 0.00 | 0.10 | 0.01 | 0.01 | 0.00 | 0.02 | 0.00 | 0.03 | 0.01 | 0.03 | 0.01 |
| **2015.12** | 0.07 | 0.02 | 0.15 | 0.01 | 0.24 | 0.03 | 0.04 | 0.01 | 0.09 | 0.03 | 0.11 | 0.02 | 0.10 | 0.04 |
| **2015.15** | 0.05 | 0.01 | NA | NA | 0.19 | 0.01 | 0.04 | 0.02 | NA | NA | NA | NA | 0.07 | 0.00 |
| **2015.16** | 0.00 | 0.00 | 0.02 | 0.00 | 0.05 | 0.00 | 0.03 | 0.03 | 0.02 | 0.02 | 0.02 | 0.02 | 0.01 | 0.01 |
| **2015.23** | 0.00 | 0.00 | 0.00 | 0.00 | 0.00 | 0.00 | 0.00 | 0.00 | 0.00 | 0.00 | 0.00 | 0.00 | 0.00 | 0.00 |
| **2015.25** | 0.10 | 0.02 | 0.16 | 0.01 | 0.22 | 0.00 | 0.11 | 0.01 | 0.10 | 0.01 | 0.13 | 0.01 | NA | NA |
| **2015.27** | 0.05 | 0.01 | 0.08 | 0.01 | 0.12 | 0.01 | 0.04 | 0.00 | 0.03 | 0.00 | 0.03 | 0.00 | NA | NA |

The method to measure various carbonyls in PBS-exposed samples has not been validated. Due to a lack of dose-dependency observed in the measured values of formaldehyde at the different smoke/aerosol concentrations, these data were not used for smoke/aerosol characterization. For the indicated nicotine doses (in mg/L) of the reference smoke and test aerosols, as well as the corresponding air controls, the carbonyls were measured in phosphate buffered saline (PBS) following a 28-minute exposure (see Testing Procedure). Abbreviations: Cig, cigarette; M, mean; NA, not available (no measurement for the indicated calendar week); SEM, standard error mean.

### 14.1.2 **Supplementary Table 2**. Descriptive Statistics of Acetaldehyde Levels Deposited in the Cultivation Base Module of the Vitrocell® 24/48 exposure system

| Descriptive Statistics: Acetaldehyde (µg/mL) | | | | | | | | | | | | | | |
|---|---|---|---|---|---|---|---|---|---|---|---|---|---|---|
| Year. Calendar Week | 3R4F (Air) | | 3R4F (0.15) | | 3R4F (0.25) | | THS2.2 (Air) | | THS2.2 (0.15) | | THS2.2 (0.27) | | THS2.2 (0.44) | |
| | M | SEM | M | SEM | M | SEM | M | SEM | M | SEM | M | SEM | M | SEM |
| **2014.14** | 0.00 | 0.00 | 1.06 | 0.09 | 1.93 | 0.17 | 0.00 | 0.00 | 0.38 | 0.02 | 0.75 | 0.13 | NA | NA |
| **2014.19** | 0.00 | 0.00 | 1.08 | 0.03 | 2.04 | 0.04 | 0.00 | 0.00 | 0.00 | 0.00 | 0.27 | 0.01 | NA | NA |
| **2014.25** | 0.00 | 0.00 | 0.86 | 0.04 | 1.95 | 0.13 | 0.00 | 0.00 | 0.00 | 0.00 | 0.18 | 0.02 | 0.45 | 0.01 |
| **2015.11** | 0.00 | 0.00 | 1.34 | 0.03 | 2.32 | 0.03 | 0.00 | 0.00 | 0.22 | 0.01 | 0.53 | 0.01 | 0.61 | 0.02 |
| **2015.12** | 0.00 | 0.00 | 1.86 | 0.14 | 3.47 | 0.47 | 0.00 | 0.00 | 0.48 | 0.11 | 1.03 | 0.09 | 1.17 | 0.23 |
| **2015.15** | 0.00 | 0.00 | NA | NA | 2.95 | 0.12 | 0.00 | 0.00 | NA | NA | NA | NA | 1.08 | 0.05 |
| **2015.16** | 0.00 | 0.00 | 0.99 | 0.06 | 1.91 | 0.03 | 0.00 | 0.00 | 0.10 | 0.01 | 0.31 | 0.04 | 0.44 | 0.02 |
| **2015.23** | 0.00 | 0.00 | 0.69 | 0.05 | 1.61 | 0.17 | 0.00 | 0.00 | 0.00 | 0.00 | 0.25 | 0.04 | 0.23 | 0.07 |
| **2015.25** | 0.00 | 0.00 | 1.88 | 0.04 | 3.55 | 0.14 | 0.00 | 0.00 | 0.35 | 0.03 | 0.94 | 0.05 | NA | NA |
| **2015.27** | 0.00 | 0.00 | 1.39 | 0.02 | 2.62 | 0.10 | 0.00 | 0.00 | 0.24 | 0.00 | 0.59 | 0.03 | NA | NA |

The method to measure various carbonyls in PBS-exposed samples has not been validated. For the indicated nicotine doses (in mg/L) of the reference smoke and test aerosols, as well as the corresponding air controls, the carbonyls were measured in phosphate buffered saline (PBS) following a 28-minute exposure (see Testing Procedure). Abbreviations: Cig, cigarette; M, mean; NA, not available (no measurement for the indicated calendar week); SEM, standard error mean.

14.1.3 **Supplementary Table 3**. Descriptive Statistics of Acetone Levels Deposited in the Cultivation Base Module of the Vitrocell® 24/48 exposure system

| Descriptive Statistics: Acetone (µg/mL) | | | | | | | | | | | | | | |
|---|---|---|---|---|---|---|---|---|---|---|---|---|---|---|
| Year. Calendar Week | 3R4F (Air) | | 3R4F (0.15) | | 3R4F (0.25) | | THS2.2 (Air) | | THS2.2 (0.15) | | THS2.2 (0.27) | | THS2.2 (0.44) | |
| | M | SEM | M | SEM | M | SEM | M | SEM | M | SEM | M | SEM | M | SEM |
| **2014.14** | 0.03 | 0.00 | 0.60 | 0.07 | 1.07 | 0.15 | 0.05 | 0.00 | 0.12 | 0.01 | 0.19 | 0.03 | NA | NA |
| **2014.19** | 0.04 | 0.00 | 0.79 | 0.02 | 1.36 | 0.02 | 0.05 | 0.00 | 0.12 | 0.00 | 0.17 | 0.01 | NA | NA |
| **2014.25** | 0.03 | 0.00 | 0.67 | 0.02 | 1.21 | 0.09 | 0.02 | 0.01 | 0.08 | 0.00 | 0.13 | 0.00 | 0.17 | 0.00 |
| **2015.11** | 0.09 | 0.04 | 0.80 | 0.03 | 1.33 | 0.03 | 0.01 | 0.01 | 0.07 | 0.00 | 0.11 | 0.00 | 0.13 | 0.01 |
| **2015.12** | 0.00 | 0.00 | 0.84 | 0.07 | 1.36 | 0.12 | 0.00 | 0.00 | 0.09 | 0.01 | 0.17 | 0.02 | 0.19 | 0.02 |
| **2015.15** | 0.03 | 0.00 | NA | NA | 1.38 | 0.03 | 0.02 | 0.01 | NA | NA | NA | NA | 0.20 | 0.00 |
| **2015.16** | 0.00 | 0.00 | 0.70 | 0.03 | 1.26 | 0.01 | 0.01 | 0.01 | 0.07 | 0.00 | 0.11 | 0.00 | 0.13 | 0.01 |
| **2015.23** | 0.00 | 0.00 | 0.62 | 0.03 | 1.12 | 0.10 | 0.00 | 0.00 | 0.06 | 0.00 | 0.12 | 0.00 | 0.12 | 0.01 |
| **2015.25** | 0.19 | 0.12 | 1.03 | 0.07 | 1.79 | 0.01 | 0.08 | 0.00 | 0.16 | 0.01 | 0.23 | 0.01 | NA | NA |
| **2015.27** | 0.03 | 0.00 | 0.78 | 0.01 | 1.35 | 0.00 | 0.02 | 0.00 | 0.08 | 0.00 | 0.13 | 0.01 | NA | NA |

The method to measure various carbonyls in PBS-exposed samples has not been validated. For the indicated nicotine doses (in mg/L) of the reference smoke and test aerosols, as well as the corresponding air controls, the carbonyls were measured in phosphate buffered saline (PBS) following a 28-minute exposure (see Testing Procedure). Abbreviations: Cig, cigarette; M, mean; NA, not available (no measurement for the indicated calendar week); SEM, standard error mean.

14.1.4 **Supplementary Table 4**. Descriptive Statistics of Acrolein Levels Deposited in the Cultivation Base Module of the Vitrocell® 24/48 exposure system

| Descriptive Statistics: Acrolein (µg/mL) | | | | | | | | | | | | | | |
|---|---|---|---|---|---|---|---|---|---|---|---|---|---|---|
| Year. Calendar Week | 3R4F (Air) | | 3R4F (0.15) | | 3R4F (0.25) | | THS2.2 (Air) | | THS2.2 (0.15) | | THS2.2 (0.27) | | THS2.2 (0.44) | |
| | M | SEM | M | SEM | M | SEM | M | SEM | M | SEM | M | SEM | M | SEM |
| **2014.14** | 0.00 | 0.00 | 0.06 | 0.00 | 0.10 | 0.00 | 0.00 | 0.00 | 0.01 | 0.00 | 0.03 | 0.01 | NA | NA |
| **2014.19** | 0.00 | 0.00 | 0.07 | 0.00 | 0.12 | 0.00 | 0.00 | 0.00 | 0.01 | 0.00 | 0.02 | 0.00 | NA | NA |
| **2014.25** | 0.00 | 0.00 | 0.08 | 0.01 | 0.15 | 0.01 | 0.00 | 0.00 | 0.01 | 0.00 | 0.02 | 0.00 | 0.03 | 0.00 |
| **2015.11** | 0.01 | 0.01 | 0.10 | 0.00 | 0.15 | 0.00 | 0.00 | 0.00 | 0.01 | 0.00 | 0.02 | 0.00 | 0.02 | 0.00 |
| **2015.12** | 0.00 | 0.00 | 0.11 | 0.01 | 0.18 | 0.01 | 0.00 | 0.00 | 0.00 | 0.00 | 0.01 | 0.01 | 0.02 | 0.02 |
| **2015.15** | 0.00 | 0.00 | NA | NA | 0.17 | 0.00 | 0.00 | 0.00 | NA | NA | NA | NA | 0.03 | 0.00 |
| **2015.16** | 0.00 | 0.00 | 0.08 | 0.00 | 0.14 | 0.00 | 0.00 | 0.00 | 0.01 | 0.00 | 0.02 | 0.00 | 0.02 | 0.00 |
| **2015.23** | 0.00 | 0.00 | 0.09 | 0.00 | 0.16 | 0.02 | 0.00 | 0.00 | 0.01 | 0.00 | 0.02 | 0.00 | 0.02 | 0.00 |
| **2015.25** | 0.00 | 0.00 | 0.12 | 0.00 | 0.22 | 0.01 | 0.00 | 0.00 | 0.01 | 0.00 | 0.02 | 0.00 | NA | NA |
| **2015.27** | 0.00 | 0.00 | 0.07 | 0.00 | 0.11 | 0.00 | 0.00 | 0.00 | 0.01 | 0.00 | 0.02 | 0.00 | NA | NA |

The method to measure various carbonyls in PBS-exposed samples has not been validated. For the indicated nicotine doses (in mg/L) of the reference smoke and test aerosols, as well as the corresponding air controls, the carbonyls were measured in phosphate buffered saline (PBS) following a 28-minute exposure (see Testing Procedure). Abbreviations: Cig, cigarette; M, mean; NA, not available (no measurement for the indicated calendar week); SEM, standard error mean.

14.1.5 **Supplementary Table 5**. Descriptive Statistics of Propionaldehyde Levels Deposited in the Cultivation Base Module of the Vitrocell® 24/48 exposure system

| Descriptive Statistics: Propionaldehyde (µg/mL) | | | | | | | | | | | | | | |
|---|---|---|---|---|---|---|---|---|---|---|---|---|---|---|
| Year. Calendar Week | 3R4F (: Pro) | | 3R4F (0.15) | | 3R4F (0.25) | | THS2.2 (Air) | | THS2.2 (0.15) | | THS2.2 (0.27) | | THS2.2 (0.44) | |
| | M | SEM | M | SEM | M | SEM | M | SEM | M | SEM | M | SEM | M | SEM |
| **2014.14** | 0.00 | 0.00 | 0.02 | 0.00 | 0.03 | 0.00 | 0.00 | 0.00 | 0.01 | 0.00 | 0.02 | 0.01 | NA | NA |
| **2014.19** | 0.00 | 0.00 | 0.06 | 0.00 | 0.11 | 0.00 | 0.00 | 0.00 | 0.02 | 0.00 | 0.03 | 0.00 | NA | NA |
| **2014.25** | 0.00 | 0.00 | 0.06 | 0.00 | 0.10 | 0.01 | 0.00 | 0.00 | 0.02 | 0.00 | 0.03 | 0.00 | 0.04 | 0.00 |
| **2015.11** | 0.01 | 0.01 | 0.08 | 0.00 | 0.13 | 0.00 | 0.00 | 0.00 | 0.02 | 0.00 | 0.03 | 0.00 | 0.04 | 0.00 |
| **2015.12** | 0.00 | 0.00 | 0.10 | 0.01 | 0.21 | 0.01 | 0.00 | 0.00 | 0.03 | 0.01 | 0.05 | 0.00 | 0.07 | 0.02 |
| **2015.15** | 0.00 | 0.00 | NA | NA | 0.18 | 0.01 | 0.00 | 0.00 | NA | NA | NA | NA | 0.07 | 0.00 |
| **2015.16** | 0.00 | 0.00 | 0.06 | 0.00 | 0.10 | 0.00 | 0.00 | 0.00 | 0.02 | 0.00 | 0.03 | 0.00 | 0.03 | 0.00 |
| **2015.23** | 0.00 | 0.00 | 0.05 | 0.00 | 0.10 | 0.01 | 0.00 | 0.00 | 0.01 | 0.00 | 0.03 | 0.00 | 0.03 | 0.00 |
| **2015.25** | 0.00 | 0.00 | 0.14 | 0.00 | 0.24 | 0.01 | 0.00 | 0.00 | 0.03 | 0.00 | 0.07 | 0.00 | NA | NA |
| **2015.27** | 0.00 | 0.00 | 0.08 | 0.00 | 0.14 | 0.00 | 0.00 | 0.00 | 0.02 | 0.00 | 0.04 | 0.00 | NA | NA |

The method to measure various carbonyls in PBS-exposed samples has not been validated. For the indicated nicotine doses (in mg/L) of the reference smoke and test aerosols, as well as the corresponding air controls, the carbonyls were measured in phosphate buffered saline (PBS) following a 28-minute exposure (see Testing Procedure). Abbreviations: Cig, cigarette; M, mean; NA, not available (no measurement for the indicated calendar week); SEM, standard error mean.

14.1.6 **Supplementary Table 6**. Descriptive Statistics of Crotonaldehyde Levels Deposited in the Cultivation Base Module of the Vitrocell® 24/48 exposure system

| Descriptive Statistics: Crotonaldehyde (µg/mL) | | | | | | | | | | | | | | |
|---|---|---|---|---|---|---|---|---|---|---|---|---|---|---|
| Year. Calendar Week | 3R4F (Air) | | 3R4F (0.15) | | 3R4F (0.25) | | THS2.2 (Air) | | THS2.2 (0.15) | | THS2.2 (0.27) | | THS2.2 (0.44) | |
| | M | SEM | M | SEM | M | SEM | M | SEM | M | SEM | M | SEM | M | SEM |
| **2014.14** | 0.00 | 0.00 | 0.08 | 0.00 | 0.14 | 0.00 | 0.00 | 0.00 | 0.01 | 0.00 | 0.02 | 0.00 | NA | NA |
| **2014.19** | 0.00 | 0.00 | 0.07 | 0.00 | 0.12 | 0.00 | 0.00 | 0.00 | 0.01 | 0.00 | 0.01 | 0.00 | NA | NA |
| **2014.25** | 0.00 | 0.00 | 0.07 | 0.00 | 0.13 | 0.01 | 0.00 | 0.00 | 0.01 | 0.00 | 0.01 | 0.00 | 0.02 | 0.00 |
| **2015.11** | 0.01 | 0.00 | 0.07 | 0.00 | 0.12 | 0.00 | 0.00 | 0.00 | 0.01 | 0.00 | 0.01 | 0.00 | 0.01 | 0.00 |
| **2015.12** | 0.00 | 0.00 | 0.07 | 0.00 | 0.12 | 0.00 | 0.00 | 0.00 | 0.01 | 0.00 | 0.01 | 0.00 | 0.02 | 0.00 |
| **2015.15** | 0.00 | 0.00 | NA | NA | 0.13 | 0.00 | 0.00 | 0.00 | NA | NA | NA | NA | 0.02 | 0.00 |
| **2015.16** | 0.00 | 0.00 | 0.07 | 0.01 | 0.13 | 0.01 | 0.00 | 0.00 | 0.01 | 0.00 | 0.01 | 0.00 | 0.01 | 0.00 |
| **2015.23** | 0.00 | 0.00 | 0.05 | 0.00 | 0.10 | 0.01 | 0.00 | 0.00 | 0.01 | 0.00 | 0.01 | 0.00 | 0.01 | 0.00 |
| **2015.25** | 0.00 | 0.00 | 0.09 | 0.01 | 0.16 | 0.02 | 0.00 | 0.00 | 0.01 | 0.00 | 0.02 | 0.00 | NA | NA |
| **2015.27** | 0.00 | 0.00 | 0.07 | 0.01 | 0.11 | 0.01 | 0.00 | 0.00 | 0.01 | 0.00 | 0.01 | 0.00 | NA | NA |

The method to measure various carbonyls in PBS-exposed samples has not been validated. For the indicated nicotine doses (in mg/L) of the reference smoke and test aerosols, as well as the corresponding air controls, the carbonyls were measured in phosphate buffered saline (PBS) following a 28-minute exposure (see Testing Procedure). Abbreviations: Cig, cigarette; M, mean; NA, not available (no measurement for the indicated calendar week); SEM, standard error mean.

14.1.7 **Supplementary Table 7**. Descriptive Statistics of Methyl Ethyl Ketone Levels Deposited in the Cultivation Base Module of the Vitrocell® 24/48 exposure system

| Descriptive Statistics: Methyl Ethyl Ketone (µg/mL) | | | | | | | | | | | | | | |
|---|---|---|---|---|---|---|---|---|---|---|---|---|---|---|
| Year. Calendar Week | 3R4F (Air) | | 3R4F (0.15) | | 3R4F (0.25) | | THS2.2 (Air) | | THS2.2 (0.15) | | THS2.2 (0.27) | | THS2.2 (0.44) | |
| | M | SEM | M | SEM | M | SEM | M | SEM | M | SEM | M | SEM | M | SEM |
| **2014.14** | 0.03 | 0.00 | 0.17 | 0.01 | 0.30 | 0.02 | 0.03 | 0.00 | 0.05 | 0.00 | 0.06 | 0.00 | NA | NA |
| **2014.19** | 0.03 | 0.00 | 0.21 | 0.00 | 0.35 | 0.00 | 0.04 | 0.00 | 0.05 | 0.00 | 0.06 | 0.00 | NA | NA |
| **2014.25** | 0.03 | 0.00 | 0.18 | 0.00 | 0.31 | 0.02 | 0.03 | 0.00 | 0.04 | 0.00 | 0.05 | 0.00 | 0.06 | 0.00 |
| **2015.11** | 0.05 | 0.02 | 0.19 | 0.01 | 0.32 | 0.00 | 0.01 | 0.01 | 0.02 | 0.00 | 0.03 | 0.00 | 0.03 | 0.00 |
| **2015.12** | 0.01 | 0.00 | 0.20 | 0.01 | 0.32 | 0.02 | 0.00 | 0.00 | 0.02 | 0.00 | 0.04 | 0.00 | 0.04 | 0.00 |
| **2015.15** | 0.02 | 0.00 | NA | NA | 0.35 | 0.00 | 0.02 | 0.00 | NA | NA | NA | NA | 0.05 | 0.00 |
| **2015.16** | 0.02 | 0.01 | 0.19 | 0.01 | 0.33 | 0.01 | 0.01 | 0.00 | 0.04 | 0.01 | 0.03 | 0.00 | 0.05 | 0.01 |
| **2015.23** | 0.01 | 0.00 | 0.16 | 0.01 | 0.29 | 0.03 | 0.01 | 0.00 | 0.02 | 0.00 | 0.03 | 0.00 | 0.03 | 0.00 |
| **2015.25** | 0.07 | 0.00 | 0.25 | 0.01 | 0.42 | 0.03 | 0.08 | 0.00 | 0.09 | 0.00 | 0.11 | 0.00 | NA | NA |
| **2015.27** | 0.02 | 0.00 | 0.22 | 0.01 | 0.35 | 0.00 | 0.02 | 0.00 | 0.03 | 0.00 | 0.04 | 0.00 | NA | NA |

The method to measure various carbonyls in PBS-exposed samples has not been validated. For the indicated nicotine doses (in mg/L) of the reference smoke and test aerosols, as well as the corresponding air controls, the carbonyls were measured in phosphate buffered saline (PBS) following a 28-minute exposure (see Testing Procedure). Abbreviations: Cig, cigarette; M, mean; NA, not available (no measurement for the indicated calendar week); SEM, standard error mean.

14.1.8 **Supplementary Table 8**. Descriptive Statistics of Butyraldehyde Levels Deposited in the Cultivation Base Module of the Vitrocell® 24/48 exposure system

| Descriptive Statistics: Butyraldehyde (µg/mL) | | | | | | | | | | | | | | |
|---|---|---|---|---|---|---|---|---|---|---|---|---|---|---|
| Year. Calendar Week | 3R4F (Air) | | 3R4F (0.15) | | 3R4F (0.25) | | THS2.2 (Air) | | THS2.2 (0.15) | | THS2.2 (0.27) | | THS2.2 (0.44) | |
| | M | SEM | M | SEM | M | SEM | M | SEM | M | SEM | M | SEM | M | SEM |
| **2014.14** | 0.00 | 0.00 | 0.03 | 0.00 | 0.04 | 0.00 | 0.00 | 0.00 | 0.02 | 0.00 | 0.03 | 0.01 | NA | NA |
| **2014.19** | 0.00 | 0.00 | 0.00 | 0.00 | 0.01 | 0.00 | 0.00 | 0.00 | 0.00 | 0.00 | 0.00 | 0.00 | NA | NA |
| **2014.25** | 0.00 | 0.00 | 0.01 | 0.00 | 0.01 | 0.00 | 0.00 | 0.00 | 0.00 | 0.00 | 0.01 | 0.00 | 0.01 | 0.00 |
| **2015.11** | 0.00 | 0.00 | 0.02 | 0.00 | 0.03 | 0.00 | 0.00 | 0.00 | 0.01 | 0.00 | 0.02 | 0.00 | 0.02 | 0.00 |
| **2015.12** | 0.00 | 0.00 | 0.02 | 0.00 | 0.03 | 0.00 | 0.00 | 0.00 | 0.01 | 0.00 | 0.03 | 0.00 | 0.03 | 0.00 |
| **2015.15** | 0.00 | 0.00 | NA | NA | 0.03 | 0.00 | 0.00 | 0.00 | NA | NA | NA | NA | 0.03 | 0.00 |
| **2015.16** | 0.00 | 0.00 | 0.02 | 0.00 | 0.03 | 0.00 | 0.00 | 0.00 | 0.01 | 0.00 | 0.02 | 0.00 | 0.02 | 0.00 |
| **2015.23** | 0.00 | 0.00 | 0.01 | 0.00 | 0.03 | 0.00 | 0.00 | 0.00 | 0.01 | 0.00 | 0.02 | 0.00 | 0.02 | 0.00 |
| **2015.25** | 0.00 | 0.00 | 0.03 | 0.00 | 0.05 | 0.00 | 0.00 | 0.00 | 0.02 | 0.00 | 0.06 | 0.03 | NA | NA |
| **2015.27** | 0.00 | 0.00 | 0.02 | 0.00 | 0.04 | 0.00 | 0.00 | 0.00 | 0.01 | 0.00 | 0.02 | 0.00 | NA | NA |

The method to measure various carbonyls in PBS-exposed samples has not been validated. Due to a lack of dose-dependency observed in the measured values of butyraldehyde at the different smoke/aerosol concentrations, these data were not used for smoke/aerosol characterization. For the indicated nicotine doses (in mg/L) of the reference smoke and test aerosols, as well as the corresponding air controls, the carbonyls were measured in phosphate buffered saline (PBS) following a 28-minute exposure (see Testing Procedure). Abbreviations: Cig, cigarette; M, mean; NA, not available (no measurement for the indicated calendar week); SEM, standard error mean.

14.1.9 **Supplementary Table 9**. Descriptive Statistics: Cytotoxicity, CYP Activity, and Inflammatory Mediators Levels of the 3R4F (0.20) Group

| **Descriptive Statistics: 3R4F (0.20) Group Applied in Experiment 2** | | | | | | | | | | | |
|---|---|---|---|---|---|---|---|---|---|---|---|
| **Type** | **Endpoint** | **Unit** | **PE [h]** | **N** | **M** | **SEM** | **Q1** | **Median** | **Q3** | **LCLM** | **UCLM** |
| AK | AK | RLU | 4:00 | 3 | 1059.67 | 186.28 | 785.00 | 979.00 | 1415.00 | 258.15 | 1861.18 |
| | | | 48:00 | 3 | 11831.00 | 1851.51 | 8163.00 | 13225.00 | 14105.00 | 3864.60 | 19797.40 |
| | | | 72:00 | 3 | 14183.67 | 4891.75 | 4643.00 | 17078.00 | 20830.00 | −6863.83 | 35231.16 |
| | Cytotoxicity | % | 4:00 | 3 | −0.01 | 0.01 | −0.02 | −0.01 | −0.00 | −0.03 | 0.01 |
| | | | 48:00 | 3 | 0.29 | 0.05 | 0.19 | 0.32 | 0.35 | 0.07 | 0.51 |
| | | | 72:00 | 3 | 0.35 | 0.13 | 0.09 | 0.43 | 0.53 | −0.23 | 0.93 |
| CYP | CYP1A1/1B1 | RLU | 24:00 | 3 | 1530.00 | 1004.90 | 420.00 | 634.00 | 3536.00 | −2793.74 | 5853.74 |
| | | | 48:00 | 3 | 3724.67 | 2285.24 | 844.00 | 2092.00 | 8238.00 | −6107.94 | 13557.27 |
| | | | 72:00 | 3 | 5304.00 | 2624.53 | 1301.00 | 4365.00 | 10246.00 | −5988.46 | 16596.46 |
| | Normalized CYP Activity | % | 24:00 | 3 | 0.03 | 0.03 | −0.01 | −0.00 | 0.09 | −0.12 | 0.17 |
| | | | 48:00 | 3 | 0.10 | 0.08 | 0.00 | 0.05 | 0.25 | −0.23 | 0.44 |
| | | | 72:00 | 3 | 0.16 | 0.09 | 0.02 | 0.12 | 0.32 | −0.23 | 0.54 |
| Inflammatory Mediators | EGF | pg/mL | 48:00 | 3 | 15.60 | 7.95 | 1.40 | 16.49 | 28.91 | −18.62 | 49.82 |
| | CXCL1 | pg/mL | 48:00 | 3 | 7349.09 | 357.11 | 6839.03 | 7171.16 | 8037.08 | 5812.58 | 8885.60 |
| | IL6 | pg/mL | 48:00 | 3 | 35.84 | 8.16 | 19.54 | 43.37 | 44.61 | 0.75 | 70.93 |
| | CXCL8 | pg/mL | 48:00 | 3 | 5380.21 | 923.93 | 4041.11 | 4947.03 | 7152.51 | 1404.87 | 9355.56 |
| | CCL20 | pg/mL | 48:00 | 3 | 51.14 | 15.27 | 22.89 | 55.21 | 75.31 | −14.57 | 116.84 |
| | MMP-1 | pg/mL | 48:00 | 3 | 1504.80 | 98.38 | 1321.55 | 1534.36 | 1658.48 | 1081.50 | 1928.10 |
| | MMP-9 | pg/mL | 48:00 | 3 | 4419.34 | 2089.68 | 1707.62 | 3021.08 | 8529.33 | −4571.83 | 13410.51 |
| | sICAM1 | pg/mL | 48:00 | 3 | 412.35 | 98.68 | 235.53 | 424.83 | 576.69 | −12.24 | 836.94 |
| | TIMP1 | pg/mL | 48:00 | 3 | 11195.16 | 2714.43 | 6132.60 | 12028.73 | 15424.16 | −484.09 | 22874.41 |
| | TNFA | pg/mL | 48:00 | 3 | 7.92 | 1.55 | 5.67 | 7.20 | 10.90 | 1.24 | 14.61 |
| | VEGFA | pg/mL | 48:00 | 3 | 377.97 | 51.45 | 309.63 | 345.52 | 478.76 | 156.60 | 599.33 |

Abbreviations: AK, adenylate kinase; CCL, chemokine (C-C motif) ligand; CXCL, chemokine (C-X-C motif) ligand; CYP, cytochrome P450; EGF, epidermal growth factor; h, hour; M, mean; N, number of samples; LCLM, lower confidence limit for the mean; MMP, matrix metalloproteinase; PE, post-exposure; Q1, first quartile; Q3, third quartile; RLU, Relative Luminescence Units; SEM, standard error of the mean; sICAM, soluble intercellular adhesion molecule; TIMP, tissue inhibitor of metalloproteinase; TNFA, tumor necrosis factor alpha; UCLM, upper confidence limit of the mean; VEGFA, vascular endothelial growth factor alpha.

14.1.10 **Supplementary Table 10**. Descriptive Statistics of Immunohistochemistry Quantification on P63 Positive Staining (%)

| | | Descriptive Statistics: P63 Positive Staining (%) | | | | | | | |
|---|---|---|---|---|---|---|---|---|---|
| **PE [h]** | **Exposure** | **N** | **M** | **SEM** | **Q1** | **Median** | **Q3** | **LCLM** | **UCLM** |
| 48:00 | 3R4F (Air) | 15 | 14.43 | 1.08 | 11.77 | 14.79 | 17.74 | 12.11 | 16.75 |
| | 3R4F (0.15) | 14 | 15.46 | 0.98 | 14.38 | 16.82 | 18.18 | 13.35 | 17.57 |
| | THS2.2 (Air) | 15 | 14.79 | 0.60 | 12.21 | 15.28 | 17.00 | 13.50 | 16.07 |
| | THS2.2 (0.15) | 15 | 15.59 | 0.78 | 13.51 | 14.18 | 18.49 | 13.92 | 17.27 |
| | THS2.2 (0.27) | 15 | 15.39 | 0.99 | 13.50 | 14.21 | 17.14 | 13.26 | 17.51 |
| | THS2.2 (0.44) | 12 | 14.46 | 1.29 | 11.28 | 15.23 | 17.91 | 11.63 | 17.30 |
| 72:00 | 3R4F (Air) | 15 | 14.92 | 1.03 | 11.76 | 14.06 | 16.99 | 12.71 | 17.13 |
| | 3R4F (0.15) | 15 | 14.26 | 1.21 | 11.19 | 15.13 | 17.71 | 11.66 | 16.87 |
| | THS2.2 (Air) | 15 | 14.51 | 0.98 | 12.24 | 14.02 | 15.14 | 12.42 | 16.60 |
| | THS2.2 (0.15) | 15 | 13.52 | 1.25 | 11.68 | 12.84 | 15.57 | 10.84 | 16.20 |
| | THS2.2 (0.27) | 15 | 13.50 | 0.89 | 10.67 | 13.33 | 15.55 | 11.60 | 15.40 |
| | THS2.2 (0.44) | 12 | 14.91 | 1.07 | 12.13 | 14.75 | 17.94 | 12.55 | 17.28 |

The proportion of positively stained cells was calculated relative to the total cell numbers. Abbreviations: h, hour; LCLM, lower confidence limit for the mean; M, mean; N, number of replicate; Q1, first quartile; Q3, third quartile; UCLM, upper confidence limit of the mean; PE, post-exposure; SEM, standard error of the mean.

14.1.11 **Supplementary Table 11**. Descriptive Statistics of Immunohistochemistry Quantification on Ki67 Positive Staining (%)

| | | Descriptive Statistics: Ki67 Positive Staining (%) | | | | | | | |
|---|---|---|---|---|---|---|---|---|---|
| **PE [h]** | **Exposure** | **N** | **M** | **SEM** | **Q1** | **Median** | **Q3** | **LCLM** | **UCLM** |
| 48:00 | 3R4F (Air) | 15 | 2.55 | 0.36 | 1.32 | 3.20 | 3.55 | 1.78 | 3.32 |
| | 3R4F (0.15) | 14 | 1.69 | 0.34 | 0.90 | 1.32 | 2.31 | 0.95 | 2.42 |
| | THS2.2 (Air) | 15 | 2.62 | 0.28 | 1.51 | 2.96 | 3.52 | 2.01 | 3.22 |
| | THS2.2 (0.15) | 15 | 2.09 | 0.30 | 1.17 | 1.64 | 2.84 | 1.45 | 2.72 |
| | THS2.2 (0.27) | 15 | 2.05 | 0.32 | 0.87 | 2.28 | 3.07 | 1.38 | 2.73 |
| | THS2.2 (0.44) | 12 | 1.71 | 0.33 | 0.79 | 1.31 | 2.61 | 0.99 | 2.43 |
| 72:00 | 3R4F (Air) | 15 | 2.15 | 0.38 | 0.98 | 1.98 | 3.50 | 1.33 | 2.97 |
| | 3R4F (0.15) | 15 | 2.11 | 0.37 | 1.22 | 1.89 | 2.83 | 1.31 | 2.90 |
| | THS2.2 (Air) | 15 | 1.93 | 0.27 | 1.03 | 1.82 | 3.07 | 1.35 | 2.50 |
| | THS2.2 (0.15) | 15 | 1.76 | 0.22 | 1.08 | 1.69 | 2.47 | 1.30 | 2.22 |
| | THS2.2 (0.27) | 15 | 1.39 | 0.22 | 0.77 | 1.20 | 1.74 | 0.92 | 1.85 |
| | THS2.2 (0.44) | 12 | 2.21 | 0.70 | 0.48 | 1.92 | 2.46 | 0.66 | 3.76 |

The proportion of positively stained cells was calculated relative to the total cell numbers. Abbreviations: h, hour; LCLM, lower confidence limit for the mean; M, mean; N, number of replicate; Q1, first quartile; Q3, third quartile; UCLM, upper confidence limit of the mean; PE, post-exposure; SEM, standard error of the mean.

14.1.12 **Supplementary Table 12**. Descriptive Statistics of Immunohistochemistry Quantification on FoxJ1 Positive Staining (%)

| | | Descriptive Statistics: FoxJ1 Positive Staining (%) | | | | | | | |
|---|---|---|---|---|---|---|---|---|---|
| **PE [h]** | **Exposure** | **N** | **M** | **SEM** | **Q1** | **Median** | **Q3** | **LCLM** | **UCLM** |
| 48:00 | 3R4F (Air) | 15 | 25.65 | 3.43 | 15.89 | 23.45 | 36.76 | 18.30 | 33.00 |
| | 3R4F (0.15) | 14 | 25.53 | 3.50 | 15.03 | 21.17 | 36.95 | 17.97 | 33.09 |
| | THS2.2 (Air) | 15 | 30.81 | 2.35 | 24.62 | 28.96 | 35.84 | 25.77 | 35.85 |
| | THS2.2 (0.15) | 15 | 26.60 | 2.27 | 21.43 | 26.22 | 32.04 | 21.73 | 31.47 |
| | THS2.2 (0.27) | 15 | 28.89 | 2.28 | 21.87 | 29.19 | 34.46 | 24.00 | 33.78 |
| | THS2.2 (0.44) | 12 | 28.61 | 3.26 | 17.73 | 29.10 | 36.51 | 21.43 | 35.79 |
| 72:00 | 3R4F (Air) | 15 | 31.76 | 2.84 | 24.98 | 33.20 | 40.08 | 25.67 | 37.84 |
| | 3R4F (0.15) | 15 | 20.84 | 2.87 | 11.68 | 18.94 | 33.57 | 14.68 | 27.01 |
| | THS2.2 (Air) | 15 | 31.96 | 2.64 | 24.26 | 32.99 | 42.20 | 26.29 | 37.63 |
| | THS2.2 (0.15) | 15 | 33.10 | 2.63 | 24.56 | 35.48 | 43.61 | 27.47 | 38.73 |
| | THS2.2 (0.27) | 15 | 33.13 | 2.37 | 24.33 | 34.98 | 39.11 | 28.04 | 38.22 |
| | THS2.2 (0.44) | 12 | 30.76 | 4.10 | 17.41 | 33.25 | 39.62 | 21.74 | 39.78 |

The proportion of positively stained cells was calculated relative to the total cell numbers. Abbreviations: h, hour; LCLM, lower confidence limit for the mean; M, mean; N, number of replicate; Q1, first quartile; Q3, third quartile; UCLM, upper confidence limit of the mean; PE, post-exposure; SEM, standard error of the mean.

## 14.1.13 **Supplementary Table 13.** Descriptive Statistics: Cytotoxicity (RLU)

| | | Descriptive Statistics | | | | | | | |
|---|---|---|---|---|---|---|---|---|---|
| **PE [h]** | **Exposure** | **N** | **M** | **SEM** | **Q1** | **Median** | **Q3** | **LCLM** | **UCLM** |
| NA | Untreated | 9 | 1244 | 195 | 1172 | 1172 | 1345 | 795 | 1694 |
| | PBS | 2 | 1139 | 166 | 973 | 1139 | 1305 | -968 | 3246 |
| | TX-100 | 7 | 73958 | 38166 | 36795 | 47434 | 47434 | -19430 | 167346 |
| 4:00 | 3R4F (Air) | 15 | 694 | 116 | 365 | 820 | 991 | 446 | 943 |
| | 3R4F (0.15) | 15 | 705 | 122 | 345 | 845 | 988 | 442 | 968 |
| | 3R4F (0.25) | 15 | 786 | 143 | 337 | 782 | 1319 | 480 | 1092 |
| | THS2.2 (Air) | 15 | 779 | 168 | 272 | 810 | 1206 | 419 | 1139 |
| | THS2.2 (0.15) | 15 | 750 | 157 | 280 | 766 | 999 | 412 | 1087 |
| | THS2.2 (0.27) | 15 | 724 | 143 | 321 | 791 | 950 | 416 | 1031 |
| | THS2.2 (0.44) | 12 | 935 | 193 | 419 | 982 | 1263 | 510 | 1360 |
| 24:00 | 3R4F (Air) | 9 | 1480 | 476 | 44 | 1273 | 2496 | 383 | 2577 |
| | 3R4F (0.15) | 9 | 3009 | 1132 | 279 | 1853 | 3969 | 399 | 5619 |
| | 3R4F (0.25) | 9 | 19438 | 6365 | 591 | 14148 | 36922 | 4761 | 34116 |
| | THS2.2 (Air) | 9 | 1670 | 603 | 86 | 1227 | 2340 | 279 | 3061 |
| | THS2.2 (0.15) | 9 | 1567 | 562 | 84 | 1146 | 1861 | 270 | 2864 |
| | THS2.2 (0.27) | 9 | 1398 | 441 | 64 | 1216 | 1671 | 380 | 2415 |
| | THS2.2 (0.44) | 9 | 3167 | 1836 | 93 | 1379 | 2784 | -1067 | 7401 |
| 48:00 | 3R4F (Air) | 15 | 1669 | 412 | 910 | 1111 | 2236 | 786 | 2553 |
| | 3R4F (0.15) | 15 | 2649 | 921 | 1154 | 1517 | 4028 | 674 | 4624 |
| | 3R4F (0.25) | 15 | 28552 | 9776 | 9164 | 13605 | 18715 | 7585 | 49518 |
| | THS2.2 (Air) | 15 | 1892 | 446 | 749 | 1573 | 2549 | 936 | 2848 |
| | THS2.2 (0.15) | 15 | 1747 | 556 | 763 | 1181 | 1586 | 555 | 2939 |
| | THS2.2 (0.27) | 15 | 1702 | 445 | 693 | 1428 | 1888 | 748 | 2655 |
| | THS2.2 (0.44) | 12 | 1941 | 644 | 430 | 1158 | 2275 | 524 | 3358 |
| 72:00 | 3R4F (Air) | 15 | 2304 | 546 | 1207 | 1841 | 2835 | 1133 | 3475 |
| | 3R4F (0.15) | 15 | 3473 | 1019 | 1474 | 1862 | 6415 | 1288 | 5657 |
| | 3R4F (0.25) | 15 | 41042 | 15255 | 11675 | 14042 | 28392 | 8322 | 73762 |
| | THS2.2 (Air) | 15 | 2200 | 498 | 930 | 2028 | 2825 | 1132 | 3269 |
| | THS2.2 (0.15) | 15 | 1912 | 509 | 924 | 1481 | 1958 | 820 | 3004 |
| | THS2.2 (0.27) | 15 | 1763 | 409 | 927 | 1571 | 2009 | 886 | 2640 |
| | THS2.2 (0.44) | 12 | 1993 | 571 | 503 | 1478 | 2464 | 735 | 3250 |

Abbreviations: h, hour; LCLM, lower confidence limit for the mean; M, mean; N, number of replicate; Q1, first quartile; Q3, third quartile; RLU, relative luminescence unit; UCLM, upper confidence limit of the mean; PBS, phosphate buffer saline; PE, post-exposure; SEM, standard error of the mean.

## 14.1.14 **Supplementary Table 14.** Descriptive Statistics: CYP1A1/1B1 Activity (RLU)

| | | Descriptive Statistics | | | | | | | |
|---|---|---|---|---|---|---|---|---|---|
| **PE[h]** | **Exposure** | **N** | **M** | **SEM** | **Q1** | **Median** | **Q3** | **LCLM** | **UCLM** |
| NA | Untreated | 7 | 836 | 124 | 674 | 814 | 1126 | 533 | 1138 |
| | TCDD | 7 | 17901 | 5517 | 4303 | 14286 | 30143 | 4402 | 31401 |
| 24:00 | 3R4F (Air) | 6 | 1938 | 259 | 1632 | 1982 | 2345 | 1273 | 2602 |
| | 3R4F (0.15) | 6 | 1519 | 341 | 777 | 1434 | 2006 | 643 | 2395 |
| | 3R4F (0.25) | 6 | 392 | 32 | 353 | 394 | 434 | 311 | 473 |
| | THS2.2 (Air) | 6 | 1468 | 317 | 814 | 1229 | 2098 | 654 | 2282 |
| | THS2.2 (0.15) | 6 | 1771 | 212 | 1327 | 1745 | 2187 | 1227 | 2315 |
| | THS2.2 (0.27) | 6 | 1599 | 213 | 1134 | 1630 | 2067 | 1052 | 2145 |
| | THS2.2 (0.44) | 3 | 1805 | 212 | 1431 | 1818 | 2165 | 893 | 2717 |
| 48:00 | 3R4F (Air) | 15 | 1298 | 224 | 561 | 1098 | 2238 | 819 | 1778 |
| | 3R4F (0.15) | 15 | 2606 | 511 | 877 | 1913 | 3393 | 1509 | 3702 |
| | 3R4F (0.25) | 15 | 551 | 85 | 258 | 431 | 807 | 369 | 732 |
| | THS2.2 (Air) | 15 | 1057 | 187 | 603 | 933 | 1272 | 655 | 1459 |
| | THS2.2 (0.15) | 15 | 1221 | 187 | 681 | 1164 | 1542 | 820 | 1622 |
| | THS2.2 (0.27) | 15 | 1244 | 200 | 742 | 1118 | 1469 | 815 | 1673 |
| | THS2.2 (0.44) | 12 | 1116 | 255 | 378 | 912 | 1646 | 556 | 1677 |
| 72:00 | 3R4F (Air) | 6 | 1794 | 306 | 1148 | 1654 | 2321 | 1008 | 2581 |
| | 3R4F (0.15) | 6 | 4849 | 650 | 3532 | 4299 | 6253 | 3178 | 6519 |
| | 3R4F (0.25) | 6 | 1266 | 285 | 529 | 1363 | 1614 | 532 | 1999 |
| | THS2.2 (Air) | 6 | 1491 | 333 | 825 | 1375 | 2321 | 635 | 2347 |
| | THS2.2 (0.15) | 6 | 1631 | 316 | 941 | 1532 | 2440 | 819 | 2443 |
| | THS2.2 (0.27) | 6 | 1667 | 314 | 977 | 1534 | 2414 | 860 | 2473 |
| | THS2.2 (0.44) | 3 | 2412 | 76 | 2260 | 2479 | 2497 | 2084 | 2740 |

Abbreviations: h, hour; LCLM, lower confidence limit for the mean; M, mean; N, number of replicate; Q1, first quartile; Q3, third quartile; RLU, relative luminescence unit; TCDD, 2,3,7,8-Tetrachlorodibenzodioxin; UCLM, upper confidence limit of the mean; PE, post-exposure; SEM, standard error of the mean.

14.1.15 **Supplementary Table 15.** Descriptive Statistics: EGF (Epidermal Growth Factor) Protein in the Basolateral Media

| | | Descriptive Statistics: EGF (pg/mL) | | | | | | | |
|---|---|---|---|---|---|---|---|---|---|
| **PE [h]** | **Exposure** | **N** | **M** | **SEM** | **Q1** | **Median** | **Q3** | **LCLM** | **UCLM** |
| 0:00 | PBS | 5 | 3.20 | 0.73 | 1.86 | 3.06 | 4.47 | 1.17 | 5.22 |
| | TNFA+IL1B | 5 | 3.33 | 0.63 | 2.20 | 2.86 | 4.51 | 1.57 | 5.08 |
| 24:00 | 3R4F (Air) | 9 | 4.06 | 1.19 | 1.40 | 1.40 | 5.45 | 1.32 | 6.79 |
| | 3R4F (0.15) | 9 | 5.29 | 1.34 | 1.40 | 3.78 | 8.55 | 2.20 | 8.38 |
| | 3R4F (0.25) | 9 | 22.75 | 3.02 | 17.16 | 23.24 | 25.93 | 15.78 | 29.73 |
| | THS2.2 (Air) | 9 | 3.68 | 0.65 | 2.18 | 3.54 | 5.34 | 2.18 | 5.19 |
| | THS2.2 (0.15) | 9 | 4.07 | 0.97 | 2.51 | 3.65 | 4.29 | 1.82 | 6.32 |
| | THS2.2 (0.27) | 9 | 3.15 | 0.51 | 1.40 | 3.87 | 4.29 | 1.97 | 4.34 |
| | THS2.2 (0.44) | 9 | 2.83 | 0.62 | 1.40 | 1.40 | 4.80 | 1.41 | 4.25 |
| 48:00 | 3R4F (Air) | 15 | 4.36 | 0.47 | 2.73 | 3.37 | 6.15 | 3.34 | 5.37 |
| | 3R4F (0.15) | 15 | 9.46 | 4.31 | 2.74 | 5.46 | 7.53 | 0.22 | 18.70 |
| | 3R4F (0.25) | 15 | 35.97 | 5.81 | 17.79 | 33.13 | 50.51 | 23.52 | 48.42 |
| | THS2.2 (Air) | 15 | 3.50 | 0.72 | 1.40 | 1.40 | 6.23 | 1.96 | 5.04 |
| | THS2.2 (0.15) | 15 | 3.63 | 0.82 | 1.40 | 1.40 | 6.42 | 1.87 | 5.38 |
| | THS2.2 (0.27) | 15 | 3.92 | 0.68 | 1.40 | 3.95 | 5.35 | 2.45 | 5.39 |
| | THS2.2 (0.44) | 12 | 4.30 | 0.85 | 1.40 | 3.50 | 7.09 | 2.44 | 6.17 |
| 72:00 | 3R4F (Air) | 9 | 10.24 | 1.69 | 6.60 | 8.31 | 12.80 | 6.33 | 14.15 |
| | 3R4F (0.15) | 9 | 15.13 | 2.72 | 9.48 | 11.36 | 20.37 | 8.85 | 21.41 |
| | 3R4F (0.25) | 9 | 49.76 | 5.29 | 35.85 | 48.58 | 62.01 | 37.56 | 61.97 |
| | THS2.2 (Air) | 9 | 6.02 | 1.03 | 3.30 | 4.66 | 9.56 | 3.63 | 8.40 |
| | THS2.2 (0.15) | 9 | 6.48 | 0.79 | 4.37 | 6.99 | 7.45 | 4.67 | 8.30 |
| | THS2.2 (0.27) | 9 | 6.99 | 2.04 | 2.52 | 4.01 | 9.99 | 2.28 | 11.69 |
| | THS2.2 (0.44) | 9 | 6.10 | 1.26 | 3.37 | 4.02 | 9.77 | 3.19 | 9.00 |

Abbreviations: h, hour; LCLM, lower confidence limit for the mean; IL, interleukin; M, mean; N, number of replicate; Q1, first quartile; Q3, third quartile; UCLM, upper confidence limit of the mean; PE, post-exposure; SEM, standard error of the mean; TNFA, tumor necrosis factor alpha.

14.1.16 **Supplementary Table 16**. Descriptive Statistics: CXCL1 (Chemokine (C-X-C motif) Ligand 1) Protein in the Basolateral Media

| | | Descriptive Statistics: CXCL1 (pg/mL) | | | | | | | |
|---|---|---|---|---|---|---|---|---|---|
| **PE [h]** | **Exposure** | **N** | **M** | **SEM** | **Q1** | **Median** | **Q3** | **LCLM** | **UCLM** |
| 0:00 | PBS | 5 | 5071.89 | 1100.26 | 3335.22 | 4078.78 | 6034.12 | 2017.08 | 8126.70 |
| | TNFA+IL1B | 5 | 121128.9 | 8229.57 | 106988.9 | 115557.7 | 126390.7 | 98279.99 | 143977.9 |
| 24:00 | 3R4F (Air) | 9 | 5351.89 | 552.28 | 4140.39 | 5259.51 | 6194.51 | 4078.34 | 6625.44 |
| | 3R4F (0.15) | 9 | 6326.36 | 883.20 | 5233.95 | 7228.37 | 8433.83 | 4289.70 | 8363.02 |
| | 3R4F (0.25) | 9 | 10900.18 | 5053.56 | 4050.09 | 5917.53 | 7079.48 | -753.34 | 22553.71 |
| | THS2.2 (Air) | 9 | 6324.83 | 864.64 | 3984.39 | 6604.90 | 7248.83 | 4330.97 | 8318.69 |
| | THS2.2 (0.15) | 9 | 4987.09 | 865.72 | 2417.02 | 5364.20 | 6648.41 | 2990.74 | 6983.45 |
| | THS2.2 (0.27) | 9 | 5808.94 | 475.15 | 5488.43 | 5934.19 | 6187.98 | 4713.24 | 6904.63 |
| | THS2.2 (0.44) | 9 | 6265.11 | 585.01 | 4993.22 | 5571.44 | 7880.10 | 4916.06 | 7614.15 |
| 48:00 | 3R4F (Air) | 15 | 9691.32 | 1675.95 | 6728.73 | 7668.36 | 10122.18 | 6096.77 | 13285.88 |
| | 3R4F (0.15) | 15 | 9019.20 | 926.18 | 6801.59 | 7810.30 | 10528.51 | 7032.73 | 11005.67 |
| | 3R4F (0.25) | 15 | 14249.19 | 2914.69 | 7829.11 | 8527.82 | 14596.31 | 7997.81 | 20500.57 |
| | THS2.2 (Air) | 15 | 6950.86 | 356.86 | 5678.62 | 6357.09 | 7869.04 | 6185.47 | 7716.26 |
| | THS2.2 (0.15) | 15 | 8266.03 | 762.74 | 6924.49 | 7648.14 | 9072.22 | 6630.12 | 9901.95 |
| | THS2.2 (0.27) | 15 | 7255.77 | 557.27 | 6154.09 | 6825.95 | 7891.67 | 6060.55 | 8451.00 |
| | THS2.2 (0.44) | 12 | 10122.04 | 3011.64 | 6215.12 | 7242.41 | 9202.05 | 3493.47 | 16750.61 |
| 72:00 | 3R4F (Air) | 9 | 10063.44 | 2240.43 | 6329.35 | 10228.57 | 12601.61 | 4897.01 | 15229.87 |
| | 3R4F (0.15) | 9 | 12423.50 | 3117.05 | 5087.14 | 10864.66 | 13951.49 | 5235.57 | 19611.43 |
| | 3R4F (0.25) | 9 | 32789.58 | 14926.96 | 1610.88 | 16553.54 | 35818.81 | -1632.06 | 67211.22 |
| | THS2.2 (Air) | 9 | 14633.48 | 2193.73 | 10767.08 | 11187.17 | 16894.15 | 9574.72 | 19692.24 |
| | THS2.2 (0.15) | 9 | 11541.41 | 1831.02 | 8705.52 | 9429.10 | 13315.52 | 7319.06 | 15763.76 |
| | THS2.2 (0.27) | 9 | 9541.45 | 778.94 | 8355.44 | 9397.21 | 10154.16 | 7745.20 | 11337.70 |
| | THS2.2 (0.44) | 9 | 16699.94 | 5447.20 | 8229.42 | 10531.16 | 16043.74 | 4138.68 | 29261.19 |

Abbreviations: h, hour; LCLM, lower confidence limit for the mean; IL, interleukin; M, mean; N, number of replicate; Q1, first quartile; Q3, third quartile; UCLM, upper confidence limit of the mean; PE, post-exposure; SEM, standard error of the mean; TNFA, tumor necrosis factor alpha.

14.1.17 **Supplementary Table 17.** Descriptive Statistics: IL6 (Interleukin 6) Protein in the Basolateral Media

| | | Descriptive Statistics: IL6 (pg/mL) | | | | | | | |
|---|---|---|---|---|---|---|---|---|---|
| **PE [h]** | **Exposure** | **N** | **M** | **SEM** | **Q1** | **Median** | **Q3** | **LCLM** | **UCLM** |
| 0:00 | PBS | 5 | 20.58 | 2.74 | 16.82 | 16.97 | 26.79 | 12.97 | 28.19 |
| | TNFA+IL1B | 5 | 303.56 | 94.21 | 134.93 | 257.91 | 383.02 | 42.00 | 565.12 |
| 24:00 | 3R4F (Air) | 9 | 24.06 | 8.01 | 10.16 | 12.59 | 19.79 | 5.59 | 42.53 |
| | 3R4F (0.15) | 9 | 52.16 | 14.85 | 17.52 | 28.80 | 73.91 | 17.92 | 86.40 |
| | 3R4F (0.25) | 9 | 25.04 | 4.11 | 18.29 | 22.31 | 38.46 | 15.56 | 34.52 |
| | THS2.2 (Air) | 9 | 21.19 | 4.15 | 11.94 | 15.76 | 27.21 | 11.62 | 30.77 |
| | THS2.2 (0.15) | 9 | 20.41 | 6.65 | 4.97 | 11.74 | 29.56 | 5.07 | 35.76 |
| | THS2.2 (0.27) | 9 | 31.74 | 8.65 | 16.55 | 21.39 | 31.36 | 11.80 | 51.68 |
| | THS2.2 (0.44) | 9 | 28.02 | 6.45 | 12.88 | 21.16 | 41.52 | 13.14 | 42.90 |
| 48:00 | 3R4F (Air) | 15 | 82.94 | 28.37 | 26.21 | 41.11 | 81.52 | 22.10 | 143.79 |
| | 3R4F (0.15) | 15 | 55.83 | 12.87 | 17.53 | 46.21 | 63.80 | 28.23 | 83.44 |
| | 3R4F (0.25) | 15 | 50.08 | 7.07 | 28.76 | 48.36 | 59.63 | 34.91 | 65.26 |
| | THS2.2 (Air) | 15 | 33.71 | 5.97 | 18.76 | 24.46 | 51.45 | 20.91 | 46.51 |
| | THS2.2 (0.15) | 15 | 44.30 | 9.15 | 17.86 | 35.11 | 55.84 | 24.67 | 63.93 |
| | THS2.2 (0.27) | 15 | 49.10 | 9.44 | 18.83 | 43.37 | 58.50 | 28.85 | 69.36 |
| | THS2.2 (0.44) | 12 | 26.94 | 4.45 | 13.77 | 26.20 | 39.70 | 17.16 | 36.73 |
| 72:00 | 3R4F (Air) | 9 | 67.85 | 13.67 | 42.11 | 49.07 | 110.67 | 36.32 | 99.38 |
| | 3R4F (0.15) | 9 | 63.88 | 13.71 | 42.89 | 49.84 | 107.85 | 32.25 | 95.50 |
| | 3R4F (0.25) | 9 | 129.86 | 46.30 | 8.39 | 87.93 | 229.06 | 23.08 | 236.64 |
| | THS2.2 (Air) | 9 | 84.14 | 25.11 | 34.90 | 53.24 | 88.80 | 26.23 | 142.05 |
| | THS2.2 (0.15) | 9 | 91.90 | 21.79 | 47.91 | 78.16 | 118.52 | 41.65 | 142.15 |
| | THS2.2 (0.27) | 9 | 57.81 | 14.81 | 27.17 | 45.12 | 60.75 | 23.66 | 91.96 |
| | THS2.2 (0.44) | 9 | 59.76 | 9.20 | 31.44 | 72.42 | 82.46 | 38.56 | 80.97 |

Abbreviations: h, hour; LCLM, lower confidence limit for the mean; IL, interleukin; M, mean; N, number of replicate; Q1, first quartile; Q3, third quartile; UCLM, upper confidence limit of the mean; PE, post-exposure; SEM, standard error of the mean; TNFA, tumor necrosis factor alpha.

14.1.18 **Supplementary Table 18.** Descriptive Statistics: CXCL8 (Chemokine (C-X-C motif) Ligand 8) Protein in the Basolateral Media

| | | Descriptive Statistics: CXCL8 (pg/mL) | | | | | | | |
|---|---|---|---|---|---|---|---|---|---|
| **PE [h]** | **Exposure** | **N** | **M** | **SEM** | **Q1** | **Median** | **Q3** | **LCLM** | **UCLM** |
| 0:00 | PBS | 5 | 2032.23 | 604.62 | 1228.08 | 1649.32 | 1989.10 | 353.53 | 3710.94 |
| | TNFA+IL1B | 5 | 60079.49 | 9171.49 | 44769.57 | 55468.73 | 64886.91 | 34615.36 | 85543.61 |
| 24:00 | 3R4F (Air) | 9 | 2699.51 | 434.90 | 1848.32 | 2277.45 | 3132.97 | 1696.63 | 3702.39 |
| | 3R4F (0.15) | 9 | 5528.48 | 881.40 | 3755.89 | 5912.49 | 6664.21 | 3495.96 | 7561.00 |
| | 3R4F (0.25) | 9 | 9098.99 | 3542.01 | 3734.16 | 6635.33 | 8089.33 | 931.10 | 17266.88 |
| | THS2.2 (Air) | 9 | 2740.19 | 430.33 | 1679.76 | 2526.01 | 3323.81 | 1747.85 | 3732.53 |
| | THS2.2 (0.15) | 9 | 2269.36 | 441.91 | 1512.60 | 2034.73 | 2397.02 | 1250.31 | 3288.41 |
| | THS2.2 (0.27) | 9 | 3345.66 | 446.52 | 2592.67 | 3286.08 | 3813.37 | 2315.98 | 4375.33 |
| | THS2.2 (0.44) | 9 | 4176.99 | 709.75 | 2308.27 | 3941.63 | 6261.52 | 2540.30 | 5813.68 |
| 48:00 | 3R4F (Air) | 15 | 4649.33 | 518.01 | 2928.77 | 4538.27 | 6500.14 | 3538.31 | 5760.34 |
| | 3R4F (0.15) | 15 | 6184.49 | 768.13 | 3794.32 | 5653.71 | 7781.69 | 4537.02 | 7831.96 |
| | 3R4F (0.25) | 15 | 10692.21 | 1882.09 | 6762.96 | 7958.62 | 11910.28 | 6655.53 | 14728.89 |
| | THS2.2 (Air) | 15 | 3191.16 | 356.02 | 2085.26 | 3092.12 | 4541.22 | 2427.57 | 3954.76 |
| | THS2.2 (0.15) | 15 | 3859.21 | 379.99 | 2609.81 | 3673.29 | 5137.36 | 3044.21 | 4674.22 |
| | THS2.2 (0.27) | 15 | 4043.76 | 459.93 | 2517.73 | 3821.72 | 5360.71 | 3057.31 | 5030.21 |
| | THS2.2 (0.44) | 12 | 4338.81 | 533.85 | 2807.40 | 4299.00 | 5666.65 | 3163.80 | 5513.81 |
| 72:00 | 3R4F (Air) | 9 | 4158.38 | 779.29 | 1831.61 | 4777.02 | 5430.75 | 2361.34 | 5955.43 |
| | 3R4F (0.15) | 9 | 6723.89 | 2156.33 | 1949.87 | 4741.21 | 9270.09 | 1751.39 | 11696.38 |
| | 3R4F (0.25) | 9 | 22023.84 | 7600.83 | 1326.91 | 20530.61 | 32222.76 | 4496.29 | 39551.39 |
| | THS2.2 (Air) | 9 | 6328.87 | 483.84 | 5219.93 | 6407.93 | 7429.27 | 5213.14 | 7444.60 |
| | THS2.2 (0.15) | 9 | 6493.90 | 624.01 | 5327.02 | 6504.66 | 7949.24 | 5054.94 | 7932.86 |
| | THS2.2 (0.27) | 9 | 6009.57 | 514.72 | 5257.60 | 5478.15 | 6909.62 | 4822.63 | 7196.52 |
| | THS2.2 (0.44) | 9 | 6991.01 | 1078.07 | 5266.06 | 6007.79 | 7356.53 | 4504.97 | 9477.05 |

Abbreviations: h, hour; LCLM, lower confidence limit for the mean; IL, interleukin; M, mean; N, number of replicate; Q1, first quartile; Q3, third quartile; UCLM, upper confidence limit of the mean; PE, post-exposure; SEM, standard error of the mean; TNFA, tumor necrosis factor alpha.

14.1.19 **Supplementary Table 19.** Descriptive Statistics: CCL20 (Chemokine (C-C motif) Ligand 20) Protein in the Basolateral Media

| | | Descriptive Statistics: CCL20 (pg/mL) | | | | | | | |
|---|---|---|---|---|---|---|---|---|---|
| **PE [h]** | **Exposure** | **N** | **M** | **SEM** | **Q1** | **Median** | **Q3** | **LCLM** | **UCLM** |
| 0:00 | PBS | 5 | 22.05 | 9.71 | 10.55 | 12.01 | 20.03 | -4.91 | 49.01 |
| | TNFA+IL1B | 5 | 4678.54 | 719.36 | 3304.41 | 4180.22 | 6174.25 | 2681.28 | 6675.80 |
| 24:00 | 3R4F (Air) | 9 | 24.07 | 7.56 | 6.75 | 12.84 | 31.46 | 6.65 | 41.50 |
| | 3R4F (0.15) | 9 | 17.79 | 4.05 | 9.38 | 11.01 | 27.43 | 8.45 | 27.13 |
| | 3R4F (0.25) | 9 | 19.78 | 8.03 | 11.04 | 11.42 | 14.69 | 1.26 | 38.30 |
| | THS2.2 (Air) | 9 | 19.61 | 2.85 | 14.60 | 17.09 | 23.25 | 13.03 | 26.20 |
| | THS2.2 (0.15) | 9 | 19.02 | 3.54 | 12.53 | 16.06 | 21.55 | 10.86 | 27.18 |
| | THS2.2 (0.27) | 9 | 19.78 | 4.30 | 8.36 | 15.37 | 25.87 | 9.86 | 29.70 |
| | THS2.2 (0.44) | 9 | 23.99 | 5.88 | 16.16 | 17.77 | 20.64 | 10.44 | 37.54 |
| 48:00 | 3R4F (Air) | 15 | 38.36 | 11.23 | 22.57 | 27.52 | 36.08 | 14.28 | 62.44 |
| | 3R4F (0.15) | 15 | 46.11 | 10.99 | 19.59 | 25.67 | 67.04 | 22.55 | 69.68 |
| | 3R4F (0.25) | 15 | 94.60 | 7.95 | 69.28 | 96.65 | 108.16 | 77.56 | 111.64 |
| | THS2.2 (Air) | 15 | 22.33 | 2.32 | 15.60 | 21.38 | 25.21 | 17.35 | 27.31 |
| | THS2.2 (0.15) | 15 | 22.89 | 2.46 | 17.42 | 21.14 | 25.32 | 17.62 | 28.17 |
| | THS2.2 (0.27) | 15 | 20.68 | 1.94 | 13.44 | 21.68 | 25.93 | 16.52 | 24.84 |
| | THS2.2 (0.44) | 12 | 20.65 | 1.56 | 16.66 | 19.19 | 25.83 | 17.20 | 24.09 |
| 72:00 | 3R4F (Air) | 9 | 58.62 | 12.92 | 25.47 | 59.37 | 84.27 | 28.84 | 88.40 |
| | 3R4F (0.15) | 9 | 102.13 | 33.29 | 27.10 | 67.45 | 126.98 | 25.35 | 178.90 |
| | 3R4F (0.25) | 9 | 184.65 | 17.46 | 152.92 | 187.65 | 234.08 | 144.39 | 224.92 |
| | THS2.2 (Air) | 9 | 77.83 | 14.92 | 39.74 | 59.64 | 104.37 | 43.43 | 112.23 |
| | THS2.2 (0.15) | 9 | 71.32 | 24.52 | 32.85 | 50.39 | 73.51 | 14.78 | 127.87 |
| | THS2.2 (0.27) | 9 | 45.91 | 6.71 | 37.94 | 42.52 | 56.94 | 30.43 | 61.39 |
| | THS2.2 (0.44) | 9 | 106.14 | 43.40 | 49.63 | 52.14 | 94.80 | 6.05 | 206.22 |

Abbreviations: h, hour; LCLM, lower confidence limit for the mean; IL, interleukin; M, mean; N, number of replicate; Q1, first quartile; Q3, third quartile; UCLM, upper confidence limit of the mean; PE, post-exposure; SEM, standard error of the mean; TNFA, tumor necrosis factor alpha.

14.1.20 **Supplementary Table 20.** Descriptive Statistics: MMP1 (Matrix Metalloproteinase 1) Protein in the Basolateral Media

| | | Descriptive Statistics: MMP1 (pg/mL) | | | | | | | |
|---|---|---|---|---|---|---|---|---|---|
| **PE [h]** | **Exposure** | **N** | **M** | **SEM** | **Q1** | **Median** | **Q3** | **LCLM** | **UCLM** |
| 0:00 | PBS | 5 | 372.94 | 107.61 | 213.27 | 304.60 | 389.94 | 74.17 | 671.72 |
| | TNFA+IL1B | 5 | 2206.95 | 687.08 | 1316.33 | 1666.96 | 1961.47 | 299.31 | 4114.58 |
| 24:00 | 3R4F (Air) | 9 | 463.14 | 91.77 | 306.18 | 337.27 | 644.37 | 251.52 | 674.77 |
| | 3R4F (0.15) | 9 | 1742.84 | 431.91 | 998.29 | 1696.04 | 1810.40 | 746.85 | 2738.83 |
| | 3R4F (0.25) | 9 | 1822.61 | 775.72 | 1054.96 | 1139.01 | 1282.37 | 33.80 | 3611.42 |
| | THS2.2 (Air) | 9 | 480.22 | 53.15 | 354.98 | 402.64 | 510.13 | 357.67 | 602.78 |
| | THS2.2 (0.15) | 9 | 433.36 | 46.03 | 351.99 | 421.86 | 480.70 | 327.21 | 539.51 |
| | THS2.2 (0.27) | 9 | 502.30 | 43.62 | 414.28 | 471.35 | 503.37 | 401.72 | 602.88 |
| | THS2.2 (0.44) | 9 | 619.08 | 105.20 | 426.03 | 512.64 | 663.84 | 376.49 | 861.67 |
| 48:00 | 3R4F (Air) | 15 | 771.82 | 135.24 | 572.33 | 647.51 | 783.27 | 481.76 | 1061.88 |
| | 3R4F (0.15) | 15 | 1893.98 | 326.46 | 1011.81 | 1453.22 | 2318.27 | 1193.80 | 2594.16 |
| | 3R4F (0.25) | 15 | 1823.27 | 271.07 | 1084.84 | 1346.36 | 2489.95 | 1241.89 | 2404.65 |
| | THS2.2 (Air) | 15 | 605.15 | 45.06 | 504.13 | 626.80 | 662.48 | 508.50 | 701.80 |
| | THS2.2 (0.15) | 15 | 695.67 | 76.63 | 425.86 | 598.20 | 931.86 | 531.33 | 860.02 |
| | THS2.2 (0.27) | 15 | 723.71 | 52.69 | 557.22 | 700.54 | 790.97 | 610.69 | 836.72 |
| | THS2.2 (0.44) | 12 | 794.25 | 54.14 | 651.50 | 775.33 | 886.28 | 675.09 | 913.42 |
| 72:00 | 3R4F (Air) | 9 | 1186.72 | 274.55 | 725.45 | 763.53 | 1313.58 | 553.62 | 1819.82 |
| | 3R4F (0.15) | 9 | 3440.89 | 1055.65 | 1661.94 | 2470.81 | 4026.71 | 1006.57 | 5875.21 |
| | 3R4F (0.25) | 9 | 7943.13 | 1502.00 | 3241.62 | 7761.98 | 11410.54 | 4479.51 | 11406.75 |
| | THS2.2 (Air) | 9 | 1587.33 | 341.51 | 1048.43 | 1170.37 | 1570.43 | 799.80 | 2374.86 |
| | THS2.2 (0.15) | 9 | 1229.88 | 172.35 | 827.75 | 1251.37 | 1380.62 | 832.44 | 1627.33 |
| | THS2.2 (0.27) | 9 | 1120.61 | 121.14 | 885.92 | 959.02 | 1315.13 | 841.25 | 1399.97 |
| | THS2.2 (0.44) | 9 | 1851.54 | 508.09 | 1220.17 | 1471.51 | 1776.16 | 679.89 | 3023.19 |

Abbreviations: h, hour; LCLM, lower confidence limit for the mean; IL, interleukin; M, mean; N, number of replicate; Q1, first quartile; Q3, third quartile; UCLM, upper confidence limit of the mean; PE, post-exposure; SEM, standard error of the mean; TNFA, tumor necrosis factor alpha.

14.1.21 **Supplementary Table 21.** Descriptive Statistics: MMP9 (Matrix Metalloproteinase 9) Protein in the Basolateral Media

| | | Descriptive Statistics: MMP9 (pg/mL) | | | | | | | |
|---|---|---|---|---|---|---|---|---|---|
| **PE [h]** | **Exposure** | **N** | **M** | **SEM** | **Q1** | **Median** | **Q3** | **LCLM** | **UCLM** |
| 0:00 | PBS | 5 | 6421.24 | 1871.00 | 3641.99 | 3917.51 | 8577.90 | 1226.51 | 11615.98 |
| | TNFA+IL1B | 5 | 9328.58 | 4853.59 | 2341.85 | 4865.65 | 9377.12 | -4147.15 | 22804.31 |
| 24:00 | 3R4F (Air) | 9 | 7730.34 | 1617.94 | 2776.31 | 8244.55 | 11014.59 | 3999.36 | 11461.32 |
| | 3R4F (0.15) | 9 | 10348.47 | 2686.13 | 2503.84 | 8876.58 | 13281.22 | 4154.24 | 16542.69 |
| | 3R4F (0.25) | 9 | 17982.27 | 12477.41 | 2335.87 | 3620.71 | 12162.10 | -10790.7 | 46755.22 |
| | THS2.2 (Air) | 9 | 9325.04 | 1241.10 | 6375.09 | 10366.17 | 12212.83 | 6463.06 | 12187.01 |
| | THS2.2 (0.15) | 9 | 8697.18 | 1287.44 | 6640.20 | 8045.38 | 9940.12 | 5728.33 | 11666.02 |
| | THS2.2 (0.27) | 9 | 11050.18 | 1260.34 | 8742.56 | 10169.97 | 14269.53 | 8143.82 | 13956.54 |
| | THS2.2 (0.44) | 9 | 12099.93 | 1908.68 | 9627.43 | 11194.21 | 16641.15 | 7698.52 | 16501.35 |
| 48:00 | 3R4F (Air) | 15 | 12276.25 | 2074.93 | 6567.99 | 10220.49 | 21832.17 | 7825.97 | 16726.53 |
| | 3R4F (0.15) | 15 | 15560.82 | 3404.91 | 2468.00 | 13211.14 | 27244.10 | 8258.00 | 22863.63 |
| | 3R4F (0.25) | 15 | 20650.56 | 3984.10 | 8419.82 | 13989.20 | 36957.80 | 12105.52 | 29195.61 |
| | THS2.2 (Air) | 15 | 11896.54 | 1813.40 | 7937.61 | 9911.56 | 18972.42 | 8007.19 | 15785.89 |
| | THS2.2 (0.15) | 15 | 13765.66 | 2039.99 | 7615.78 | 11170.05 | 22724.42 | 9390.31 | 18141.01 |
| | THS2.2 (0.27) | 15 | 11972.42 | 1945.75 | 5934.71 | 8086.68 | 15809.89 | 7799.20 | 16145.64 |
| | THS2.2 (0.44) | 12 | 11761.05 | 1836.90 | 6372.36 | 11077.63 | 18041.76 | 7718.07 | 15804.03 |
| 72:00 | 3R4F (Air) | 9 | 27995.42 | 6166.16 | 5767.12 | 31214.16 | 43405.03 | 13776.22 | 42214.62 |
| | 3R4F (0.15) | 9 | 35416.63 | 11594.21 | 4068.99 | 26717.57 | 51376.45 | 8680.33 | 62152.92 |
| | 3R4F (0.25) | 9 | 73516.06 | 21005.51 | 37200.16 | 56827.41 | 63841.83 | 25077.27 | 121954.9 |
| | THS2.2 (Air) | 9 | 30682.14 | 3757.03 | 21245.49 | 30983.19 | 36271.84 | 22018.42 | 39345.87 |
| | THS2.2 (0.15) | 9 | 29365.74 | 3925.91 | 20338.79 | 29487.11 | 35085.91 | 20312.58 | 38418.90 |
| | THS2.2 (0.27) | 9 | 25903.88 | 2646.04 | 19168.15 | 28409.00 | 31047.65 | 19802.11 | 32005.66 |
| | THS2.2 (0.44) | 9 | 34538.70 | 6383.95 | 26499.26 | 31820.69 | 34384.50 | 19817.28 | 49260.12 |

Abbreviations: h, hour; LCLM, lower confidence limit for the mean; IL, interleukin; M, mean; N, number of replicate; Q1, first quartile; Q3, third quartile; UCLM, upper confidence limit of the mean; PE, post-exposure; SEM, standard error of the mean; TNFA, tumor necrosis factor alpha.

14.1.22 **Supplementary Table 22.** Descriptive Statistics: sICAM1 (soluble Inter-Cellular Adhesion Molecule 1) Protein in the Basolateral Media

| | | Descriptive Statistics: sICAM1 (pg/mL) | | | | | | | |
|---|---|---|---|---|---|---|---|---|---|
| **PE [h]** | **Exposure** | **N** | **M** | **SEM** | **Q1** | **Median** | **Q3** | **LCLM** | **UCLM** |
| 0:00 | PBS | 5 | 66.22 | 18.54 | 39.96 | 40.13 | 90.33 | 14.76 | 117.68 |
| | TNFA+IL1B | 5 | 649.06 | 44.03 | 584.76 | 599.87 | 749.88 | 526.80 | 771.31 |
| 24:00 | 3R4F (Air) | 9 | 83.96 | 21.09 | 35.54 | 67.66 | 132.10 | 35.34 | 132.59 |
| | 3R4F (0.15) | 9 | 114.62 | 47.67 | 42.40 | 77.12 | 115.17 | 4.69 | 224.54 |
| | 3R4F (0.25) | 9 | 567.74 | 298.54 | 186.93 | 262.59 | 367.14 | -120.70 | 1256.18 |
| | THS2.2 (Air) | 9 | 77.57 | 12.62 | 42.31 | 79.14 | 102.86 | 48.47 | 106.67 |
| | THS2.2 (0.15) | 9 | 70.38 | 12.69 | 51.21 | 56.00 | 110.04 | 41.13 | 99.64 |
| | THS2.2 (0.27) | 9 | 83.11 | 15.57 | 56.95 | 70.70 | 88.59 | 47.21 | 119.01 |
| | THS2.2 (0.44) | 9 | 97.94 | 10.11 | 90.22 | 97.15 | 114.41 | 74.63 | 121.26 |
| 48:00 | 3R4F (Air) | 15 | 169.10 | 43.71 | 74.20 | 134.01 | 192.41 | 75.35 | 262.84 |
| | 3R4F (0.15) | 15 | 168.00 | 32.63 | 83.41 | 122.15 | 230.12 | 98.01 | 237.99 |
| | 3R4F (0.25) | 15 | 680.96 | 161.76 | 291.91 | 571.68 | 709.98 | 334.03 | 1027.89 |
| | THS2.2 (Air) | 15 | 104.98 | 7.42 | 82.31 | 107.31 | 121.63 | 89.08 | 120.89 |
| | THS2.2 (0.15) | 15 | 119.30 | 11.60 | 87.15 | 96.37 | 145.01 | 94.42 | 144.18 |
| | THS2.2 (0.27) | 15 | 114.27 | 8.32 | 92.20 | 100.21 | 149.17 | 96.43 | 132.10 |
| | THS2.2 (0.44) | 12 | 102.66 | 7.53 | 81.53 | 98.41 | 121.54 | 86.09 | 119.23 |
| 72:00 | 3R4F (Air) | 9 | 232.36 | 45.92 | 143.03 | 187.50 | 282.38 | 126.47 | 338.26 |
| | 3R4F (0.15) | 9 | 190.75 | 46.01 | 113.80 | 156.78 | 222.41 | 84.65 | 296.85 |
| | 3R4F (0.25) | 9 | 936.92 | 263.21 | 464.87 | 594.28 | 1301.37 | 329.97 | 1543.88 |
| | THS2.2 (Air) | 9 | 274.68 | 44.91 | 155.90 | 239.51 | 385.30 | 171.11 | 378.25 |
| | THS2.2 (0.15) | 9 | 275.65 | 78.52 | 167.39 | 193.62 | 281.48 | 94.58 | 456.73 |
| | THS2.2 (0.27) | 9 | 209.26 | 25.95 | 130.33 | 191.02 | 274.49 | 149.41 | 269.11 |
| | THS2.2 (0.44) | 9 | 251.43 | 40.91 | 171.89 | 224.60 | 326.32 | 157.09 | 345.76 |

Abbreviations: h, hour; LCLM, lower confidence limit for the mean; IL, interleukin; M, mean; N, number of replicate; Q1, first quartile; Q3, third quartile; UCLM, upper confidence limit of the mean; PE, post-exposure; SEM, standard error of the mean; TNFA, tumor necrosis factor alpha.

14.1.23 **Supplementary Table 23.** Descriptive Statistics: TIMP1 (Tissue Inhibitor of Metalloproteinase 1) Protein in the Basolateral Media

| | | Descriptive Statistics: TIMP1 (pg/mL) | | | | | | | |
|---|---|---|---|---|---|---|---|---|---|
| **PE [h]** | **Exposure** | **N** | **M** | **SEM** | **Q1** | **Median** | **Q3** | **LCLM** | **UCLM** |
| 0:00 | PBS | 5 | 1645.09 | 378.31 | 1064.48 | 1242.44 | 1896.73 | 594.72 | 2695.46 |
| | TNFA+IL1B | 5 | 2462.56 | 639.92 | 1666.21 | 1739.94 | 2793.17 | 685.86 | 4239.27 |
| 24:00 | 3R4F (Air) | 9 | 1275.56 | 239.12 | 649.94 | 1335.91 | 1491.20 | 724.14 | 1826.98 |
| | 3R4F (0.15) | 9 | 3029.81 | 542.28 | 2065.67 | 3268.60 | 3655.18 | 1779.32 | 4280.30 |
| | 3R4F (0.25) | 9 | 3452.07 | 1327.92 | 1096.36 | 2403.58 | 3027.82 | 389.89 | 6514.26 |
| | THS2.2 (Air) | 9 | 1571.09 | 131.76 | 1416.16 | 1442.03 | 1884.09 | 1267.24 | 1874.94 |
| | THS2.2 (0.15) | 9 | 1535.65 | 151.06 | 1391.25 | 1496.24 | 1594.26 | 1187.30 | 1883.99 |
| | THS2.2 (0.27) | 9 | 1933.31 | 211.36 | 1537.89 | 1913.70 | 2255.96 | 1445.91 | 2420.70 |
| | THS2.2 (0.44) | 9 | 2203.79 | 432.61 | 1517.77 | 1896.19 | 2365.77 | 1206.20 | 3201.39 |
| 48:00 | 3R4F (Air) | 15 | 3375.41 | 340.76 | 2316.57 | 3349.87 | 4165.38 | 2644.56 | 4106.26 |
| | 3R4F (0.15) | 15 | 11077.62 | 1335.03 | 5434.83 | 10471.34 | 15252.51 | 8214.26 | 13940.98 |
| | 3R4F (0.25) | 15 | 10946.92 | 1809.96 | 4742.77 | 8843.06 | 16586.09 | 7064.93 | 14828.90 |
| | THS2.2 (Air) | 15 | 3725.09 | 579.47 | 2381.97 | 2599.85 | 4789.40 | 2482.25 | 4967.93 |
| | THS2.2 (0.15) | 15 | 3204.03 | 387.70 | 2199.42 | 2334.91 | 4450.58 | 2372.49 | 4035.57 |
| | THS2.2 (0.27) | 15 | 3970.27 | 504.92 | 2470.43 | 3328.05 | 5206.55 | 2887.33 | 5053.21 |
| | THS2.2 (0.44) | 12 | 4463.50 | 719.38 | 2617.80 | 4061.59 | 6056.48 | 2880.15 | 6046.86 |
| 72:00 | 3R4F (Air) | 9 | 7539.66 | 1737.08 | 3517.94 | 6860.36 | 12949.38 | 3533.94 | 11545.37 |
| | 3R4F (0.15) | 9 | 26113.71 | 4234.55 | 16131.52 | 23483.27 | 29373.54 | 16348.81 | 35878.61 |
| | 3R4F (0.25) | 9 | 16496.58 | 3810.68 | 4103.46 | 17034.09 | 22081.56 | 7709.14 | 25284.02 |
| | THS2.2 (Air) | 9 | 3706.74 | 494.74 | 3324.76 | 3839.17 | 4155.62 | 2565.87 | 4847.60 |
| | THS2.2 (0.15) | 9 | 5231.98 | 1173.28 | 2928.38 | 4055.27 | 8381.10 | 2526.39 | 7937.56 |
| | THS2.2 (0.27) | 9 | 4532.08 | 819.92 | 3103.05 | 3808.40 | 4830.24 | 2641.33 | 6422.83 |
| | THS2.2 (0.44) | 9 | 8916.24 | 3436.23 | 4272.38 | 4666.64 | 6829.31 | 992.27 | 16840.20 |

Abbreviations: h, hour; LCLM, lower confidence limit for the mean; IL, interleukin; M, mean; N, number of replicate; Q1, first quartile; Q3, third quartile; UCLM, upper confidence limit of the mean; PE, post-exposure; SEM, standard error of the mean; TNFA, tumor necrosis factor alpha.

14.1.24 **Supplementary Table 24**. Descriptive Statistics: TNFA (Tumor Necrosis Factor Alpha) Protein in the Basolateral Media

| | | Descriptive Statistics: TNFA (pg/mL) | | | | | | | |
|---|---|---|---|---|---|---|---|---|---|
| **PE [h]** | **Exposure** | **N** | **M** | **SEM** | **Q1** | **Median** | **Q3** | **LCLM** | **UCLM** |
| 0:00 | PBS | 5 | 10.07 | 3.22 | 5.78 | 7.24 | 11.97 | 1.13 | 19.02 |
| | TNFA+IL1B | 5 | 8269.19 | 1427.58 | 7398.61 | 7966.91 | 8230.91 | 4305.60 | 12232.78 |
| 24:00 | 3R4F (Air) | 9 | 8.48 | 1.40 | 6.44 | 8.16 | 9.09 | 5.25 | 11.70 |
| | 3R4F (0.15) | 9 | 8.04 | 1.10 | 4.84 | 8.84 | 10.45 | 5.51 | 10.58 |
| | 3R4F (0.25) | 9 | 15.44 | 4.77 | 8.79 | 11.42 | 14.96 | 4.45 | 26.44 |
| | THS2.2 (Air) | 9 | 9.10 | 0.95 | 7.45 | 8.79 | 9.60 | 6.92 | 11.28 |
| | THS2.2 (0.15) | 9 | 7.86 | 1.71 | 5.31 | 6.62 | 11.66 | 3.92 | 11.81 |
| | THS2.2 (0.27) | 9 | 9.93 | 1.27 | 8.28 | 9.80 | 10.88 | 7.00 | 12.86 |
| | THS2.2 (0.44) | 9 | 8.98 | 1.54 | 5.99 | 8.62 | 12.64 | 5.42 | 12.55 |
| 48:00 | 3R4F (Air) | 15 | 16.85 | 3.60 | 10.83 | 13.53 | 17.05 | 9.14 | 24.57 |
| | 3R4F (0.15) | 15 | 8.81 | 1.76 | 4.74 | 7.06 | 10.54 | 5.03 | 12.59 |
| | 3R4F (0.25) | 15 | 14.90 | 2.13 | 7.75 | 14.08 | 17.36 | 10.32 | 19.48 |
| | THS2.2 (Air) | 15 | 10.24 | 1.44 | 5.64 | 9.36 | 13.85 | 7.14 | 13.33 |
| | THS2.2 (0.15) | 15 | 11.73 | 1.43 | 6.80 | 11.80 | 15.02 | 8.66 | 14.80 |
| | THS2.2 (0.27) | 15 | 11.60 | 1.44 | 6.55 | 11.59 | 15.06 | 8.52 | 14.68 |
| | THS2.2 (0.44) | 12 | 8.73 | 0.95 | 6.37 | 9.12 | 10.94 | 6.63 | 10.83 |
| 72:00 | 3R4F (Air) | 9 | 18.82 | 4.29 | 9.23 | 20.66 | 26.88 | 8.92 | 28.72 |
| | 3R4F (0.15) | 9 | 12.89 | 1.78 | 10.72 | 13.78 | 15.90 | 8.77 | 17.00 |
| | 3R4F (0.25) | 9 | 32.15 | 7.63 | 15.76 | 21.20 | 44.20 | 14.56 | 49.75 |
| | THS2.2 (Air) | 9 | 25.53 | 2.81 | 19.54 | 22.26 | 29.71 | 19.04 | 32.01 |
| | THS2.2 (0.15) | 9 | 29.58 | 4.39 | 20.00 | 27.51 | 43.42 | 19.45 | 39.71 |
| | THS2.2 (0.27) | 9 | 20.90 | 2.86 | 14.92 | 17.54 | 30.52 | 14.31 | 27.48 |
| | THS2.2 (0.44) | 9 | 22.70 | 3.05 | 14.30 | 23.28 | 26.34 | 15.66 | 29.73 |

Abbreviations: h, hour; LCLM, lower confidence limit for the mean; IL, interleukin; M, mean; N, number of replicate; Q1, first quartile; Q3, third quartile; UCLM, upper confidence limit of the mean; PE, post-exposure; SEM, standard error of the mean; TNFA, tumor necrosis factor alpha.

14.1.25 **Supplementary Table 25**. Descriptive Statistics of VEGFA (Vascular Endothelial Growth Factor Alpha) Protein in the Basolateral Media

| | | Descriptive Statistics: VEGFA (pg/mL) | | | | | | | |
|---|---|---|---|---|---|---|---|---|---|
| **PE [h]** | **Exposure** | **N** | **M** | **SEM** | **Q1** | **Median** | **Q3** | **LCLM** | **UCLM** |
| 0:00 | PBS | 5 | 101.39 | 44.13 | 28.83 | 47.95 | 201.79 | -21.13 | 223.91 |
| | TNFA+IL1B | 5 | 445.49 | 161.51 | 66.99 | 575.04 | 666.35 | -2.95 | 893.92 |
| 24:00 | 3R4F (Air) | 9 | 127.26 | 34.05 | 30.43 | 100.29 | 196.34 | 48.74 | 205.78 |
| | 3R4F (0.15) | 9 | 460.91 | 86.56 | 284.90 | 384.26 | 677.14 | 261.30 | 660.51 |
| | 3R4F (0.25) | 9 | 230.63 | 43.07 | 111.90 | 219.65 | 236.79 | 131.31 | 329.95 |
| | THS2.2 (Air) | 9 | 155.43 | 35.31 | 57.43 | 130.00 | 246.23 | 74.01 | 236.85 |
| | THS2.2 (0.15) | 9 | 132.97 | 27.41 | 44.30 | 156.66 | 204.43 | 69.77 | 196.17 |
| | THS2.2 (0.27) | 9 | 218.60 | 50.81 | 72.48 | 256.12 | 353.28 | 101.43 | 335.77 |
| | THS2.2 (0.44) | 9 | 312.90 | 68.13 | 175.72 | 279.31 | 492.80 | 155.78 | 470.02 |
| 48:00 | 3R4F (Air) | 15 | 162.50 | 55.69 | 24.07 | 56.15 | 296.16 | 43.06 | 281.94 |
| | 3R4F (0.15) | 15 | 715.52 | 181.24 | 211.54 | 419.87 | 1011.59 | 326.79 | 1104.24 |
| | 3R4F (0.25) | 15 | 318.81 | 43.91 | 195.55 | 310.25 | 401.17 | 224.64 | 412.98 |
| | THS2.2 (Air) | 15 | 219.21 | 68.10 | 44.42 | 102.78 | 290.74 | 73.16 | 365.26 |
| | THS2.2 (0.15) | 15 | 194.54 | 53.03 | 41.60 | 115.66 | 313.28 | 80.80 | 308.28 |
| | THS2.2 (0.27) | 15 | 235.89 | 66.41 | 54.16 | 89.57 | 418.02 | 93.45 | 378.32 |
| | THS2.2 (0.44) | 12 | 413.44 | 107.72 | 148.98 | 257.38 | 622.46 | 176.35 | 650.54 |
| 72:00 | 3R4F (Air) | 9 | 823.22 | 128.57 | 501.12 | 947.22 | 1036.85 | 526.74 | 1119.69 |
| | 3R4F (0.15) | 9 | 1394.00 | 223.32 | 976.07 | 1268.77 | 1915.82 | 879.02 | 1908.99 |
| | 3R4F (0.25) | 9 | 756.71 | 119.50 | 573.72 | 828.16 | 878.42 | 481.14 | 1032.28 |
| | THS2.2 (Air) | 9 | 586.97 | 178.37 | 60.57 | 496.37 | 1093.60 | 175.65 | 998.29 |
| | THS2.2 (0.15) | 9 | 338.84 | 96.25 | 70.33 | 277.65 | 459.87 | 116.88 | 560.81 |
| | THS2.2 (0.27) | 9 | 576.86 | 166.71 | 134.06 | 447.78 | 966.56 | 192.42 | 961.30 |
| | THS2.2 (0.44) | 9 | 744.48 | 208.88 | 125.41 | 592.09 | 1429.85 | 262.79 | 1226.16 |

Abbreviations: h, hour; LCLM, lower confidence limit for the mean; IL, interleukin; M, mean; N, number of replicate; Q1, first quartile; Q3, third quartile; UCLM, upper confidence limit of the mean; PE, post-exposure; SEM, standard error of the mean; TNFA, tumor necrosis factor alpha.

14.1.26 **Supplementary Table 26**. Descriptive Statistics of CCL11 (Chemokine (C-C motif) Ligand 11) Protein in the Basolateral Media

| | | Descriptive Statistics: CCL11 (pg/mL) | | | | | | | |
|---|---|---|---|---|---|---|---|---|---|
| **PE[h]** | **Exposure** | **N** | **M** | **SEM** | **Q1** | **Median** | **Q3** | **LCLM** | **UCLM** |
| 0:00 | PBS | 1 | 2.00 | . | 2.00 | 2.00 | 2.00 | . | . |
| | TNFA+IL1B | 1 | 4.05 | . | 4.05 | 4.05 | 4.05 | . | . |
| 48:00 | 3R4F (Air) | 3 | 2.00 | 0.00 | 2.00 | 2.00 | 2.00 | . | . |
| | 3R4F (0.15) | 3 | 3.74 | 1.74 | 2.00 | 2.00 | 7.22 | -3.75 | 11.23 |
| | 3R4F (0.25) | 3 | 4.56 | 2.56 | 2.00 | 2.00 | 9.69 | -6.46 | 15.59 |
| | THS2.2 (Air) | 3 | 10.15 | 0.63 | 8.96 | 10.41 | 11.08 | 7.46 | 12.84 |
| | THS2.2 (0.15) | 3 | 10.06 | 0.16 | 9.78 | 10.06 | 10.35 | 9.35 | 10.77 |
| | THS2.2 (0.27) | 3 | 11.08 | 0.75 | 10.32 | 10.32 | 12.59 | 7.84 | 14.32 |

Abbreviations: h, hour; LCLM, lower confidence limit for the mean; IL, interleukin; M, mean; N, number of replicate; Q1, first quartile; Q3, third quartile; UCLM, upper confidence limit of the mean; PE, post-exposure; SEM, standard error of the mean; TNFA, tumor necrosis factor alpha.

14.1.27 **Supplementary Table 27**. Descriptive Statistics of CSF3 (colony-stimulating factor 3) Protein in the Basolateral Media

| | | Descriptive Statistics: CSF3 (pg/mL) | | | | | | | |
|---|---|---|---|---|---|---|---|---|---|
| **PE[h]** | **Exposure** | **N** | **M** | **SEM** | **Q1** | **Median** | **Q3** | **LCLM** | **UCLM** |
| 0:00 | PBS | 1 | 8.64 | . | 8.64 | 8.64 | 8.64 | . | . |
| | TNFA+IL1B | 1 | 58968.00 | . | 58968.00 | 58968.00 | 58968.00 | . | . |
| 48:00 | 3R4F (Air) | 3 | 91.24 | 65.88 | 11.73 | 40.00 | 221.98 | -192.22 | 374.70 |
| | 3R4F (0.15) | 3 | 24.79 | 9.36 | 12.63 | 18.54 | 43.19 | -15.48 | 65.05 |
| | 3R4F (0.25) | 3 | 31.21 | 8.98 | 21.17 | 23.33 | 49.13 | -7.43 | 69.85 |
| | THS2.2 (Air) | 3 | 11.30 | 0.80 | 10.50 | 10.50 | 12.90 | 7.85 | 14.74 |
| | THS2.2 (0.15) | 3 | 26.57 | 11.46 | 9.40 | 22.03 | 48.30 | -22.73 | 75.87 |
| | THS2.2 (0.27) | 3 | 21.92 | 12.06 | 6.70 | 13.33 | 45.73 | -29.95 | 73.80 |

Abbreviations: h, hour; LCLM, lower confidence limit for the mean; IL, interleukin; M, mean; N, number of replicate; Q1, first quartile; Q3, third quartile; UCLM, upper confidence limit of the mean; PE, post-exposure; SEM, standard error of the mean; TNFA, tumor necrosis factor alpha.

14.1.28 **Supplementary Table 28**. Descriptive Statistics of CSF2 (colony-stimulating factor 2) Protein in the Basolateral Media

| | | Descriptive Statistics: CSF2 (pg/mL) | | | | | | | |
|---|---|---|---|---|---|---|---|---|---|
| **PE[h]** | **Exposure** | **N** | **M** | **SEM** | **Q1** | **Median** | **Q3** | **LCLM** | **UCLM** |
| 0:00 | PBS | 1 | 31.54 | . | 31.54 | 31.54 | 31.54 | . | . |
| | TNFA+IL1B | 1 | 308.80 | . | 308.80 | 308.80 | 308.80 | . | . |
| 48:00 | 3R4F (Air) | 3 | 136.39 | 16.41 | 103.95 | 148.35 | 156.88 | 65.80 | 206.99 |
| | 3R4F (0.15) | 3 | 67.41 | 2.55 | 63.32 | 66.82 | 72.10 | 56.43 | 78.39 |
| | 3R4F (0.25) | 3 | 63.17 | 20.95 | 36.76 | 48.22 | 104.54 | -26.96 | 153.31 |
| | THS2.2 (Air) | 3 | 72.15 | 8.98 | 54.31 | 79.27 | 82.87 | 33.50 | 110.79 |
| | THS2.2 (0.15) | 3 | 123.33 | 23.68 | 76.23 | 142.54 | 151.21 | 21.45 | 225.21 |
| | THS2.2 (0.27) | 3 | 125.18 | 20.21 | 98.35 | 112.41 | 164.79 | 38.21 | 212.16 |

Abbreviations: h, hour; LCLM, lower confidence limit for the mean; IL, interleukin; M, mean; N, number of replicate; Q1, first quartile; Q3, third quartile; UCLM, upper confidence limit of the mean; PE, post-exposure; SEM, standard error of the mean; TNFA, tumor necrosis factor alpha.

14.1.29 **Supplementary Table 29**. Descriptive Statistics of IL1A (Interleukin 1 Alpha) Protein in the Basolateral Media

| | | Descriptive Statistics: IL1A (pg/mL) | | | | | | | |
|---|---|---|---|---|---|---|---|---|---|
| **PE[h]** | **Exposure** | **N** | **M** | **SEM** | **Q1** | **Median** | **Q3** | **LCLM** | **UCLM** |
| 0:00 | PBS | 1 | 4.70 | . | 4.70 | 4.70 | 4.70 | . | . |
| | TNFA+IL1B | 1 | 4.70 | . | 4.70 | 4.70 | 4.70 | . | . |
| 48:00 | 3R4F (Air) | 3 | 4.70 | 0.00 | 4.70 | 4.70 | 4.70 | . | . |
| | 3R4F (0.15) | 3 | 4.70 | 0.00 | 4.70 | 4.70 | 4.70 | . | . |
| | 3R4F (0.25) | 3 | 6.79 | 2.09 | 4.70 | 4.70 | 10.97 | -2.20 | 15.78 |
| | THS2.2 (Air) | 3 | 4.70 | 0.00 | 4.70 | 4.70 | 4.70 | . | . |
| | THS2.2 (0.15) | 3 | 4.70 | 0.00 | 4.70 | 4.70 | 4.70 | . | . |
| | THS2.2 (0.27) | 3 | 5.78 | 1.08 | 4.70 | 4.70 | 7.94 | 1.13 | 10.43 |

Abbreviations: h, hour; LCLM, lower confidence limit for the mean; IL, interleukin; M, mean; N, number of replicate; Q1, first quartile; Q3, third quartile; UCLM, upper confidence limit of the mean; PE, post-exposure; SEM, standard error of the mean; TNFA, tumor necrosis factor alpha.

14.1.30 **Supplementary Table 30**. Descriptive Statistics of IL1B (Interleukin 1 Beta) Protein in the Basolateral Media

| | | Descriptive Statistics: IL1B (pg/mL) | | | | | | | |
|---|---|---|---|---|---|---|---|---|---|
| **PE[h]** | **Exposure** | **N** | **M** | **SEM** | **Q1** | **Median** | **Q3** | **LCLM** | **UCLM** |
| 0:00 | PBS | 1 | 0.53 | . | 0.53 | 0.53 | 0.53 | . | . |
| | TNFA+IL1B | 1 | 8631.40 | . | 8631.40 | 8631.40 | 8631.40 | . | . |
| 48:00 | 3R4F (Air) | 3 | 0.40 | 0.00 | 0.40 | 0.40 | 0.40 | . | . |
| | 3R4F (0.15) | 3 | 0.40 | 0.00 | 0.40 | 0.40 | 0.40 | . | . |
| | 3R4F (0.25) | 3 | 0.40 | 0.00 | 0.40 | 0.40 | 0.40 | . | . |
| | THS2.2 (Air) | 3 | 0.40 | 0.00 | 0.40 | 0.40 | 0.40 | . | . |
| | THS2.2 (0.15) | 3 | 0.40 | 0.00 | 0.40 | 0.40 | 0.40 | . | . |
| | THS2.2 (0.27) | 3 | 0.40 | 0.00 | 0.40 | 0.40 | 0.40 | . | . |

Abbreviations: h, hour; LCLM, lower confidence limit for the mean; IL, interleukin; M, mean; N, number of replicate; Q1, first quartile; Q3, third quartile; UCLM, upper confidence limit of the mean; PE, post-exposure; SEM, standard error of the mean; TNFA, tumor necrosis factor alpha.

## 14.1.31 **Supplementary Table 31**. Descriptive Statistics of IL10 (Interleukin 10) Protein in the Basolateral Media

| | | Descriptive Statistics: IL10 (pg/mL) | | | | | | | |
|---|---|---|---|---|---|---|---|---|---|
| **PE[h]** | **Exposure** | **N** | **M** | **SEM** | **Q1** | **Median** | **Q3** | **LCLM** | **UCLM** |
| 0:00 | PBS | 1 | 0.55 | . | 0.55 | 0.55 | 0.55 | . | . |
| | TNFA+IL1B | 1 | 0.55 | . | 0.55 | 0.55 | 0.55 | . | . |
| 48:00 | 3R4F (Air) | 3 | 0.55 | 0.00 | 0.55 | 0.55 | 0.55 | . | . |
| | 3R4F (0.15) | 3 | 0.55 | 0.00 | 0.55 | 0.55 | 0.55 | . | . |
| | 3R4F (0.25) | 3 | 0.55 | 0.00 | 0.55 | 0.55 | 0.55 | . | . |
| | THS2.2 (Air) | 3 | 0.55 | 0.00 | 0.55 | 0.55 | 0.55 | . | . |
| | THS2.2 (0.15) | 3 | 0.55 | 0.00 | 0.55 | 0.55 | 0.55 | . | . |
| | THS2.2 (0.27) | 3 | 0.55 | 0.00 | 0.55 | 0.55 | 0.55 | . | . |

Abbreviations: h, hour; LCLM, lower confidence limit for the mean; IL, interleukin; M, mean; N, number of replicate; Q1, first quartile; Q3, third quartile; UCLM, upper confidence limit of the mean; PE, post-exposure; SEM, standard error of the mean; TNFA, tumor necrosis factor alpha.

## 14.1.32 **Supplementary Table 32**. Descriptive Statistics of IL13 (Interleukin 13) Protein in the Basolateral Media

| | | Descriptive Statistics: IL13 (pg/mL) | | | | | | | |
|---|---|---|---|---|---|---|---|---|---|
| **PE[h]** | **Exposure** | **N** | **M** | **SEM** | **Q1** | **Median** | **Q3** | **LCLM** | **UCLM** |
| 0:00 | PBS | 1 | 0.65 | . | 0.65 | 0.65 | 0.65 | . | . |
| | TNFA+IL1B | 1 | 0.65 | . | 0.65 | 0.65 | 0.65 | . | . |
| 48:00 | 3R4F (Air) | 3 | 0.65 | 0.00 | 0.65 | 0.65 | 0.65 | . | . |
| | 3R4F (0.15) | 3 | 0.65 | 0.00 | 0.65 | 0.65 | 0.65 | . | . |
| | 3R4F (0.25) | 3 | 0.65 | 0.00 | 0.65 | 0.65 | 0.65 | . | . |
| | THS2.2 (Air) | 3 | 0.88 | 0.23 | 0.65 | 0.65 | 1.33 | -0.10 | 1.85 |
| | THS2.2 (0.15) | 3 | 0.65 | 0.00 | 0.65 | 0.65 | 0.65 | . | . |
| | THS2.2 (0.27) | 3 | 0.65 | 0.00 | 0.65 | 0.65 | 0.65 | . | . |

Abbreviations: h, hour; LCLM, lower confidence limit for the mean; IL, interleukin; M, mean; N, number of replicate; Q1, first quartile; Q3, third quartile; UCLM, upper confidence limit of the mean; PE, post-exposure; SEM, standard error of the mean; TNFA, tumor necrosis factor alpha.

14.1.33 **Supplementary Table 33**. Descriptive Statistics of CXCL10 (chemokine (C-X-C motif) ligand)) Protein in the Basolateral Media

| | | Descriptive Statistics: CXCL10 (pg/mL) | | | | | | | |
|---|---|---|---|---|---|---|---|---|---|
| **PE[h]** | **Exposure** | **N** | **M** | **SEM** | **Q1** | **Median** | **Q3** | **LCLM** | **UCLM** |
| 0:00 | PBS | 1 | 41.43 | . | 41.43 | 41.43 | 41.43 | . | . |
| | TNFA+IL1B | 1 | 1232.74 | . | 1232.74 | 1232.74 | 1232.74 | . | . |
| 48:00 | 3R4F (Air) | 3 | 126.78 | 11.14 | 105.71 | 131.04 | 143.59 | 78.85 | 174.71 |
| | 3R4F (0.15) | 3 | 28.53 | 11.47 | 16.73 | 17.40 | 51.47 | -20.82 | 77.88 |
| | 3R4F (0.25) | 3 | 82.86 | 64.44 | 14.68 | 22.25 | 211.66 | -194.38 | 360.11 |
| | THS2.2 (Air) | 3 | 81.78 | 12.82 | 59.60 | 81.74 | 104.01 | 26.63 | 136.94 |
| | THS2.2 (0.15) | 3 | 131.91 | 18.47 | 108.44 | 118.94 | 168.36 | 52.43 | 211.40 |
| | THS2.2 (0.27) | 3 | 78.45 | 4.70 | 73.58 | 73.93 | 87.84 | 58.24 | 98.65 |

Abbreviations: h, hour; LCLM, lower confidence limit for the mean; IL, interleukin; M, mean; N, number of replicate; Q1, first quartile; Q3, third quartile; UCLM, upper confidence limit of the mean; PE, post-exposure; SEM, standard error of the mean; TNFA, tumor necrosis factor alpha.

14.1.34 **Supplementary Table 34**. Descriptive Statistics of CCL2 (Chemokine (C-C motif) Ligand 2) Protein in the Basolateral Media

| | | Descriptive Statistics: CCL2 (pg/mL) | | | | | | | |
|---|---|---|---|---|---|---|---|---|---|
| **PE[h]** | **Exposure** | **N** | **M** | **SEM** | **Q1** | **Median** | **Q3** | **LCLM** | **UCLM** |
| 0:00 | PBS | 1 | 75.47 | . | 75.47 | 75.47 | 75.47 | . | . |
| | TNFA+IL1B | 1 | 23860.69 | . | 23860.69 | 23860.69 | 23860.69 | . | . |
| 48:00 | 3R4F (Air) | 3 | 227.58 | 55.85 | 165.24 | 178.47 | 339.02 | -12.74 | 467.89 |
| | 3R4F (0.15) | 3 | 651.57 | 569.87 | 74.05 | 89.40 | 1791.27 | -1800.37 | 3103.51 |
| | 3R4F (0.25) | 3 | 1071.59 | 772.48 | 232.95 | 367.22 | 2614.62 | -2252.14 | 4395.32 |
| | THS2.2 (Air) | 3 | 117.19 | 9.84 | 98.27 | 121.94 | 131.36 | 74.83 | 159.55 |
| | THS2.2 (0.15) | 3 | 106.21 | 6.20 | 94.44 | 108.71 | 115.47 | 79.54 | 132.87 |
| | THS2.2 (0.27) | 3 | 116.98 | 12.00 | 100.29 | 110.39 | 140.27 | 65.35 | 168.62 |

Abbreviations: h, hour; LCLM, lower confidence limit for the mean; IL, interleukin; M, mean; N, number of replicate; Q1, first quartile; Q3, third quartile; UCLM, upper confidence limit of the mean; PE, post-exposure; SEM, standard error of the mean; TNFA, tumor necrosis factor alpha.

14.1.35 **Supplementary Table 35**. Descriptive Statistics of CCL5 (Chemokine (C-C motif) Ligand 5) Protein in the Basolateral Media

| | | Descriptive Statistics: CCL5 (pg/mL) | | | | | | | |
|---|---|---|---|---|---|---|---|---|---|
| **PE[h]** | **Exposure** | **N** | **M** | **SEM** | **Q1** | **Median** | **Q3** | **LCLM** | **UCLM** |
| 0:00 | PBS | 1 | 7.97 | . | 7.97 | 7.97 | 7.97 | . | . |
| | TNFA+IL1B | 1 | 68.86 | . | 68.86 | 68.86 | 68.86 | . | . |
| 48:00 | 3R4F (Air) | 3 | 18.15 | 1.45 | 16.26 | 17.19 | 21.01 | 11.90 | 24.40 |
| | 3R4F (0.15) | 3 | 12.76 | 0.29 | 12.32 | 12.66 | 13.31 | 11.51 | 14.01 |
| | 3R4F (0.25) | 3 | 13.83 | 4.59 | 7.49 | 11.24 | 22.76 | -5.93 | 33.60 |
| | THS2.2 (Air) | 3 | 15.69 | 2.01 | 12.92 | 14.54 | 19.61 | 7.02 | 24.35 |
| | THS2.2 (0.15) | 3 | 17.48 | 1.56 | 14.98 | 17.11 | 20.34 | 10.77 | 24.19 |
| | THS2.2 (0.27) | 3 | 17.70 | 1.27 | 15.77 | 17.23 | 20.09 | 12.24 | 23.15 |

Abbreviations: h, hour; LCLM, lower confidence limit for the mean; IL, interleukin; M, mean; N, number of replicate; Q1, first quartile; Q3, third quartile; UCLM, upper confidence limit of the mean; PE, post-exposure; SEM, standard error of the mean; TNFA, tumor necrosis factor alpha.

14.1.36 **Supplementary Table 36**. Descriptive Statistics of TSLP (Thymic Stromal Lymphopoietin) Protein in the Basolateral Media

| | | Descriptive Statistics: TLSP (pg/mL) | | | | | | | |
|---|---|---|---|---|---|---|---|---|---|
| **PE[h]** | **Exposure** | **N** | **M** | **SEM** | **Q1** | **Median** | **Q3** | **LCLM** | **UCLM** |
| 0:00 | PBS | 1 | 1.55 | . | 1.55 | 1.55 | 1.55 | . | . |
| | TNFA+IL1B | 1 | 3.50 | . | 3.50 | 3.50 | 3.50 | . | . |
| 48:00 | 3R4F (Air) | 3 | 1.55 | 0.00 | 1.55 | 1.55 | 1.55 | . | . |
| | 3R4F (0.15) | 3 | 1.55 | 0.00 | 1.55 | 1.55 | 1.55 | . | . |
| | 3R4F (0.25) | 3 | 1.55 | 0.00 | 1.55 | 1.55 | 1.55 | . | . |
| | THS2.2 (Air) | 3 | 1.55 | 0.00 | 1.55 | 1.55 | 1.55 | . | . |
| | THS2.2 (0.15) | 3 | 1.55 | 0.00 | 1.55 | 1.55 | 1.55 | . | . |
| | THS2.2 (0.27) | 3 | 1.55 | 0.00 | 1.55 | 1.55 | 1.55 | . | . |

Abbreviations: h, hour; LCLM, lower confidence limit for the mean; IL, interleukin; M, mean; N, number of replicate; Q1, first quartile; Q3, third quartile; UCLM, upper confidence limit of the mean; PE, post-exposure; SEM, standard error of the mean; TNFA, tumor necrosis factor alpha.

14.1.37 **Supplementary Table 37**. Descriptive Statistics: Cytotoxicity (%) in Dose Range Assessment of THS2.2

| | | Descriptive Statistics: Cytotoxicity (RLU) | | | | | | | |
|---|---|---|---|---|---|---|---|---|---|
| **PE [h]** | **Exposure** | N | M | SEM | Q1 | Median | Q3 | LCLM | UCLM |
| 72:00 | THS2.2 (Air) | 3 | 4713 | 184 | 4346 | 4882 | 4910 | 3923 | 5502 |
| | THS2.2 (0.14) | 3 | 4920 | 199 | 4523 | 5105 | 5132 | 4065 | 5775 |
| | THS2.2 (0.22) | 3 | 4984 | 247 | 4495 | 5168 | 5290 | 3921 | 6048 |
| | THS2.2 (0.37) | 3 | 4263 | 453 | 3378 | 4540 | 4871 | 2315 | 6211 |
| | THS2.2 (0.55) | 3 | 5989 | 900 | 4755 | 5471 | 7742 | 2115 | 9863 |
| | THS2.2 (0.77) | 3 | 7929 | 92 | 7747 | 8000 | 8040 | 7534 | 8324 |
| | THS2.2 (1.02) | 3 | 48796 | 15843 | 17229 | 62192 | 66966 | −19373 | 116964 |
| | THS2.2 (1.79) | 3 | 102518 | 2615 | 98733 | 101285 | 107536 | 91267 | 113769 |

Abbreviations: h, hour; LCLM, lower confidence limit for the mean; M, mean; N, number of replicate; Q1, first quartile; Q3, third quartile; UCLM, upper confidence limit of the mean; SEM, standard error of the mean.

## 14.2 Supplementary Figures

### 14.2.1 **Supplementary Figure 1**. Individual Plots of the Inflammatory Mediators Secreted into the Basolateral Media

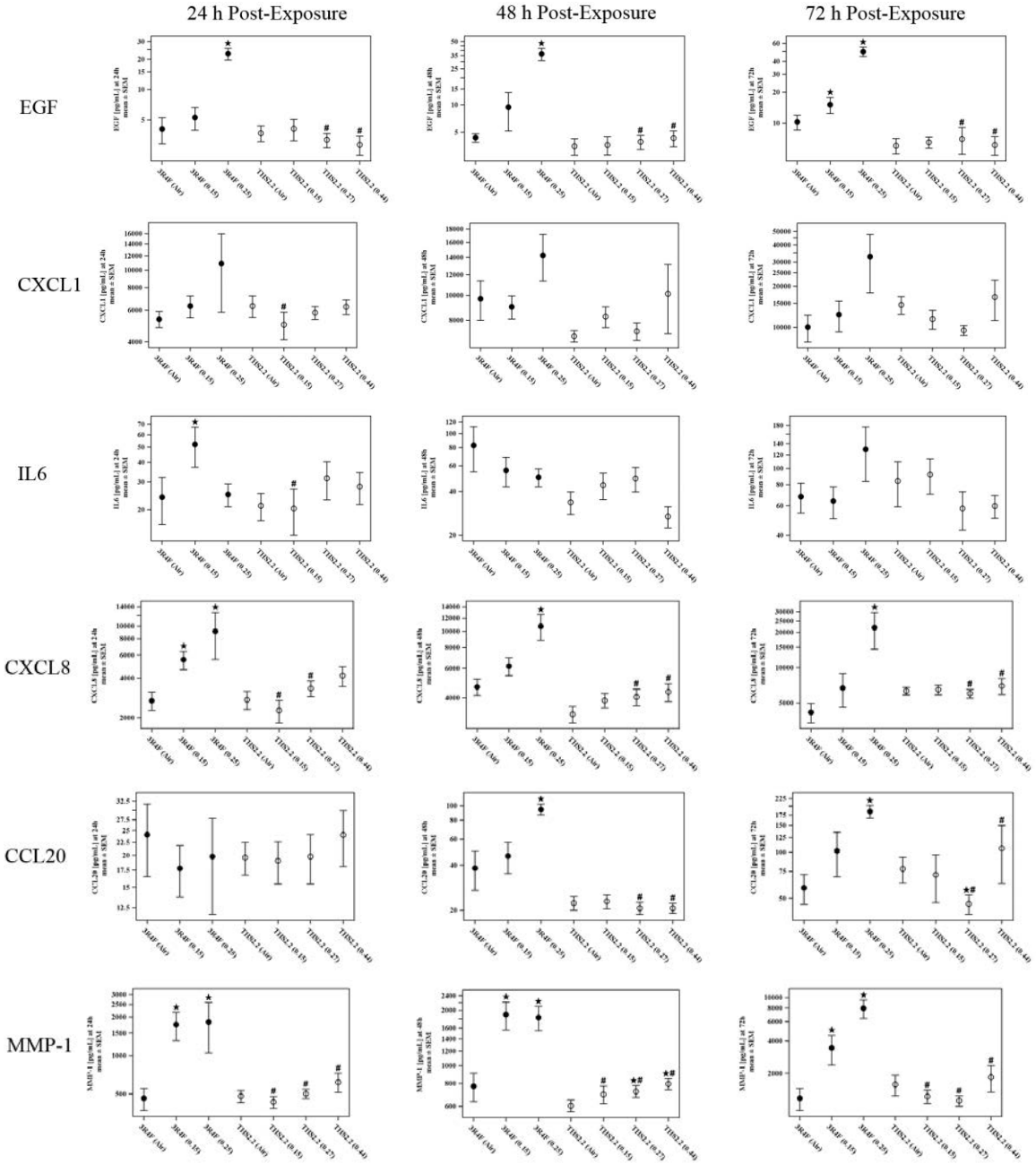
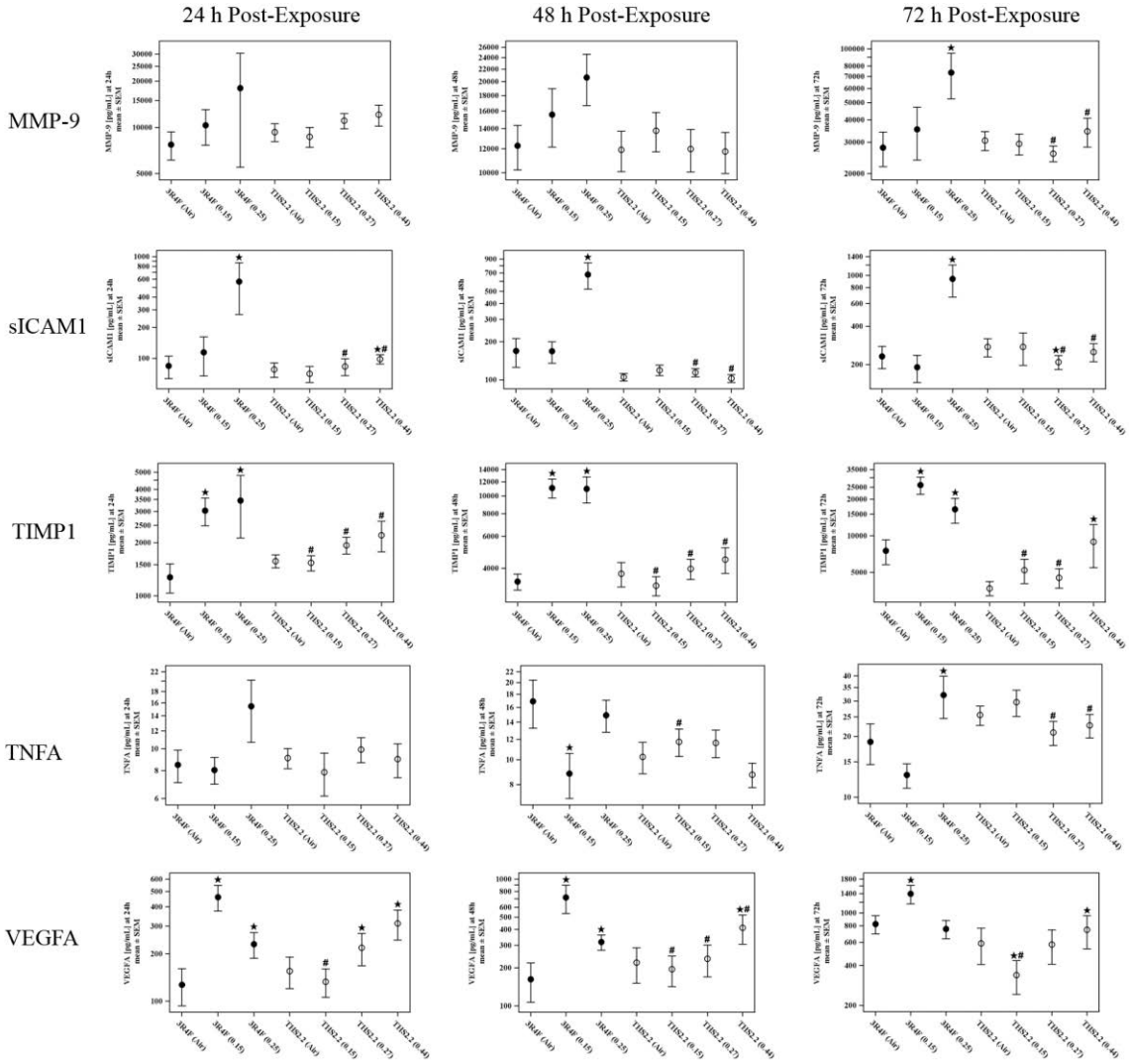


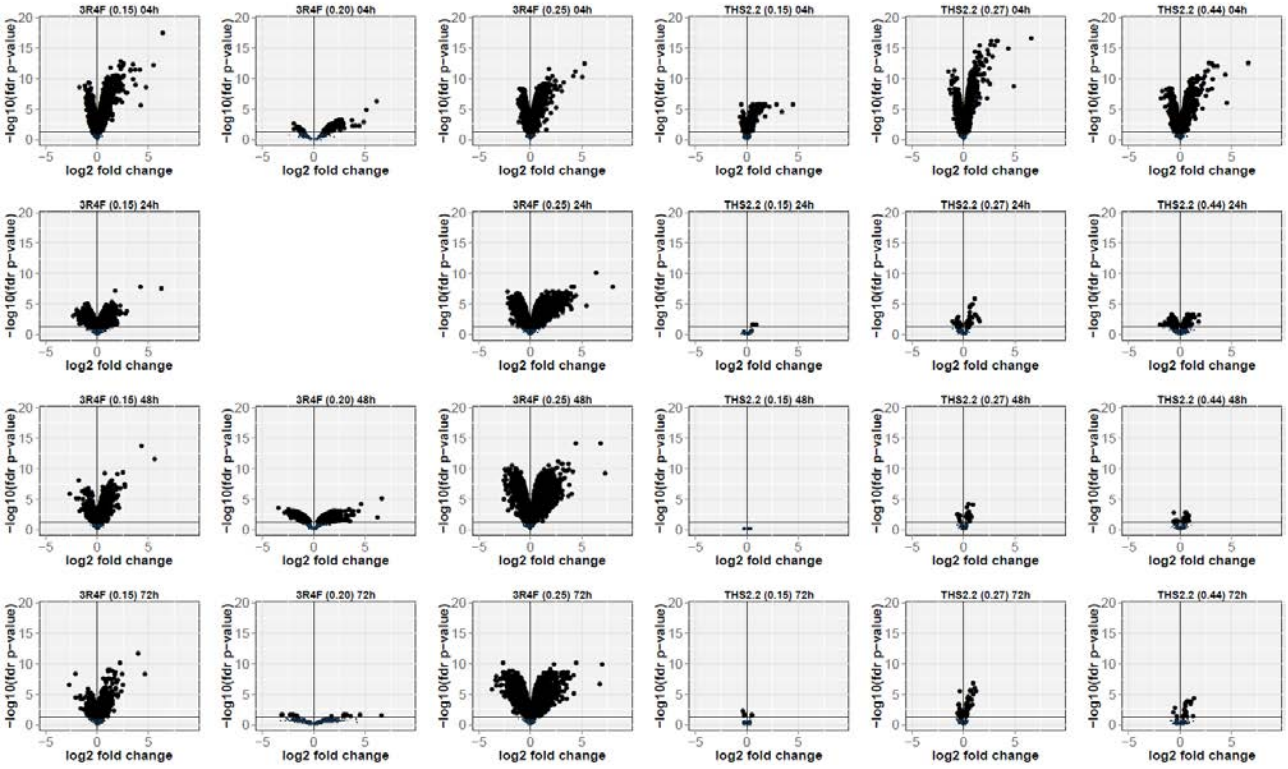

Figure continues




**Supplementary Figure 1. Individual plots of the inflammatory mediators secreted into the basolateral media.**

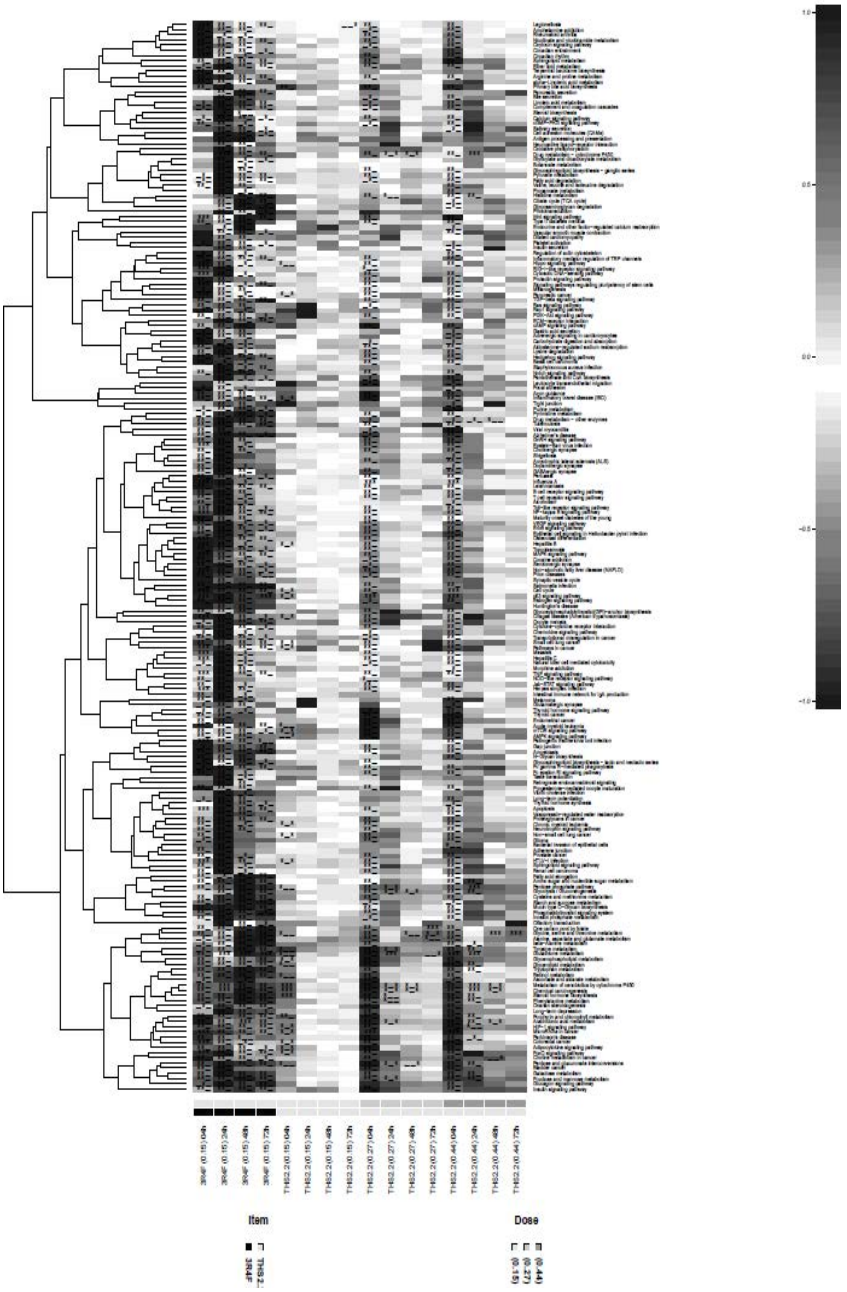
The mean concentration of the indicated mediator and SEM (N = 9–15, from five experimental repetitions with three exposure runs/repetition) are shown. ⋆ indicates a significant difference compared with the corresponding air controls (*p*-values <0.05). # indicates a significant difference compared with 3R4F at the comparable nicotine concentration (*p*-values <0.05). Abbreviations: CCL, chemokine (C-C motif) ligand; CXCL, chemokine (C-X-C motif) ligand; EGF, epidermal growth factor; h, hour; IL, interleukin; MMP, matrix metalloproteinase; SEM, standard error of the mean; sICAM, soluble inter-cellular adhesion molecule; TIMP, tissue inhibitor of metalloproteinase; TNFA, tumor necrosis factor alpha, VEGFA, vascular endothelial growth factor alpha.

14.2.2 **Supplementary Figure 2**. Volcano Plots of the Differentially Expressed Genes (DEGs) in All Experimental Groups Relative to Air Controls




**Supplementary Figure 2. Volcano plots representing the differentially expressed genes.**
Each dot represents a gene generated from five experimental repetitions, N = 9–15 (with the exception of 3R4F (0.20), which was only tested once, N = 3). Gene expression changes compared with the corresponding air controls (x-axis) are expressed as $\log_2(fold-change)$; increased when >0 and decreased when <0. Statistical significance (y-axis) is represented as the −log10 (adjusted *p*-value FDR). The horizontal line represents statistical significance ($-\log_{10}(0.05)$). No 3R4F (0.20)-exposed cultures were collected 24 h post-exposure.

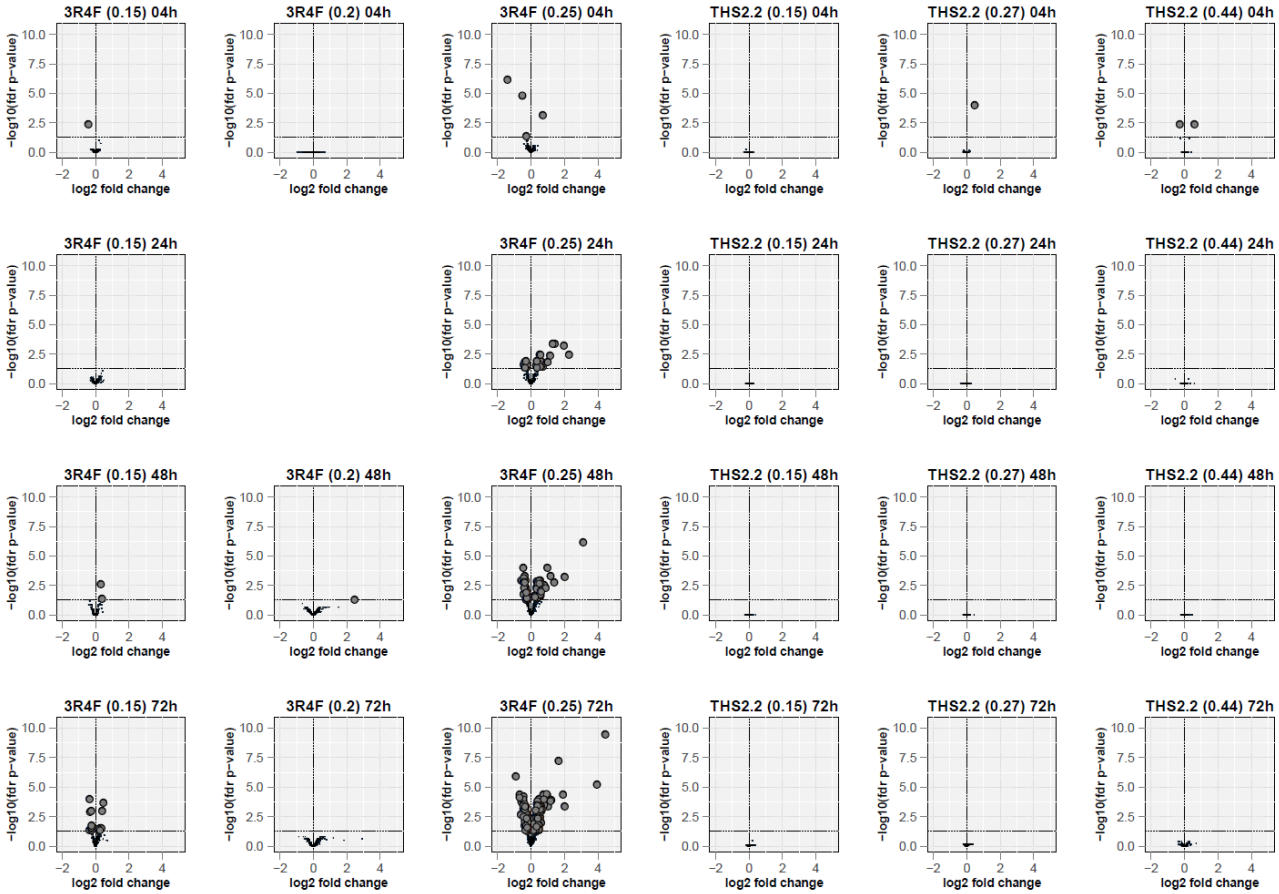
14.2.3 **Supplementary Figure 3**. Gene-set Analysis of the Differentially Expressed Genes




**Supplementary Figure 3. Gene-set analysis of the differentially expressed genes.**

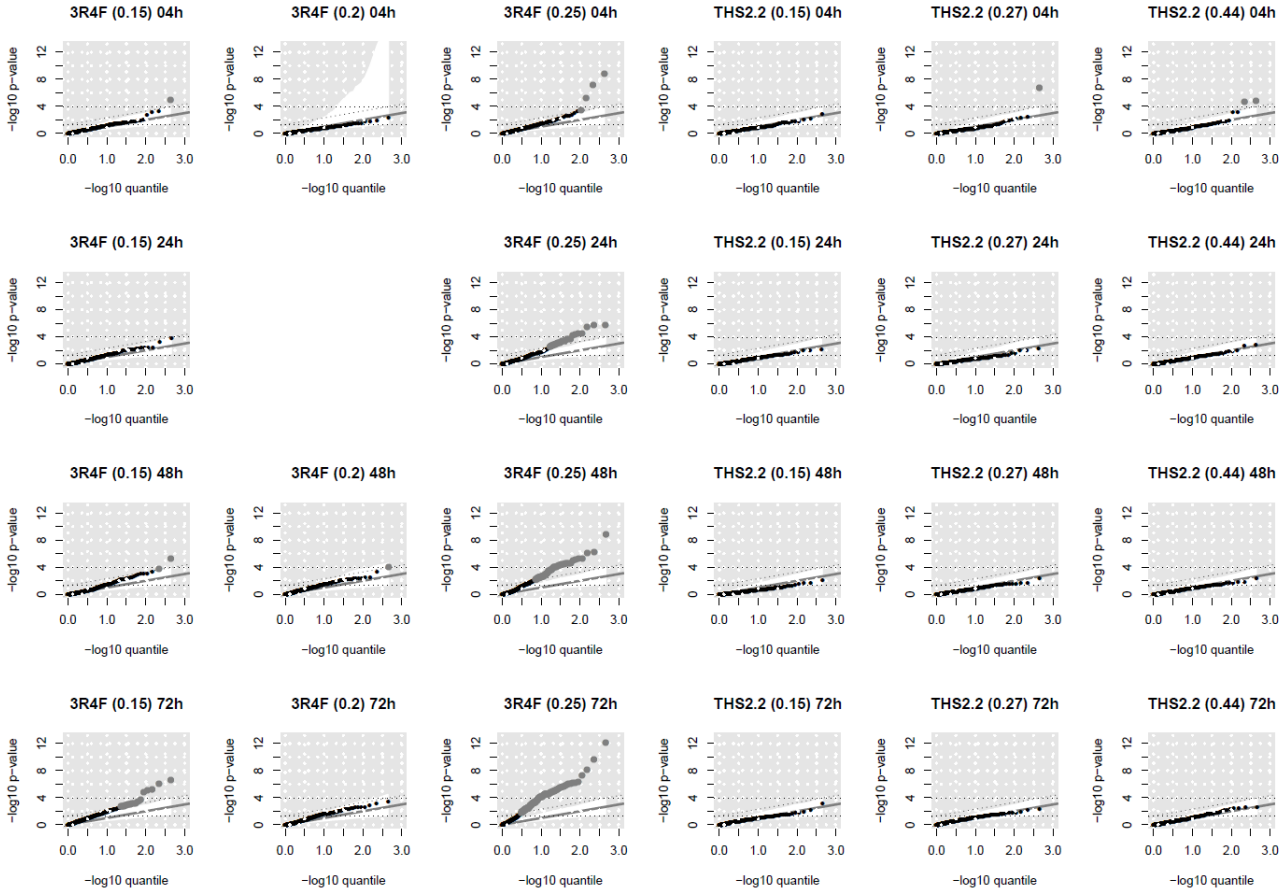
Gene-set enrichment was assessed using over-representation analysis and gene-set analysis. Three types of significance (*) are marked in each cell for each annotation: The first character indicates the adjusted Fisher p-value; the second character indicates the GSA Q2 test; and the third character indicates the over-representation analysis test. Non-significance statistics are indicated with "-" symbol.

14.2.4 **Supplementary Figure 4**. Volcano Plots of the Differentially Expressed miRNAs in All Experimental Groups Relative to Air Controls




**Supplementary Figure 4. Volcano plots representing the differentially expressed miRNAs.**
Each dot represents a miRNA generated from five experimental repetitions, N = 9–15 (with the exception of 3R4F (0.20), which was only tested once, N = 3). MiRNA expression changes (x-axis) compared with the corresponding air controls are expressed as $\log_2(fold - change)$; up-regulated when >0 and down-regulated when <0. Statistical significance (y-axis) is represented as −log10 (adjusted *p*-value FDR). The horizontal line represents statistical significance ($-\log_{10}(0.05)$). No 3R4F (0.20)-exposed cultures were collected 24 h post-exposure.

14.2.5 **Supplementary Figure 5**. Quantile-Quantile (QQ) Plots of the Differentially Expressed miRNA in All Experimental Groups




**Supplementary Figure 5. Quantile-quantile (QQ) plots representing the significance of the miRNA differential expression profiles.**

Each dot represents a miRNA generated from five experimental repetitions, N = 9–15 (with the exception of 3R4F (0.20), which was only tested once, N = 3). Statistical significance (y-axis) is proportionally expressed as $-\log_{10}(raw\ p-value)$. The corresponding quantiles are plotted on the x-axis. A miRNA is considered to be significantly differentially expressed if it falls above the oblique gray line. No 3R4F (0.20)-exposed cultures were collected 24 h post-exposure.

--- End of Document ---